(12) INTERNATIONAL APPLICATION PUBLISHED UNDER THE PATENT COOPERATION TREATY (PCT)

(19) World Intellectual Property Organization
International Bureau

(43) International Publication Date
16 March 2017 (16.03.2017)

WIPO | PCT

(10) International Publication Number
WO 2017/044272 A1

(51) International Patent Classification:
G01S 11/02 (2010.01) *G01S 5/14* (2006.01)

(21) International Application Number:
PCT/US2016/047448

(22) International Filing Date:
18 August 2016 (18.08.2016)

(25) Filing Language: English

(26) Publication Language: English

(30) Priority Data:
14/850,071 10 September 2015 (10.09.2015) US

(71) Applicant: **CPG TECHNOLOGIES, LLC.** [US/US]; 202N I-35, Suite C, Red Oak, TX 75154 (US).

(72) Inventors: **CORUM, James, F.**; 202N I-35, Suite C, Red Oak, TX 75154 (US). **CORUM, Kenneth, L.**; 202N I-35, Suite C, Red Oak, TX 75154 (US). **LILLY, James, D.**; 202N I-35, Suite C, Red Oak, TX 75154 (US). **D'AURELIO, Michael, J.**; 202N I-35, Suite C, Red Oak, TX 75154 (US).

(74) Agents: **D'AURELIO, Michael, J.** et al.; Thomas | Horstemeyer, LLP., 400 Interstate North Parkway, Ste. 1500, Atlanta, GA 30339 (US).

(81) Designated States *(unless otherwise indicated, for every kind of national protection available)*: AE, AG, AL, AM, AO, AT, AU, AZ, BA, BB, BG, BH, BN, BR, BW, BY, BZ, CA, CH, CL, CN, CO, CR, CU, CZ, DE, DK, DM, DO, DZ, EC, EE, EG, ES, FI, GB, GD, GE, GH, GM, GT, HN, HR, HU, ID, IL, IN, IR, IS, JP, KE, KG, KN, KP, KR, KZ, LA, LC, LK, LR, LS, LU, LY, MA, MD, ME, MG, MK, MN, MW, MX, MY, MZ, NA, NG, NI, NO, NZ, OM, PA, PE, PG, PH, PL, PT, QA, RO, RS, RU, RW, SA, SC, SD, SE, SG, SK, SL, SM, ST, SV, SY, TH, TJ, TM, TN, TR, TT, TZ, UA, UG, US, UZ, VC, VN, ZA, ZM, ZW.

(84) Designated States *(unless otherwise indicated, for every kind of regional protection available)*: ARIPO (BW, GH, GM, KE, LR, LS, MW, MZ, NA, RW, SD, SL, ST, SZ, TZ, UG, ZM, ZW), Eurasian (AM, AZ, BY, KG, KZ, RU, TJ, TM), European (AL, AT, BE, BG, CH, CY, CZ, DE, DK, EE, ES, FI, FR, GB, GR, HR, HU, IE, IS, IT, LT, LU, LV, MC, MK, MT, NL, NO, PL, PT, RO, RS, SE, SI, SK,

[Continued on next page]

(54) Title: GEOLOCATION USING GUIDED SURFACE WAVES

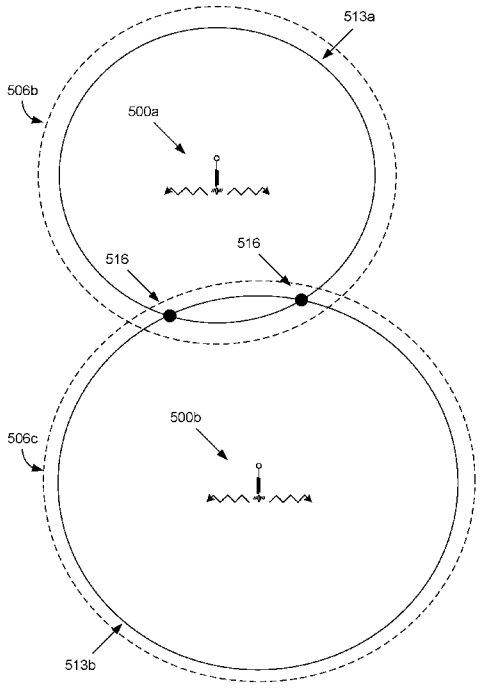


FIG. 24

(57) Abstract: Disclosed are various approaches for determining a location using guided surface waves. A wavelength and a phase of a base guided surface wave launched from a ground station and received by the guided surface wave receive structure are identified. A range of an overlaid guided surface wave launched from the ground station and received by the guided surface wave receive structure are identified., wherein the range of the overlaid guided surface wave is measured as a number of wavelengths of the base guided surface wave. A distance of the guided surface wave receive structure from the ground station based at least in part on the phase of the base guided surface wave and the range of the overlaid guided surface wave is calculated. Finally, a location of the guided surface wave receive structure based at least in part on the distance of the guided surface wave receive structure from the ground station is determined.

WO 2017/044272 A1

SM, TR), OAPI (BF, BJ, CF, CG, CI, CM, GA, GN, GQ, GW, KM, ML, MR, NE, SN, TD, TG).

Declarations under Rule 4.17:

— *as to applicant's entitlement to apply for and be granted a patent (Rule 4.17(ii))*

— *as to the applicant's entitlement to claim the priority of the earlier application (Rule 4.17(iii))*

Published:

— *with international search report (Art. 21(3))*

GEOLOCATION USING GUIDED SURFACE WAVES

CROSS REFERENCE TO RELATED APPLICATIONS

[0001] This application claims priority to, and the benefit of, U.S. Patent Application No. 14/850,071, entitled "Geolocation Using Guided Surface Waves" and filed on September 10, 2015, which is incorporated by reference as if set forth herein in its entirety.

[0002] This application is related to co-pending U.S. Non-provisional Patent Application entitled "Excitation and Use of Guided Surface Wave Modes on Lossy Media," which was filed on March 7, 2013 and assigned Application Number 13/789,538, and was published on September 11, 2014 as Publication Number US2014/0252886 A1, and which is incorporated herein by reference in its entirety. This application is also related to co-pending U.S. Non-provisional Patent Application entitled "Excitation and Use of Guided Surface Wave Modes on Lossy Media," which was filed on March 7, 2013 and assigned Application Number 13/789,525, and was published on September 11, 2014 as Publication Number US2014/0252865 A1, and which is incorporated herein by reference in its entirety. This application is further related to co-pending U.S. Non-provisional Patent Application entitled "Excitation and Use of Guided Surface Wave Modes on Lossy Media," which was filed on September 10, 2014 and assigned Application Number 14/483,089, and which is incorporated herein by reference in its entirety. This application is further related to co-pending U.S. Non-provisional Patent Application entitled "Excitation and Use of Guided Surface Waves," which was filed on June 2, 2015 and assigned Application Number 14/728,507, and which is incorporated herein by reference in its entirety. This application is further related to co-pending U.S. Non-provisional Patent Application entitled "Excitation and Use of Guided Surface Waves," which was filed on June 2, 2015 and assigned Application Number 14/728,492, and which is incorporated herein by reference in its entirety.

BACKGROUND

[0003] For over a century, signals transmitted by radio waves involved radiation fields launched using conventional antenna structures. In contrast to radio science, electrical power distribution systems in the last century involved the transmission of energy guided along electrical conductors. This understanding of the distinction between radio frequency (RF) and power transmission has existed since the early 1900's.

SUMMARY

[0004] Disclosed are various embodiments of an apparatus for determining geolocation using guided surface waves. The apparatus can include a charge terminal elevated over a lossy conducting medium; a receiver network coupled between the charge terminal and the lossy conducting medium, the receiver network having a phase delay (Φ) that matches a wave tilt angle (Ψ) associated with the guided surface wave, the wave tilt angle (Ψ) based at least in part upon characteristics of the lossy conducting medium in a vicinity of the receiving structure; a processor; a memory; and an application stored in the memory and executable by the processor, wherein the application causes the apparatus to perform at least the following actions when executed by the processor: identify a wavelength and a phase of a base guided surface wave launched from a ground station and received by the receiver network; identify a range of an overlaid guided surface wave launched from the ground station and received by the receiver network, wherein the range of the overlaid guided surface wave is measured as a number of wavelengths of the base guided surface wave; calculate a distance of the receiver network from the ground station based at least in part on the phase of the base guided surface wave and the range of the overlaid guided surface wave; and determine a location of the receiver network based at least in part on the distance of the receiver network from the ground station. In one or more embodiments, the application, when executed by the processor, further causes the apparatus to at least: identify a second wavelength and a second phase of a second base guided surface wave launched from a second ground station and received by the receiver network; identify a second range of a second overlaid guided surface wave launched from the second ground station and received by the receiver network, wherein the second range of the second overlaid guided surface wave is measured as a second number of wavelengths of the second based guided surface wave; and calculate a second distance of the receiver network from the second ground station based at least in part on the second phase of the second base guided surface wave and the second range of the second overlaid guided surface wave. In some of these embodiments, causing the apparatus to determine the location of the receiver network is further based at least in part on the second distance of the receiver network from the second ground station. In one or more embodiments, the overlaid guided surface wave has a higher frequency than the base guided surface wave. In one or more embodiments, the application, when executed by the processor, further causes the apparatus to at least identify an approximate position of the receiver network based at least in part on inertial data associated with the apparatus. In some of these embodiments, the inertial data is stored in the memory of the apparatus. In some of these embodiments, causing the apparatus to determine the location of the receiver network is further based at least in part on the approximate position of the receiver network. In one or more

embodiments, the application, when executed by the processor, further causes the apparatus to at least identify an approximate position of the receiver network is based at least in part on an identity of a cellular network tower within range of the receiver network. In some of these embodiments, causing the apparatus to determine the location of the receiver network is further based at least in part on the approximate position of the receiver network. In one or more embodiments, the application, when executed by the processor, further causes the apparatus to at least identify an approximate position of the receiver network based at least in part on an identity of a radio transmission tower within range of the receiver network. In some of these embodiments, causing the apparatus to determine the location of the receiver network is further based at least in part on the approximate position of the receiver network. In one or more embodiments, the charge terminal is height adjustable such that a change in a height of the charge terminal causes a change in the phase delay (Φ).

[0005] Disclosed are various methods for determining geolocation using guided surface waves. For example, the method can include receiving a base guided surface wave launched from a ground station; identifying a wavelength and a phase of the base guided surface wave; receiving an overlaid guided surface wave launched from the ground station; identifying a range of the overlaid guided surface wave, wherein the range of the overlaid guided surface wave is measured as a number of wavelengths of the base guided surface wave; calculating a distance from the ground station based at least in part on the phase of the base guided surface wave and the range of the overlaid guided surface wave; and determining a current location based at least in part on the distance from the ground station. In one or more embodiments, the method can further include receiving a second based guided surface wave launched from a second ground station; identifying a second wavelength and a second phase of the second base guided surface wave; receiving a second overlaid guided surface wave launched from a second ground station; identifying a second range of the second overlaid guided surface wave launched, wherein the second range of the second overlaid guided surface wave is measured as a second number of wavelengths of the second based guided surface wave; and calculating a second distance from the second ground station based at least in part on the second phase of the second base guided surface wave and the second range of the second overlaid guided surface wave. In some of these embodiments, determining the location is further based at least in part on the second distance from the second ground station. In one or more embodiments, the overlaid guided surface wave has a higher frequency than the base guided surface wave. In one or more embodiments, the method further includes identifying an approximate position based at least in part on inertial data. In some of these embodiments, determining the current location is further based at least in part on the approximate position. In one or more embodiments, the method further includes identifying an approximate position based at

least in part on an identity of a cellular network tower. In some of these embodiments, determining the current location is further based at least in part on the approximate position. In one or more embodiments, the method further includes receiving a broadcast transmission and identifying an approximate position based at least in part on an identity of the broadcast transmission. In some of these embodiments, determining the current location is further based at least in part on the approximate position. In one or more embodiments, the method further includes receiving a signal from a wireless network; identifying a media access control (MAC) address associated with an access point for the wireless network; and identifying an approximate position based at least in part on the MAC address. In some of these embodiments, determining the current location is further based at least in part on the approximate position.

[0006] Disclosed are various embodiments for a system for performing geolocation using guided surface waves. The system can include a guided surface wave receive structure configured to obtain electrical energy from a guided surface wave traveling along a terrestrial medium; a processor; a memory; and an application stored in the memory that, when executed by the processor, causes the apparatus to at least: identify a wavelength and a phase of a base guided surface wave launched from a ground station and received by the guided surface wave receive structure; identify a range of an overlaid guided surface wave launched from the ground station and received by the guided surface wave receive structure, wherein the range of the overlaid guided surface wave is measured as a number of wavelengths of the base guided surface wave; calculate a distance of the guided surface wave receive structure from the ground station based at least in part on the phase of the base guided surface wave and the range of the overlaid guided surface wave; and determine a location of the guided surface wave receive structure based at least in part on the distance of the guided surface wave receive structure from the ground station. In one or more embodiments, the application, when executed by the processor, further causes the system to at least: identify a second wavelength and a second phase of a second base guided surface wave launched from a second ground station and received by the guided surface wave receive structure; identify a second range of a second overlaid guided surface wave launched from the second ground station and received by the guided surface wave receive structure, wherein the second range of the second overlaid guided surface wave is measured as a second number of wavelengths of the second based guided surface wave; and calculate a second distance of the guided surface wave receive structure from the second ground station based at least in part on the second phase of the second base guided surface wave and the second range of the second overlaid guided surface wave. In some of these embodiments, causing the apparatus to determine the location of the guided surface wave receive structure is further based at least in part on the second distance of the guided

surface wave receive structure from the second ground station. In one or more embodiments, the overlaid guided surface wave has a higher frequency than the base guided surface wave. In one or more embodiments, the application, when executed by the processor, further causes the system to at least identify an approximate position of guided surface wave receive structure based at least in part on inertial data associated with the system, wherein the inertial data is stored in the memory of the system. In some of these embodiments, causing the system to determine the location of the guided surface wave receive structure is further based at least in part on the approximate position of the guided surface wave receive structure. In one or more embodiments, the application, when executed by the processor, further causes the system to at least identify an approximate position of the guided surface wave receive structure based at least in part on inertial data associated with the system, wherein the inertial data is stored in the memory of the system. In some of these embodiments, causing the system to determine the location of the guided surface wave receive structure is further based at least in part on the approximate position of the guided surface wave receive structure. In one or more embodiments, the application, when executed by the processor, further causes the system to at least identify an approximate position of the guided surface wave receive structure based at least in part on an identity of a radio transmission tower within range of the guided surface wave receive structure. In some of these embodiments, causing the apparatus to determine the location of the guided surface wave receive structure is further based at least in part on the approximate position of the guided surface wave receive structure.

[0007] Other systems, methods, features, and advantages of the present disclosure will be or become apparent to one with skill in the art upon examination of the following drawings and detailed description. It is intended that all such additional systems, methods, features, and advantages be included within this description, be within the scope of the present disclosure, and be protected by the accompanying claims.

[0008] In addition, all optional and preferred features and modifications of the described embodiments are usable in all aspects of the entire disclosure taught herein. Furthermore, the individual features of the dependent claims, as well as all optional and preferred features and modifications of the described embodiments are combinable and interchangeable with one another.

BRIEF DESCRIPTION OF THE DRAWINGS

[0009] Many aspects of the present disclosure can be better understood with reference to the following drawings. The components in the drawings are not necessarily to scale, emphasis instead being placed upon clearly illustrating the principles of the disclosure.

Moreover, in the drawings, like reference numerals designate corresponding parts throughout the several views.

[0010] FIG. 1 is a chart that depicts field strength as a function of distance for a guided electromagnetic field and a radiated electromagnetic field.

[0011] FIG. 2 is a drawing that illustrates a propagation interface with two regions employed for transmission of a guided surface wave according to various embodiments of the present disclosure.

[0012] FIG. 3 is a drawing that illustrates a guided surface waveguide probe disposed with respect to a propagation interface of FIG. 2 according to various embodiments of the present disclosure.

[0013] FIG. 4 is a plot of an example of the magnitudes of close-in and far-out asymptotes of first order Hankel functions according to various embodiments of the present disclosure.

[0014] FIGS. 5A and 5B are drawings that illustrate a complex angle of incidence of an electric field synthesized by a guided surface waveguide probe according to various embodiments of the present disclosure.

[0015] FIG. 6 is a graphical representation illustrating the effect of elevation of a charge terminal on the location where the electric field of FIG. 5A intersects with the lossy conducting medium at a Brewster angle according to various embodiments of the present disclosure.

[0016] FIG. 7 is a graphical representation of an example of a guided surface waveguide probe according to various embodiments of the present disclosure.

[0017] FIGS. 8A through 8C are graphical representations illustrating examples of equivalent image plane models of the guided surface waveguide probe of FIGS. 3 and 7 according to various embodiments of the present disclosure.

[0018] FIGS. 9A and 9B are graphical representations illustrating examples of single-wire transmission line and classic transmission line models of the equivalent image plane models of FIGS. 8B and 8C according to various embodiments of the present disclosure.

[0019] FIG. 10 is a flow chart illustrating an example of adjusting a guided surface waveguide probe of FIGS. 3 and 7 to launch a guided surface wave along the surface of a lossy conducting medium according to various embodiments of the present disclosure.

[0020] FIG. 11 is a plot illustrating an example of the relationship between a wave tilt angle and the phase delay of a guided surface waveguide probe of FIGS. 3 and 7 according to various embodiments of the present disclosure.

[0021] FIG. 12 is a drawing that illustrates an example of a guided surface waveguide probe according to various embodiments of the present disclosure.

[0022] FIG. 13 is a graphical representation illustrating the incidence of a synthesized electric field at a complex Brewster angle to match the guided surface waveguide mode at the Hankel crossover distance according to various embodiments of the present disclosure.

[0023] FIG. 14 is a graphical representation of an example of a guided surface waveguide probe of FIG. 12 according to various embodiments of the present disclosure.

[0024] FIG. 15A includes plots of an example of the imaginary and real parts of a phase delay (Φ_U) of a charge terminal T_1 of a guided surface waveguide probe according to various embodiments of the present disclosure.

[0025] FIG. 15B is a schematic diagram of the guided surface waveguide probe of FIG. 14 according to various embodiments of the present disclosure.

[0026] FIG. 16 is a drawing that illustrates an example of a guided surface waveguide probe according to various embodiments of the present disclosure.

[0027] FIG. 17 is a graphical representation of an example of a guided surface waveguide probe of FIG. 16 according to various embodiments of the present disclosure.

[0028] FIGS. 18A through 18C depict examples of receiving structures that can be employed to receive energy transmitted in the form of a guided surface wave launched by a guided surface waveguide probe according to the various embodiments of the present disclosure.

[0029] FIG. 18D is a flow chart illustrating an example of adjusting a receiving structure according to various embodiments of the present disclosure.

[0030] FIG. 19 depicts an example of an additional receiving structure that can be employed to receive energy transmitted in the form of a guided surface wave launched by a guided surface waveguide probe according to the various embodiments of the present disclosure.

[0031] FIGS. 20A-E depict various circuit symbols used in the discussion of the application of guided surface waves for geolocation according to various embodiments of the present disclosure.

[0032] FIG. 21 is schematic block diagram depicting a navigation unit capable of determining its location based upon guided surface waves launched by one or more guided surface wave probes, according to various embodiments of the present disclosure.

[0033] FIG. 22 illustrates the principles underlying the operation of the navigation unit, according to various embodiments of the present disclosure.

[0034] FIG. 23 illustrate the principles underlying the operation of the navigation unit, according to various embodiments of the present disclosure.

[0035] FIG. 24 illustrates the principles underlying the operation of the navigation unit, according to various embodiments of the present disclosure.

[0036] FIG. 25 is a flowchart depicting the operation of various components of the navigation unit according to various embodiments of the present disclosure.

DETAILED DESCRIPTION

[0037] To begin, some terminology shall be established to provide clarity in the discussion of concepts to follow. First, as contemplated herein, a formal distinction is drawn between ***radiated*** electromagnetic fields and ***guided*** electromagnetic fields.

[0038] As contemplated herein, a radiated electromagnetic field comprises electromagnetic energy that is emitted from a source structure in the form of waves that are not bound to a waveguide. For example, a radiated electromagnetic field is generally a field that leaves an electric structure such as an antenna and propagates through the atmosphere or other medium and is not bound to any waveguide structure. Once radiated electromagnetic waves leave an electric structure such as an antenna, they continue to propagate in the medium of propagation (such as air) independent of their source until they dissipate regardless of whether the source continues to operate. Once electromagnetic waves are radiated, they are not recoverable unless intercepted, and, if not intercepted, the energy inherent in the radiated electromagnetic waves is lost forever. Electrical structures such as antennas are designed to radiate electromagnetic fields by maximizing the ratio of the radiation resistance to the structure loss resistance. Radiated energy spreads out in space and is lost regardless of whether a receiver is present. The energy density of the radiated fields is a function of distance due to geometric spreading. Accordingly, the term “radiate” in all its forms as used herein refers to this form of electromagnetic propagation.

[0039] A guided electromagnetic field is a propagating electromagnetic wave whose energy is concentrated within or near boundaries between media having different electromagnetic properties. In this sense, a guided electromagnetic field is one that is bound to a waveguide and may be characterized as being conveyed by the current flowing in the waveguide. If there is no load to receive and/or dissipate the energy conveyed in a guided electromagnetic wave, then no energy is lost except for that dissipated in the conductivity of the guiding medium. Stated another way, if there is no load for a guided electromagnetic wave, then no energy is consumed. Thus, a generator or other source generating a guided electromagnetic field does not deliver real power unless a resistive load is present. To this end, such a generator or other source essentially runs idle until a load is presented. This is akin to running a generator to generate a 60 Hertz electromagnetic wave that is transmitted over power lines where there is no electrical load. It should be noted that a guided electromagnetic field or wave is the equivalent to what is termed a “transmission line mode.” This contrasts with radiated electromagnetic waves in which real power is supplied at all

times in order to generate radiated waves. Unlike radiated electromagnetic waves, guided electromagnetic energy does not continue to propagate along a finite length waveguide after the energy source is turned off. Accordingly, the term "guide" in all its forms as used herein refers to this transmission mode of electromagnetic propagation.

[0040] Referring now to FIG. 1, shown is a graph 100 of field strength in decibels (dB) above an arbitrary reference in volts per meter as a function of distance in kilometers on a log-dB plot to further illustrate the distinction between radiated and guided electromagnetic fields. The graph 100 of FIG. 1 depicts a guided field strength curve 103 that shows the field strength of a guided electromagnetic field as a function of distance. This guided field strength curve 103 is essentially the same as a transmission line mode. Also, the graph 100 of FIG. 1 depicts a radiated field strength curve 106 that shows the field strength of a radiated electromagnetic field as a function of distance.

[0041] Of interest are the shapes of the curves 103 and 106 for *guided wave* and for *radiation* propagation, respectively. The radiated field strength curve 106 falls off geometrically ($1/d$, where d is distance), which is depicted as a straight line on the log-log scale. The guided field strength curve 103, on the other hand, has a characteristic exponential decay of $e^{-\alpha d}/\sqrt{d}$ and exhibits a distinctive knee 109 on the log-log scale. The guided field strength curve 103 and the radiated field strength curve 106 intersect at point 112, which occurs at a crossing distance. At distances less than the crossing distance at intersection point 112, the field strength of a guided electromagnetic field is significantly greater at most locations than the field strength of a radiated electromagnetic field. At distances greater than the crossing distance, the opposite is true. Thus, the guided and radiated field strength curves 103 and 106 further illustrate the fundamental propagation difference between guided and radiated electromagnetic fields. For an informal discussion of the difference between guided and radiated electromagnetic fields, reference is made to Milligan, T., Modern Antenna Design, McGraw-Hill, 1st Edition, 1985, pp.8-9, which is incorporated herein by reference in its entirety.

[0042] The distinction between radiated and guided electromagnetic waves, made above, is readily expressed formally and placed on a rigorous basis. That two such diverse solutions could emerge from one and the same linear partial differential equation, the wave equation, analytically follows from the boundary conditions imposed on the problem. The Green function for the wave equation, itself, contains the distinction between the nature of radiation and guided waves.

[0043] In empty space, the wave equation is a differential operator whose eigenfunctions possess a *continuous* spectrum of eigenvalues on the complex wave-number plane. This transverse electro-magnetic (TEM) field is called the radiation field, and those

propagating fields are called "Hertzian waves." However, in the presence of a conducting boundary, the wave equation plus boundary conditions mathematically lead to a spectral representation of wave-numbers composed of a continuous spectrum *plus* a sum of *discrete* spectra. To this end, reference is made to Sommerfeld, A., "Uber die Ausbreitung der Wellen in der Drahtlosen Telegraphie," Annalen der Physik, Vol. 28, 1909, pp. 665-736. Also see Sommerfeld, A., "Problems of Radio," published as Chapter 6 in Partial Differential Equations in Physics – Lectures on Theoretical Physics: Volume VI, Academic Press, 1949, pp. 236-289, 295-296; Collin, R. E., "Hertzian Dipole Radiating Over a Lossy Earth or Sea: Some Early and Late 20th Century Controversies," IEEE Antennas and Propagation Magazine, Vol. 46, No. 2, April 2004, pp. 64-79; and Reich, H. J., Ordnung, P.F, Krauss, H.L., and Skalnik, J.G., Microwave Theory and Techniques, Van Nostrand, 1953, pp. 291-293, each of these references being incorporated herein by reference in its entirety.

[0044] The terms *"ground wave"* and *"surface wave"* identify two distinctly different physical propagation phenomena. A surface wave arises analytically from a distinct *pole* yielding a *discrete* component in the plane wave spectrum. See, e.g., "The Excitation of Plane Surface Waves" by Cullen, A.L., (Proceedings of the IEE (British), Vol. 101, Part IV, August 1954, pp. 225-235). In this context, a *surface wave* is considered to be a guided *surface wave*. The *surface wave* (in the Zenneck-Sommerfeld guided wave sense) is, physically and mathematically, not the same as the *ground wave* (in the Weyl-Norton-FCC sense) that is now so familiar from radio broadcasting. These two propagation mechanisms arise from the excitation of different types of eigenvalue spectra (continuum or discrete) on the complex plane. The field strength of the guided *surface wave* decays exponentially with distance as illustrated by curve 103 of FIG. 1 (much like propagation in a lossy waveguide) and resembles propagation in a radial transmission line, as opposed to the classical Hertzian radiation of the *ground wave*, which propagates spherically, possesses a *continuum* of eigenvalues, falls off geometrically as illustrated by curve 106 of FIG. 1, and results from branch-cut integrals. As experimentally demonstrated by C.R. Burrows in "The Surface Wave in Radio Propagation over Plane Earth" (Proceedings of the IRE, Vol. 25, No. 2, February, 1937, pp. 219-229) and "The Surface Wave in Radio Transmission" (Bell Laboratories Record, Vol. 15, June 1937, pp. 321-324), vertical antennas radiate *ground waves* but do not launch guided *surface waves*.

[0045] To summarize the above, first, the *continuous* part of the wave-number eigenvalue spectrum, corresponding to *branch-cut integrals*, produces the radiation field, and second, the *discrete* spectra, and corresponding *residue sum* arising from the poles enclosed by the contour of integration, result in non-TEM traveling surface waves that are exponentially damped in the direction transverse to the propagation. Such surface waves are guided transmission line modes. For further explanation, reference is made to Friedman, B.,

Principles and Techniques of Applied Mathematics, Wiley, 1956, pp. pp. 214, 283-286, 290, 298-300.

[0046] In free space, antennas excite the *continuum* eigenvalues of the wave equation, which is a radiation field, where the outwardly propagating RF energy with E_z and H_ϕ in-phase is lost forever. On the other hand, waveguide probes excite *discrete* eigenvalues, which results in transmission line propagation. See Collin, R. E., Field Theory of Guided Waves, McGraw-Hill, 1960, pp. 453, 474-477. While such theoretical analyses have held out the hypothetical possibility of launching open surface guided waves over planar or spherical surfaces of lossy, homogeneous media, for more than a century no known structures in the engineering arts have existed for accomplishing this with any practical efficiency. Unfortunately, since it emerged in the early 1900's, the theoretical analysis set forth above has essentially remained a theory and there have been no known structures for practically accomplishing the launching of open surface guided waves over planar or spherical surfaces of lossy, homogeneous media.

[0047] According to the various embodiments of the present disclosure, various guided surface waveguide probes are described that are configured to excite electric fields that couple into a guided surface waveguide mode along the surface of a lossy conducting medium. Such guided electromagnetic fields are substantially mode-matched in magnitude and phase to a guided surface wave mode on the surface of the lossy conducting medium. Such a guided surface wave mode can also be termed a Zenneck waveguide mode. By virtue of the fact that the resultant fields excited by the guided surface waveguide probes described herein are substantially mode-matched to a guided surface waveguide mode on the surface of the lossy conducting medium, a guided electromagnetic field in the form of a guided surface wave is launched along the surface of the lossy conducting medium. According to one embodiment, the lossy conducting medium comprises a terrestrial medium such as the Earth.

[0048] Referring to FIG. 2, shown is a propagation interface that provides for an examination of the boundary value solutions to Maxwell's equations derived in 1907 by Jonathan Zenneck as set forth in his paper Zenneck, J., "On the Propagation of Plane Electromagnetic Waves Along a Flat Conducting Surface and their Relation to Wireless Telegraphy," Annalen der Physik, Serial 4, Vol. 23, September 20, 1907, pp. 846-866. FIG. 2 depicts cylindrical coordinates for radially propagating waves along the interface between a lossy conducting medium specified as Region 1 and an insulator specified as Region 2. Region 1 can comprise, for example, any lossy conducting medium. In one example, such a lossy conducting medium can comprise a terrestrial medium such as the Earth or other medium. Region 2 is a second medium that shares a boundary interface with Region 1 and

has different constitutive parameters relative to Region 1. Region 2 can comprise, for example, any insulator such as the atmosphere or other medium. The reflection coefficient for such a boundary interface goes to zero only for incidence at a *complex* Brewster angle. See Stratton, J.A., Electromagnetic Theory, McGraw-Hill, 1941, p. 516.

[0049] According to various embodiments, the present disclosure sets forth various guided surface waveguide probes that generate electromagnetic fields that are substantially mode-matched to a guided surface waveguide mode on the surface of the lossy conducting medium comprising Region 1. According to various embodiments, such electromagnetic fields substantially synthesize a wave front incident at a complex Brewster angle of the lossy conducting medium that can result in zero reflection.

[0050] To explain further, in Region 2, where an $e^{j\omega t}$ field variation is assumed and where $\rho \neq 0$ and $z \geq 0$ (with z being the vertical coordinate normal to the surface of Region 1, and ρ being the radial dimension in cylindrical coordinates), Zenneck's closed-form exact solution of Maxwell's equations satisfying the boundary conditions along the interface are expressed by the following electric field and magnetic field components:

$$H_{2\phi} = Ae^{-u_2 z}\ H_1^{(2)}(-j\gamma\rho), \tag{1}$$

$$E_{2\rho} = A\left(\frac{u_2}{j\omega\varepsilon_o}\right)e^{-u_2 z}\ H_1^{(2)}(-j\gamma\rho), \text{ and} \tag{2}$$

$$E_{2z} = A\left(\frac{-\gamma}{\omega\varepsilon_o}\right)e^{-u_2 z}\ H_0^{(2)}(-j\gamma\rho). \tag{3}$$

[0051] In Region 1, where the $e^{j\omega t}$ field variation is assumed and where $\rho \neq 0$ and $z \leq 0$, Zenneck's closed-form exact solution of Maxwell's equations satisfying the boundary conditions along the interface is expressed by the following electric field and magnetic field components:

$$H_{1\phi} = Ae^{u_1 z}\ H_1^{(2)}(-j\gamma\rho), \tag{4}$$

$$E_{1\rho} = A\left(\frac{-u_1}{\sigma_1 + j\omega\varepsilon_1}\right)e^{u_1 z}\ H_1^{(2)}(-j\gamma\rho), \text{ and} \tag{5}$$

$$E_{1z} = A\left(\frac{-j\gamma}{\sigma_1 + j\omega\varepsilon_1}\right)e^{u_1 z}\ H_0^{(2)}(-j\gamma\rho). \tag{6}$$

[0052] In these expressions, z is the vertical coordinate normal to the surface of Region 1 and ρ is the radial coordinate, $H_n^{(2)}(-j\gamma\rho)$ is a complex argument Hankel function of the second kind and order n, u_1 is the propagation constant in the positive vertical (z) direction in Region 1, u_2 is the propagation constant in the vertical (z) direction in Region 2, σ_1 is the conductivity of Region 1, ω is equal to $2\pi f$, where f is a frequency of excitation, ε_o is the permittivity of free space, ε_1 is the permittivity of Region 1, A is a source constant imposed by the source, and γ is a surface wave radial propagation constant.

[0053] The propagation constants in the $\pm z$ directions are determined by separating the wave equation above and below the interface between Regions 1 and 2, and imposing the boundary conditions. This exercise gives, in Region 2,

$$u_2 = \frac{-jk_o}{\sqrt{1+(\varepsilon_r - jx)}} \tag{7}$$

and gives, in Region 1,

$$u_1 = -u_2(\varepsilon_r - jx). \tag{8}$$

The radial propagation constant γ is given by

$$\gamma = j\sqrt{k_o^2 + u_2^2} = j\frac{k_o n}{\sqrt{1+n^2}}, \tag{9}$$

which is a complex expression where n is the complex index of refraction given by

$$n = \sqrt{\varepsilon_r - jx}. \tag{10}$$

In all of the above Equations,

$$x = \frac{\sigma_1}{\omega\varepsilon_o}, \text{ and} \tag{11}$$

$$k_o = \omega\sqrt{\mu_o\varepsilon_o} = \frac{\lambda_o}{2\pi}, \tag{12}$$

where ε_r comprises the relative permittivity of Region 1, σ_1 is the conductivity of Region 1, ε_o is the permittivity of free space, and μ_o comprises the permeability of free space. Thus, the generated surface wave propagates parallel to the interface and exponentially decays vertical to it. This is known as evanescence.

[0054] Thus, Equations (1)-(3) can be considered to be a cylindrically-symmetric, radially-propagating waveguide mode. See Barlow, H. M., and Brown, J., Radio Surface Waves, Oxford University Press, 1962, pp. 10-12, 29-33. The present disclosure details structures that excite this "open boundary" waveguide mode. Specifically, according to various embodiments, a guided surface waveguide probe is provided with a charge terminal of appropriate size that is fed with voltage and/or current and is positioned relative to the boundary interface between Region 2 and Region 1. This may be better understood with reference to FIG. 3, which shows an example of a guided surface waveguide probe 200a that includes a charge terminal T_1 elevated above a lossy conducting medium 203 (e.g., the Earth) along a vertical axis z that is normal to a plane presented by the lossy conducting medium 203. The lossy conducting medium 203 makes up Region 1, and a second medium 206 makes up Region 2 and shares a boundary interface with the lossy conducting medium 203.

[0055] According to one embodiment, the lossy conducting medium 203 can comprise a terrestrial medium such as the planet Earth. To this end, such a terrestrial medium comprises all structures or formations included thereon whether natural or man-made. For example, such a terrestrial medium can comprise natural elements such as rock, soil, sand, fresh water, sea water, trees, vegetation, and all other natural elements that make up our

planet. In addition, such a terrestrial medium can comprise man-made elements such as concrete, asphalt, building materials, and other man-made materials. In other embodiments, the lossy conducting medium 203 can comprise some medium other than the Earth, whether naturally occurring or man-made. In other embodiments, the lossy conducting medium 203 can comprise other media such as man-made surfaces and structures such as automobiles, aircraft, man-made materials (such as plywood, plastic sheeting, or other materials) or other media.

[0056] In the case where the lossy conducting medium 203 comprises a terrestrial medium or Earth, the second medium 206 can comprise the atmosphere above the ground. As such, the atmosphere can be termed an "atmospheric medium" that comprises air and other elements that make up the atmosphere of the Earth. In addition, it is possible that the second medium 206 can comprise other media relative to the lossy conducting medium 203.

[0057] The guided surface waveguide probe 200a includes a feed network 209 that couples an excitation source 212 to the charge terminal T_1 via, e.g., a vertical feed line conductor. According to various embodiments, a charge Q_1 is imposed on the charge terminal T_1 to synthesize an electric field based upon the voltage applied to terminal T_1 at any given instant. Depending on the angle of incidence (θ_i) of the electric field (E), it is possible to substantially mode-match the electric field to a guided surface waveguide mode on the surface of the lossy conducting medium 203 comprising Region 1.

[0058] By considering the Zenneck closed-form solutions of Equations (1)-(6), the Leontovich impedance boundary condition between Region 1 and Region 2 can be stated as

$$\hat{z} \times \vec{H}_2(\rho, \varphi, 0) = \vec{J}_S, \tag{13}$$

where $\hat{z}$ is a unit normal in the positive vertical ($+z$) direction and $\vec{H}_2$ is the magnetic field strength in Region 2 expressed by Equation (1) above. Equation (13) implies that the electric and magnetic fields specified in Equations (1)-(3) may result in a radial surface current density along the boundary interface, where the radial surface current density can be specified by

$$J_\rho(\rho') = -A\, H_1^{(2)}(-j\gamma\rho') \tag{14}$$

where A is a constant. Further, it should be noted that close-in to the guided surface waveguide probe 200 (for $\rho \ll \lambda$), Equation (14) above has the behavior

$$J_{close}(\rho') = \frac{-A(j2)}{\pi(-j\gamma\rho')} = -H_\phi = -\frac{I_o}{2\pi\rho'}. \tag{15}$$

The negative sign means that when source current (I_o) flows vertically upward as illustrated in FIG. 3, the "close-in" ground current flows radially *inward.* By field matching on H_ϕ "close-in," it can be determined that

$$A = -\frac{I_o\gamma}{4} = -\frac{\omega q_1 \gamma}{4} \tag{16}$$

where $q_1 = C_1V_1$, in Equations (1)-(6) and (14). Therefore, the radial surface current density of Equation (14) can be restated as

$$J_\rho(\rho') = \frac{I_o\gamma}{4} H_1^{(2)}(-j\gamma\rho'). \quad (17)$$

The fields expressed by Equations (1)-(6) and (17) have the nature of *a transmission line mode* bound to a lossy interface, *not radiation fields* that are associated with groundwave propagation. See Barlow, H. M. and Brown, J., Radio Surface Waves, Oxford University Press, 1962, pp. 1-5.

[0059] At this point, a review of the nature of the Hankel functions used in Equations (1)-(6) and (17) is provided for these solutions of the wave equation. One might observe that the Hankel functions of the first and second kind and order n are defined as complex combinations of the standard Bessel functions of the first and second kinds

$$H_n^{(1)}(x) = J_n(x) + jN_n(x), \text{ and} \quad (18)$$

$$H_n^{(2)}(x) = J_n(x) - jN_n(x), \quad (19)$$

These functions represent cylindrical waves propagating radially inward ($H_n^{(1)}$) and outward ($H_n^{(2)}$), respectively. The definition is analogous to the relationship $e^{\pm jx} = \cos x \pm j \sin x$. See, for example, Harrington, R.F., Time-Harmonic Fields, McGraw-Hill, 1961, pp. 460-463.

[0060] That $H_n^{(2)}(k_\rho\rho)$ is an outgoing wave can be recognized from its large argument asymptotic behavior that is obtained directly from the series definitions of $J_n(x)$ and $N_n(x)$. Far-out from the guided surface waveguide probe:

$$H_n^{(2)}(x) \underset{x\to\infty}{\longrightarrow} \sqrt{\frac{2j}{\pi x}}\, j^n e^{-jx} = \sqrt{\frac{2}{\pi x}}\, j^n e^{-j\left(x-\frac{\pi}{4}\right)}, \quad (20a)$$

which, when multiplied by $e^{j\omega t}$, is an outward propagating cylindrical wave of the form $e^{j(\omega t - k\rho)}$ with a $1/\sqrt{\rho}$ spatial variation. The first order ($n = 1$) solution can be determined from Equation (20a) to be

$$H_1^{(2)}(x) \underset{x\to\infty}{\longrightarrow} j\sqrt{\frac{2j}{\pi x}}\, e^{-jx} = \sqrt{\frac{2}{\pi x}}\, e^{-j\left(x-\frac{\pi}{2}-\frac{\pi}{4}\right)}. \quad (20b)$$

Close-in to the guided surface waveguide probe (for $\rho \ll \lambda$), the Hankel function of first order and the second kind behaves as

$$H_1^{(2)}(x) \underset{x\to 0}{\longrightarrow} \frac{2j}{\pi x}. \quad (21)$$

Note that these asymptotic expressions are complex quantities. When x is a real quantity, Equations (20b) and (21) differ in phase by $\sqrt{j}$, which corresponds to an extra phase advance or "phase boost" of 45° or, equivalently, λ/8. The close-in and far-out asymptotes of the first order Hankel function of the second kind have a Hankel "crossover" or transition point where they are of equal magnitude at a distance of $\rho = R_x$.

[0061] Thus, beyond the Hankel crossover point the "far out" representation predominates over the "close-in" representation of the Hankel function. The distance to the Hankel crossover point (or Hankel crossover distance) can be found by equating Equations (20b) and (21) for $-j\gamma\rho$, and solving for R_x. With $x = \sigma/\omega\varepsilon_o$, it can be seen that the far-out and close-in Hankel function asymptotes are frequency dependent, with the Hankel crossover point moving out as the frequency is lowered. It should also be noted that the Hankel function asymptotes may also vary as the conductivity (σ) of the lossy conducting medium changes. For example, the conductivity of the soil can vary with changes in weather conditions.

[0062] Referring to FIG. 4, shown is an example of a plot of the magnitudes of the first order Hankel functions of Equations (20b) and (21) for a Region 1 conductivity of σ = 0.010 mhos/m and relative permittivity ε_r = 15, at an operating frequency of 1850 kHz. Curve 115 is the magnitude of the far-out asymptote of Equation (20b) and curve 118 is the magnitude of the close-in asymptote of Equation (21), with the Hankel crossover point 121 occurring at a distance of R_x = 54 feet. While the magnitudes are equal, a phase offset exists between the two asymptotes at the Hankel crossover point 121. It can also be seen that the Hankel crossover distance is much less than a wavelength of the operation frequency.

[0063] Considering the electric field components given by Equations (2) and (3) of the Zenneck closed-form solution in Region 2, it can be seen that the ratio of E_z and E_ρ asymptotically passes to

$$\frac{E_z}{E_\rho} = \left(\frac{-j\gamma}{u_2}\right)\frac{H_0^{(2)}(-j\gamma\rho)}{H_1^{(2)}(-j\gamma\rho)} \underset{\rho\to\infty}{\longrightarrow} \sqrt{\varepsilon_r - j\frac{\sigma}{\omega\varepsilon_o}} = n = \tan\theta_i, \tag{22}$$

where n is the complex index of refraction of Equation (10) and θ_i is the angle of incidence of the electric field. In addition, the vertical component of the mode-matched electric field of Equation (3) asymptotically passes to

$$E_{2z} \underset{\rho\to\infty}{\longrightarrow} \left(\frac{q_{free}}{\varepsilon_o}\right)\sqrt{\frac{\gamma^3}{8\pi}}\, e^{-u_2 z}\, \frac{e^{-j(\gamma\rho-\pi/4)}}{\sqrt{\rho}}, \tag{23}$$

which is linearly proportional to free charge on the isolated component of the elevated charge terminal's capacitance at the terminal voltage, $q_{free} = C_{free} \times V_T$.

[0064] For example, the height H_1 of the elevated charge terminal T_1 in FIG. 3 affects the amount of free charge on the charge terminal T_1. When the charge terminal T_1 is near the ground plane of Region 1, most of the charge Q_1 on the terminal is "bound." As the charge terminal T_1 is elevated, the bound charge is lessened until the charge terminal T_1 reaches a height at which substantially all of the isolated charge is free.

[0065] The advantage of an increased capacitive elevation for the charge terminal T_1 is that the charge on the elevated charge terminal T_1 is further removed from the ground plane,

resulting in an increased amount of free charge q_{free} to couple energy into the guided surface waveguide mode. As the charge terminal T_1 is moved away from the ground plane, the charge distribution becomes more uniformly distributed about the surface of the terminal. The amount of free charge is related to the self-capacitance of the charge terminal T_1.

[0066] For example, the capacitance of a spherical terminal can be expressed as a function of physical height above the ground plane. The capacitance of a sphere at a physical height of h above a perfect ground is given by

$$C_{\text{elevated sphere}} = 4\pi\varepsilon_o a(1 + \mathrm{M} + \mathrm{M}^2 + \mathrm{M}^3 + 2\mathrm{M}^4 + 3\mathrm{M}^5 + \cdots), \quad (24)$$

where the diameter of the sphere is $2a$, and where $\mathrm{M} = a/2h$ with h being the height of the spherical terminal. As can be seen, an increase in the terminal height h reduces the capacitance C of the charge terminal. It can be shown that for elevations of the charge terminal T_1 that are at a height of about four times the diameter ($4D = 8a$) or greater, the charge distribution is approximately uniform about the spherical terminal, which can improve the coupling into the guided surface waveguide mode.

[0067] In the case of a sufficiently isolated terminal, the self-capacitance of a conductive sphere can be approximated by $C = 4\pi\varepsilon_o a$, where a is the radius of the sphere in meters, and the self-capacitance of a disk can be approximated by $C = 8\varepsilon_o a$, where a is the radius of the disk in meters. The charge terminal T_1 can include any shape such as a sphere, a disk, a cylinder, a cone, a torus, a hood, one or more rings, or any other randomized shape or combination of shapes. An equivalent spherical diameter can be determined and used for positioning of the charge terminal T_1.

[0068] This may be further understood with reference to the example of FIG. 3, where the charge terminal T_1 is elevated at a physical height of $h_p = \mathrm{H}_1$ above the lossy conducting medium 203. To reduce the effects of the "bound" charge, the charge terminal T_1 can be positioned at a physical height that is at least four times the spherical diameter (or equivalent spherical diameter) of the charge terminal T_1 to reduce the bounded charge effects.

[0069] Referring next to FIG. 5A, shown is a ray optics interpretation of the electric field produced by the elevated charge Q_1 on charge terminal T_1 of FIG. 3. As in optics, minimizing the reflection of the incident electric field can improve and/or maximize the energy coupled into the guided surface waveguide mode of the lossy conducting medium 203. For an electric field ($E_{\|}$) that is polarized parallel to the plane of incidence (not the boundary interface), the amount of reflection of the incident electric field may be determined using the Fresnel reflection coefficient, which can be expressed as

$$\Gamma_{\|}(\theta_i) = \frac{E_{\|,R}}{E_{\|,i}} = \frac{\sqrt{(\varepsilon_r - jx) - \sin^2\theta_i} - (\varepsilon_r - jx)\cos\theta_i}{\sqrt{(\varepsilon_r - jx) - \sin^2\theta_i} + (\varepsilon_r - jx)\cos\theta_i}, \quad (25)$$

where θ_i is the conventional angle of incidence measured with respect to the surface normal.

[0070] In the example of FIG. 5A, the ray optic interpretation shows the incident field polarized parallel to the plane of incidence having an angle of incidence of θ_i, which is measured with respect to the surface normal ($\hat{z}$). There will be no reflection of the incident electric field when $\Gamma_{\parallel}(\theta_i) = 0$ and thus the incident electric field will be completely coupled into a guided surface waveguide mode along the surface of the lossy conducting medium 203. It can be seen that the numerator of Equation (25) goes to zero when the angle of incidence is

$$\theta_i = \arctan\left(\sqrt{\varepsilon_r - jx}\right) = \theta_{i,B}, \tag{26}$$

where $x = \sigma/\omega\varepsilon_o$. This complex angle of incidence ($\theta_{i,B}$) is referred to as the Brewster angle. Referring back to Equation (22), it can be seen that the same complex Brewster angle ($\theta_{i,B}$) relationship is present in both Equations (22) and (26).

[0071] As illustrated in FIG. 5A, the electric field vector $\boldsymbol{E}$ can be depicted as an incoming non-uniform plane wave, polarized parallel to the plane of incidence. The electric field vector $\boldsymbol{E}$ can be created from independent horizontal and vertical components as

$$\vec{E}(\theta_i) = E_\rho\,\hat{\rho} + E_z\,\hat{z}. \tag{27}$$

Geometrically, the illustration in FIG. 5A suggests that the electric field vector $\boldsymbol{E}$ can be given by

$$E_\rho(\rho, z) = \boldsymbol{E}(\rho, z)\cos\theta_i, \text{ and} \tag{28a}$$

$$E_z(\rho, z) = \boldsymbol{E}(\rho, z)\cos\left(\frac{\pi}{2} - \theta_i\right) = \boldsymbol{E}(\rho, z)\sin\theta_i, \tag{28b}$$

which means that the field ratio is

$$\frac{E_\rho}{E_z} = \frac{1}{\tan\theta_i} = \tan\psi_i. \tag{29}$$

[0072] A generalized parameter W, called "wave tilt," is noted herein as the ratio of the horizontal electric field component to the vertical electric field component given by

$$W = \frac{E_\rho}{E_z} = |W|e^{j\Psi}, \text{ or} \tag{30a}$$

$$\frac{1}{W} = \frac{E_z}{E_\rho} = \tan\theta_i = \frac{1}{|W|}e^{-j\Psi}, \tag{30b}$$

which is complex and has both magnitude and phase. For an electromagnetic wave in Region 2, the wave tilt angle (Ψ) is equal to the angle between the normal of the wave-front at the boundary interface with Region 1 and the tangent to the boundary interface. This may be easier to see in FIG. 5B, which illustrates equi-phase surfaces of an electromagnetic wave and their normals for a radial cylindrical guided surface wave. At the boundary interface (z = 0) with a perfect conductor, the wave-front normal is parallel to the tangent of the boundary interface, resulting in W = 0. However, in the case of a lossy dielectric, a wave

tilt W exists because the wave-front normal is not parallel with the tangent of the boundary interface at z = 0.

[0073] Applying Equation (30b) to a guided surface wave gives

$$\tan\theta_{i,B} = \frac{E_z}{E_\rho} = \frac{u_2}{\gamma} = \sqrt{\varepsilon_r - jx} = n = \frac{1}{W} = \frac{1}{|W|}e^{-j\Psi}. \tag{31}$$

With the angle of incidence equal to the complex Brewster angle ($\theta_{i,B}$), the Fresnel reflection coefficient of Equation (25) vanishes, as shown by

$$\Gamma_{\parallel}(\theta_{i,B}) = \frac{\sqrt{(\varepsilon_r - jx) - \sin^2\theta_i} - (\varepsilon_r - jx)\cos\theta_i}{\sqrt{(\varepsilon_r - jx) - \sin^2\theta_i} + (\varepsilon_r - jx)\cos\theta_i}\Bigg|_{\theta_i = \theta_{i,B}} = 0. \tag{32}$$

By adjusting the complex field ratio of Equation (22), an incident field can be synthesized to be incident at a complex angle at which the reflection is reduced or eliminated. Establishing this ratio as $n = \sqrt{\varepsilon_r - jx}$ results in the synthesized electric field being incident at the complex Brewster angle, making the reflections vanish.

[0074] The concept of an electrical effective height can provide further insight into synthesizing an electric field with a complex angle of incidence with a guided surface waveguide probe 200. The electrical effective height (h_{eff}) has been defined as

$$h_{eff} = \frac{1}{I_0}\int_0^{h_p} I(z)dz \tag{33}$$

for a monopole with a physical height (or length) of h_p. Since the expression depends upon the magnitude and phase of the source distribution along the structure, the effective height (or length) is complex in general. The integration of the distributed current $I(z)$ of the structure is performed over the physical height of the structure (h_p), and normalized to the ground current (I_0) flowing upward through the base (or input) of the structure. The distributed current along the structure can be expressed by

$$I(z) = I_C\cos(\beta_0 z), \tag{34}$$

where β_0 is the propagation factor for current propagating on the structure. In the example of FIG. 3, I_C is the current that is distributed along the vertical structure of the guided surface waveguide probe 200a.

[0075] For example, consider a feed network 209 that includes a low loss coil (*e.g.*, a helical coil) at the bottom of the structure and a vertical feed line conductor connected between the coil and the charge terminal T_1. The phase delay due to the coil (or helical delay line) is $\theta_c = \beta_p l_C$, with a physical length of l_C and a propagation factor of

$$\beta_p = \frac{2\pi}{\lambda_p} = \frac{2\pi}{V_f\lambda_0}, \tag{35}$$

where V_f is the velocity factor on the structure, λ_0 is the wavelength at the supplied frequency, and λ_p is the propagation wavelength resulting from the velocity factor V_f. The phase delay is measured relative to the ground (stake) current I_0.

[0076] In addition, the spatial phase delay along the length l_w of the vertical feed line conductor can be given by $\theta_y = \beta_w l_w$ where β_w is the propagation phase constant for the vertical feed line conductor. In some implementations, the spatial phase delay may be approximated by $\theta_y = \beta_w h_p$, since the difference between the physical height h_p of the guided surface waveguide probe 200a and the vertical feed line conductor length l_w is much less than a wavelength at the supplied frequency (λ_0). As a result, the total phase delay through the coil and vertical feed line conductor is $\Phi = \theta_c + \theta_y$, and the current fed to the top of the coil from the bottom of the physical structure is

$$I_C(\theta_c + \theta_y) = I_0 e^{j\Phi}, \tag{36}$$

with the total phase delay Φ measured relative to the ground (stake) current I_0. Consequently, the electrical effective height of a guided surface waveguide probe 200 can be approximated by

$$h_{eff} = \frac{1}{I_0}\int_0^{h_p} I_0 e^{j\Phi}\cos(\beta_0 z)\, dz \cong h_p e^{j\Phi}, \tag{37}$$

for the case where the physical height $h_p \ll \lambda_0$. The complex effective height of a monopole, $h_{eff} = h_p$ at an angle (or phase shift) of Φ, may be adjusted to cause the source fields to match a guided surface waveguide mode and cause a guided surface wave to be launched on the lossy conducting medium 203.

[0077] In the example of FIG. 5A, ray optics are used to illustrate the complex angle trigonometry of the incident electric field (E) having a complex Brewster angle of incidence ($\theta_{i,B}$) at the Hankel crossover distance (R_x) 121. Recall from Equation (26) that, for a lossy conducting medium, the Brewster angle is complex and specified by

$$\tan\theta_{i,B} = \sqrt{\varepsilon_r - j\frac{\sigma}{\omega\varepsilon_o}} = n\ . \tag{38}$$

Electrically, the geometric parameters are related by the electrical effective height (h_{eff}) of the charge terminal T_1 by

$$R_x \tan\psi_{i,B} = R_x \times W = h_{eff} = h_p e^{j\Phi}, \tag{39}$$

where $\psi_{i,B} = (\pi/2) - \theta_{i,B}$ is the Brewster angle measured from the surface of the lossy conducting medium. To couple into the guided surface waveguide mode, the wave tilt of the electric field at the Hankel crossover distance can be expressed as the ratio of the electrical effective height and the Hankel crossover distance

$$\frac{h_{eff}}{R_x} = \tan\psi_{i,B} = W_{Rx}. \tag{40}$$

Since both the physical height (h_p) and the Hankel crossover distance (R_x) are real quantities, the angle (Ψ) of the desired guided surface wave tilt at the Hankel crossover distance (R_x) is equal to the phase (Φ) of the complex effective height (h_{eff}). This implies that by varying the phase at the supply point of the coil, and thus the phase shift in Equation

(37), the phase, Φ, of the complex effective height can be manipulated to match the angle of the wave tilt, Ψ, of the guided surface waveguide mode at the Hankel crossover point 121: Φ = Ψ.

[0078] In FIG. 5A, a right triangle is depicted having an adjacent side of length R_x along the lossy conducting medium surface and a complex Brewster angle $\psi_{i,B}$ measured between a ray 124 extending between the Hankel crossover point 121 at R_x and the center of the charge terminal T_1, and the lossy conducting medium surface 127 between the Hankel crossover point 121 and the charge terminal T_1. With the charge terminal T_1 positioned at physical height h_p and excited with a charge having the appropriate phase delay Φ, the resulting electric field is incident with the lossy conducting medium boundary interface at the Hankel crossover distance R_x, and at the Brewster angle. Under these conditions, the guided surface waveguide mode can be excited without reflection or substantially negligible reflection.

[0079] If the physical height of the charge terminal T_1 is decreased without changing the phase shift Φ of the effective height (h_{eff}), the resulting electric field intersects the lossy conducting medium 203 at the Brewster angle at a reduced distance from the guided surface waveguide probe 200. FIG. 6 graphically illustrates the effect of decreasing the physical height of the charge terminal T_1 on the distance where the electric field is incident at the Brewster angle. As the height is decreased from h_3 through h_2 to h_1, the point where the electric field intersects with the lossy conducting medium (*e.g.*, the Earth) at the Brewster angle moves closer to the charge terminal position. However, as Equation (39) indicates, the height H_1 (FIG. 3) of the charge terminal T_1 should be at or higher than the physical height (h_p) in order to excite the far-out component of the Hankel function. With the charge terminal T_1 positioned at or above the effective height (h_{eff}), the lossy conducting medium 203 can be illuminated at the Brewster angle of incidence ($\psi_{i,B} = (\pi/2) - \theta_{i,B}$) at or beyond the Hankel crossover distance (R_x) 121 as illustrated in FIG. 5A. To reduce or minimize the bound charge on the charge terminal T_1, the height should be at least four times the spherical diameter (or equivalent spherical diameter) of the charge terminal T_1 as mentioned above.

[0080] A guided surface waveguide probe 200 can be configured to establish an electric field having a wave tilt that corresponds to a wave illuminating the surface of the lossy conducting medium 203 at a complex Brewster angle, thereby exciting radial surface currents by substantially mode-matching to a guided surface wave mode at (or beyond) the Hankel crossover point 121 at R_x.

[0081] Referring to FIG. 7, shown is a graphical representation of an example of a guided surface waveguide probe 200b that includes a charge terminal T_1. An AC source 212

acts as the excitation source for the charge terminal T_1, which is coupled to the guided surface waveguide probe 200b through a feed network 209 (FIG. 3) comprising a coil 215 such as, *e.g.*, a helical coil. In other implementations, the AC source 212 can be inductively coupled to the coil 215 through a primary coil. In some embodiments, an impedance matching network may be included to improve and/or maximize coupling of the AC source 212 to the coil 215.

[0082] As shown in FIG. 7, the guided surface waveguide probe 200b can include the upper charge terminal T_1 (*e.g.*, a sphere at height h_p) that is positioned along a vertical axis z that is substantially normal to the plane presented by the lossy conducting medium 203. A second medium 206 is located above the lossy conducting medium 203. The charge terminal T_1 has a self-capacitance C_T. During operation, charge Q_1 is imposed on the terminal T_1 depending on the voltage applied to the terminal T_1 at any given instant.

[0083] In the example of FIG. 7, the coil 215 is coupled to a ground stake 218 at a first end and to the charge terminal T_1 via a vertical feed line conductor 221. In some implementations, the coil connection to the charge terminal T_1 can be adjusted using a tap 224 of the coil 215 as shown in FIG. 7. The coil 215 can be energized at an operating frequency by the AC source 212 through a tap 227 at a lower portion of the coil 215. In other implementations, the AC source 212 can be inductively coupled to the coil 215 through a primary coil.

[0084] The construction and adjustment of the guided surface waveguide probe 200 is based upon various operating conditions, such as the transmission frequency, conditions of the lossy conducting medium (*e.g.*, soil conductivity σ and relative permittivity ε_r), and size of the charge terminal T_1. The index of refraction can be calculated from Equations (10) and (11) as

$$n = \sqrt{\varepsilon_r - jx}, \tag{41}$$

where $x = \sigma/\omega\varepsilon_o$ with $\omega = 2\pi f$. The conductivity σ and relative permittivity ε_r can be determined through test measurements of the lossy conducting medium 203. The complex Brewster angle ($\theta_{i,B}$) measured from the surface normal can also be determined from Equation (26) as

$$\theta_{i,B} = \arctan\left(\sqrt{\varepsilon_r - jx}\right), \tag{42}$$

or measured from the surface as shown in FIG. 5A as

$$\psi_{i,B} = \frac{\pi}{2} - \theta_{i,B}. \tag{43}$$

The wave tilt at the Hankel crossover distance (W_{Rx}) can also be found using Equation (40).

[0085] The Hankel crossover distance can also be found by equating the magnitudes of Equations (20b) and (21) for $-j\gamma\rho$, and solving for R_x as illustrated by FIG. 4. The electrical

effective height can then be determined from Equation (39) using the Hankel crossover distance and the complex Brewster angle as

$$h_{eff} = h_p e^{j\Phi} = R_x \tan \psi_{i,B}. \quad (44)$$

As can be seen from Equation (44), the complex effective height (h_{eff}) includes a magnitude that is associated with the physical height (h_p) of the charge terminal T_1 and a phase delay (Φ) that is to be associated with the angle (Ψ) of the wave tilt at the Hankel crossover distance (R_x). With these variables and the selected charge terminal T_1 configuration, it is possible to determine the configuration of a guided surface waveguide probe 200.

[0086] With the charge terminal T_1 positioned at or above the physical height (h_p), the feed network 209 (FIG. 3) and/or the vertical feed line connecting the feed network to the charge terminal T_1 can be adjusted to match the phase (Φ) of the charge Q_1 on the charge terminal T_1 to the angle (Ψ) of the wave tilt (W). The size of the charge terminal T_1 can be chosen to provide a sufficiently large surface for the charge Q_1 imposed on the terminals. In general, it is desirable to make the charge terminal T_1 as large as practical. The size of the charge terminal T_1 should be large enough to avoid ionization of the surrounding air, which can result in electrical discharge or sparking around the charge terminal.

[0087] The phase delay θ_c of a helically-wound coil can be determined from Maxwell's equations as has been discussed by Corum, K.L. and J.F. Corum, "RF Coils, Helical Resonators and Voltage Magnification by Coherent Spatial Modes," Microwave Review, Vol. 7, No. 2, September 2001, pp. 36-45., which is incorporated herein by reference in its entirety. For a helical coil with $H/D > 1$, the ratio of the velocity of propagation (v) of a wave along the coil's longitudinal axis to the speed of light (c), or the "velocity factor," is given by

$$V_f = \frac{v}{c} = \frac{1}{\sqrt{1+20\left(\frac{D}{s}\right)^{2.5}\left(\frac{D}{\lambda_O}\right)^{0.5}}}, \quad (45)$$

where H is the axial length of the solenoidal helix, D is the coil diameter, N is the number of turns of the coil, $s = H/N$ is the turn-to-turn spacing (or helix pitch) of the coil, and λ_o is the free-space wavelength. Based upon this relationship, the electrical length, or phase delay, of the helical coil is given by

$$\theta_c = \beta_p H = \frac{2\pi}{\lambda_p} H = \frac{2\pi}{V_f \lambda_0} H. \quad (46)$$

The principle is the same if the helix is wound spirally or is short and fat, but V_f and θ_c are easier to obtain by experimental measurement. The expression for the characteristic (wave) impedance of a helical transmission line has also been derived as

$$Z_c = \frac{60}{V_f}\left[\ell n\left(\frac{V_f \lambda_0}{D}\right) - 1.027\right]. \quad (47)$$

[0088] The spatial phase delay θ_y of the structure can be determined using the traveling wave phase delay of the vertical feed line conductor 221 (FIG. 7). The capacitance of a cylindrical vertical conductor above a prefect ground plane can be expressed as

$$C_A = \frac{2\pi\varepsilon_o h_w}{\ell n\left(\frac{h}{a}\right)-1} \text{ Farads,} \tag{48}$$

where h_w is the vertical length (or height) of the conductor and a is the radius (in mks units). As with the helical coil, the traveling wave phase delay of the vertical feed line conductor can be given by

$$\theta_y = \beta_w h_w = \frac{2\pi}{\lambda_w} h_w = \frac{2\pi}{V_w \lambda_0} h_w, \tag{49}$$

where β_w is the propagation phase constant for the vertical feed line conductor, h_w is the vertical length (or height) of the vertical feed line conductor, V_w is the velocity factor on the wire, λ_0 is the wavelength at the supplied frequency, and λ_w is the propagation wavelength resulting from the velocity factor V_w. For a uniform cylindrical conductor, the velocity factor is a constant with $V_w \approx 0.94$, or in a range from about 0.93 to about 0.98. If the mast is considered to be a uniform transmission line, its average characteristic impedance can be approximated by

$$Z_w = \frac{60}{V_w}\left[\ell n\left(\frac{h_w}{a}\right) - 1\right], \tag{50}$$

where $V_w \approx 0.94$ for a uniform cylindrical conductor and a is the radius of the conductor. An alternative expression that has been employed in amateur radio literature for the characteristic impedance of a single-wire feed line can be given by

$$Z_w = 138\, log\left(\frac{1.123\, V_w \lambda_0}{2\pi a}\right). \tag{51}$$

Equation (51) implies that Z_w for a single-wire feeder varies with frequency. The phase delay can be determined based upon the capacitance and characteristic impedance.

[0089] With a charge terminal T_1 positioned over the lossy conducting medium 203 as shown in FIG. 3, the feed network 209 can be adjusted to excite the charge terminal T_1 with the phase shift (Φ) of the complex effective height (h_{eff}) equal to the angle (Ψ) of the wave tilt at the Hankel crossover distance, or $\Phi = \Psi$. When this condition is met, the electric field produced by the charge oscillating Q_1 on the charge terminal T_1 is coupled into a guided surface waveguide mode traveling along the surface of a lossy conducting medium 203. For example, if the Brewster angle ($\theta_{i,B}$), the phase delay (θ_y) associated with the vertical feed line conductor 221 (FIG. 7), and the configuration of the coil 215 (FIG. 7) are known, then the position of the tap 224 (FIG. 7) can be determined and adjusted to impose an oscillating charge Q_1 on the charge terminal T_1 with phase $\Phi = \Psi$. The position of the tap 224 may be adjusted to maximize coupling the traveling surface waves into the guided surface waveguide mode. Excess coil length beyond the position of the tap 224 can be removed to

reduce the capacitive effects. The vertical wire height and/or the geometrical parameters of the helical coil may also be varied.

[0090] The coupling to the guided surface waveguide mode on the surface of the lossy conducting medium 203 can be improved and/or optimized by tuning the guided surface waveguide probe 200 for standing wave resonance with respect to a complex image plane associated with the charge Q_1 on the charge terminal T_1. By doing this, the performance of the guided surface waveguide probe 200 can be adjusted for increased and/or maximum voltage (and thus charge Q_1) on the charge terminal T_1. Referring back to FIG. 3, the effect of the lossy conducting medium 203 in Region 1 can be examined using image theory analysis.

[0091] Physically, an elevated charge Q_1 placed over a perfectly conducting plane attracts the free charge on the perfectly conducting plane, which then "piles up" in the region under the elevated charge Q_1. The resulting distribution of "bound" electricity on the perfectly conducting plane is similar to a bell-shaped curve. The superposition of the potential of the elevated charge Q_1, plus the potential of the induced "piled up" charge beneath it, forces a zero equipotential surface for the perfectly conducting plane. The boundary value problem solution that describes the fields in the region above the perfectly conducting plane may be obtained using the classical notion of image charges, where the field from the elevated charge is superimposed with the field from a corresponding "image" charge below the perfectly conducting plane.

[0092] This analysis may also be used with respect to a lossy conducting medium 203 by assuming the presence of an effective image charge Q_1' beneath the guided surface waveguide probe 200. The effective image charge Q_1' coincides with the charge Q_1 on the charge terminal T_1 about a conducting image ground plane 130, as illustrated in FIG. 3. However, the image charge Q_1' is not merely located at some real depth and 180º out of phase with the primary source charge Q_1 on the charge terminal T_1, as they would be in the case of a perfect conductor. Rather, the lossy conducting medium 203 (e.g., a terrestrial medium) presents a *phase shifted* image. That is to say, the image charge Q_1' is at a complex depth below the surface (or physical boundary) of the lossy conducting medium 203. For a discussion of complex image depth, reference is made to Wait, J. R., "Complex Image Theory—Revisited," IEEE Antennas and Propagation Magazine, Vol. 33, No. 4, August 1991, pp. 27-29, which is incorporated herein by reference in its entirety.

[0093] Instead of the image charge Q_1' being at a depth that is equal to the physical height (H_1) of the charge Q_1, the conducting image ground plane 130 (representing a perfect conductor) is located at a complex depth of $z = -\mathrm{d}/2$ and the image charge Q_1' appears at

a complex depth (*i.e.*, the "depth" has both magnitude and phase), given by $-\mathrm{D}_1 = -(\mathrm{d}/2 + \mathrm{d}/2 + \mathrm{H}_1) \neq \mathrm{H}_1$. For vertically polarized sources over the Earth,

$$\mathrm{d} = \frac{2\sqrt{\gamma_e^2 + k_0^2}}{\gamma_e^2} \approx \frac{2}{\gamma_e} = d_r + jd_i = |d|\angle\zeta \,, \tag{52}$$

where

$$\gamma_e^2 = j\omega\mu_1\sigma_1 - \omega^2\mu_1\varepsilon_1, \text{ and} \tag{53}$$

$$k_o = \omega\sqrt{\mu_o\varepsilon_o}, \tag{54}$$

as indicated in Equation (12). The complex spacing of the image charge, in turn, implies that the external field will experience *extra phase shifts* not encountered when the interface is either a dielectric or a perfect conductor. In the lossy conducting medium, the wave front normal is parallel to the tangent of the conducting image ground plane 130 at $z = -\mathrm{d}/2$, and not at the boundary interface between Regions 1 and 2.

[0094] Consider the case illustrated in FIG. 8A where the lossy conducting medium 203 is a finitely conducting Earth 133 with a physical boundary 136. The *finitely* conducting Earth 133 may be replaced by a *perfectly* conducting image ground plane 139 as shown in FIG.8B, which is located at a complex depth z_1 below the physical boundary 136. This equivalent representation exhibits the *same* impedance when looking down into the interface at the physical boundary 136. The equivalent representation of FIG. 8B can be modeled as an equivalent transmission line, as shown in FIG. 8C. The cross-section of the equivalent structure is represented as a (z-directed) end-loaded transmission line, with the impedance of the perfectly conducting image plane being a short circuit ($z_s = 0$). The depth z_1 can be determined by equating the TEM wave impedance looking down at the Earth to an image ground plane impedance z_{in} seen looking into the transmission line of FIG. 8C.

[0095] In the case of FIG. 8A, the propagation constant and wave intrinsic impedance in the upper region (air) 142 are

$$\gamma_o = j\omega\sqrt{\mu_o\varepsilon_o} = 0 + j\beta_o \text{ , and} \tag{55}$$

$$z_o = \frac{j\omega\mu_o}{\gamma_o} = \sqrt{\frac{\mu_o}{\varepsilon_o}}. \tag{56}$$

In the lossy Earth 133, the propagation constant and wave intrinsic impedance are

$$\gamma_e = \sqrt{j\omega\mu_1(\sigma_1 + j\omega\varepsilon_1)} \text{ , and} \tag{57}$$

$$Z_e = \frac{j\omega\mu_1}{\gamma_e}. \tag{58}$$

For normal incidence, the equivalent representation of FIG. 8B is equivalent to a TEM transmission line whose characteristic impedance is that of air (z_o), with propagation constant of γ_o, and whose length is z_1. As such, the image ground plane impedance Z_{in} seen at the interface for the shorted transmission line of FIG. 8C is given by

$$Z_{in} = Z_o \tanh(\gamma_o z_1). \tag{59}$$

Equating the image ground plane impedance Z_{in} associated with the equivalent model of FIG. 8C to the normal incidence wave impedance of FIG. 8A and solving for z_1 gives the distance to a short circuit (the *perfectly conducting* image ground plane 139) as

$$z_1 = \frac{1}{\gamma_o}\tanh^{-1}\left(\frac{Z_e}{Z_o}\right) = \frac{1}{\gamma_o}\tanh^{-1}\left(\frac{\gamma_o}{\gamma_e}\right) \approx \frac{1}{\gamma_e}, \quad (60)$$

where only the first term of the series expansion for the inverse hyperbolic tangent is considered for this approximation. Note that in the air region 142, the propagation constant is $\gamma_o = j\beta_o$, so $Z_{in} = jZ_o \tan \beta_o z_1$ (which is a purely imaginary quantity for a real z_1), but z_e is a complex value if $\sigma \neq 0$. Therefore, $Z_{in} = Z_e$ only when z_1 is a *complex distance*.

[0096] Since the equivalent representation of FIG. 8B includes a *perfectly conducting* image ground plane 139, the image depth for a charge or current *lying at the surface of the Earth* (physical boundary 136) is equal to distance z_1 on the other side of the image ground plane 139, or $\mathrm{d} = 2 \times z_1$ beneath the Earth's surface (which is located at $z = 0$). Thus, the distance to the perfectly conducting image ground plane 139 can be approximated by

$$\mathrm{d} = 2z_1 \approx \frac{2}{\gamma_e}. \quad (61)$$

Additionally, the "image charge" will be *"equal and opposite"* to the real charge, so the potential of the perfectly conducting image ground plane 139 at depth $z_1 = -\mathrm{d}/2$ will be zero.

[0097] If a charge Q_1 is elevated a distance H_1 above the surface of the Earth as illustrated in FIG. 3, then the image charge Q_1' resides at a complex distance of $\mathrm{D}_1 = \mathrm{d} + \mathrm{H}_1$ below the surface, or a complex distance of $\mathrm{d}/2 + \mathrm{H}_1$ below the image ground plane 130. The guided surface waveguide probe 200b of FIG. 7 can be modeled as an equivalent single-wire transmission line image plane model that can be based upon the perfectly conducting image ground plane 139 of FIG. 8B. FIG. 9A shows an example of the equivalent single-wire transmission line image plane model, and FIG. 9B illustrates an example of the equivalent classic transmission line model, including the shorted transmission line of FIG. 8C.

[0098] In the equivalent image plane models of FIGS. 9A and 9B, $\Phi = \theta_y + \theta_c$ is the traveling wave phase delay of the guided surface waveguide probe 200 referenced to Earth 133 (or the lossy conducting medium 203), $\theta_c = \beta_p H$ is the electrical length of the coil 215 (FIG. 7), of physical length H, expressed in degrees, $\theta_y = \beta_w h_w$ is the electrical length of the vertical feed line conductor 221 (FIG. 7), of physical length h_w, expressed in degrees, and $\theta_d = \beta_o \mathrm{d}/2$ is the phase shift between the image ground plane 139 and the physical boundary 136 of the Earth 133 (or lossy conducting medium 203). In the example of FIGS. 9A and 9B, Z_w is the characteristic impedance of the elevated vertical feed line conductor

221 in ohms, Z_c is the characteristic impedance of the coil 215 in ohms, and Z_O is the characteristic impedance of free space.

[0099] At the base of the guided surface waveguide probe 200, the impedance seen "looking up" into the structure is $Z_{\uparrow} = Z_{base}$. With a load impedance of:

$$Z_L = \frac{1}{j\omega C_T}, \tag{62}$$

where C_T is the self-capacitance of the charge terminal T_1, the impedance seen "looking up" into the vertical feed line conductor 221 (FIG. 7) is given by:

$$Z_2 = Z_W \frac{Z_L + Z_w \tanh(j\beta_w h_w)}{Z_w + Z_L \tanh(j\beta_w h_w)} = Z_W \frac{Z_L + Z_w \tanh(j\theta_y)}{Z_w + Z_L \tanh(j\theta_y)}, \tag{63}$$

and the impedance seen "looking up" into the coil 215 (FIG. 7) is given by:

$$Z_{base} = Z_c \frac{Z_2 + Z_c \tanh(j\beta_p H)}{Z_c + Z_2 \tanh(j\beta_p H)} = Z_c \frac{Z_2 + Z_c \tanh(j\theta_c)}{Z_c + Z_2 \tanh(j\theta_c)}. \tag{64}$$

At the base of the guided surface waveguide probe 200, the impedance seen "looking down" into the lossy conducting medium 203 is $Z_{\downarrow} = Z_{in}$, which is given by:

$$Z_{in} = Z_o \frac{Z_s + Z_o \tanh[j\beta_o(\mathrm{d}/2)]}{Z_o + Z_s \tanh[j\beta_o(\mathrm{d}/2)]} = Z_o \tanh(j\theta_d), \tag{65}$$

where $Z_s = 0$.

[0100] Neglecting losses, the equivalent image plane model can be tuned to resonance when $Z_{\downarrow} + Z_{\uparrow} = 0$ at the physical boundary 136. Or, in the low loss case, $X_{\downarrow} + X_{\uparrow} = 0$ at the physical boundary 136, where X is the corresponding reactive component. Thus, the impedance at the physical boundary 136 "looking up" into the guided surface waveguide probe 200 is the conjugate of the impedance at the physical boundary 136 "looking down" into the lossy conducting medium 203. By adjusting the load impedance Z_L of the charge terminal T_1 while maintaining the traveling wave phase delay Φ equal to the angle of the media's wave tilt Ψ, so that $\Phi = \Psi$, which improves and/or maximizes coupling of the probe's electric field to a guided surface waveguide mode along the surface of the lossy conducting medium 203 (e.g., Earth), the equivalent image plane models of FIGS. 9A and 9B can be tuned to resonance with respect to the image ground plane 139. In this way, the impedance of the equivalent complex image plane model is purely resistive, which maintains a superposed standing wave on the probe structure that maximizes the voltage and elevated charge on terminal T_1, and by equations (1)-(3) and (16) maximizes the propagating surface wave.

[0101] It follows from the Hankel solutions, that the guided surface wave excited by the guided surface waveguide probe 200 is an outward propagating traveling wave. The source distribution along the feed network 209 between the charge terminal T_1 and the ground stake 218 of the guided surface waveguide probe 200 (FIGS. 3 and 7) is actually composed of a superposition of a traveling wave plus a standing wave on the structure. With the charge

terminal T_1 positioned at or above the physical height h_p, the phase delay of the traveling wave moving through the feed network 209 is matched to the angle of the wave tilt associated with the lossy conducting medium 203. This mode-matching allows the traveling wave to be launched along the lossy conducting medium 203. Once the phase delay has been established for the traveling wave, the load impedance Z_L of the charge terminal T_1 is adjusted to bring the probe structure into standing wave resonance with respect to the image ground plane (130 of FIG. 3 or 139 of FIG. 8), which is at a complex depth of $-\mathrm{d}/2$. In that case, the impedance seen from the image ground plane has zero reactance and the charge on the charge terminal T_1 is maximized.

[0102] The distinction between the traveling wave phenomenon and standing wave phenomena is that (1) the phase delay of traveling waves ($\theta = \beta d$) on a section of transmission line of length d (sometimes called a "delay line") is due to propagation time delays; whereas (2) the position-dependent phase of standing waves (which are composed of forward and backward propagating waves) depends on both the line length propagation time delay and impedance transitions at interfaces between line sections of different characteristic impedances. In addition to the phase delay that arises due to the physical length of a section of transmission line operating in sinusoidal steady-state, there is an extra reflection coefficient phase at impedance discontinuities that is due to the ratio of Z_{oa}/Z_{ob}, where Z_{oa} and Z_{ob} are the characteristic impedances of two sections of a transmission line such as, e.g., a helical coil section of characteristic impedance $Z_{oa} = Z_c$ (FIG. 9B) and a straight section of vertical feed line conductor of characteristic impedance $Z_{ob} = Z_w$ (FIG. 9B).

[0103] As a result of this phenomenon, two *relatively short* transmission line sections of widely differing characteristic impedance may be used to provide a *very large* phase shift. For example, a probe structure composed of two sections of transmission line, one of low impedance and one of high impedance, together totaling a physical length of, say, 0.05 λ, may be fabricated to provide a phase shift of 90° which is equivalent to a 0.25 λ resonance. This is due to the large jump in characteristic impedances. In this way, a physically short probe structure can be electrically longer than the two physical lengths combined. This is illustrated in FIGS. 9A and 9B, where the discontinuities in the impedance ratios provide large jumps in phase. The impedance discontinuity provides a substantial phase shift where the sections are joined together.

[0104] Referring to FIG. 10, shown is a flow chart 150 illustrating an example of adjusting a guided surface waveguide probe 200 (FIGS. 3 and 7) to substantially mode-match to a guided surface waveguide mode on the surface of the lossy conducting medium, which launches a guided surface traveling wave along the surface of a lossy conducting

medium 203 (FIG. 3). Beginning with 153, the charge terminal T_1 of the guided surface waveguide probe 200 is positioned at a defined height above a lossy conducting medium 203. Utilizing the characteristics of the lossy conducting medium 203 and the operating frequency of the guided surface waveguide probe 200, the Hankel crossover distance can also be found by equating the magnitudes of Equations (20b) and (21) for $-j\gamma\rho$, and solving for R_x as illustrated by FIG. 4. The complex index of refraction (n) can be determined using Equation (41), and the complex Brewster angle ($\theta_{i,B}$) can then be determined from Equation (42). The physical height (h_p) of the charge terminal T_1 can then be determined from Equation (44). The charge terminal T_1 should be at or higher than the physical height (h_p) in order to excite the far-out component of the Hankel function. This height relationship is initially considered when launching surface waves. To reduce or minimize the bound charge on the charge terminal T_1, the height should be at least four times the spherical diameter (or equivalent spherical diameter) of the charge terminal T_1.

[0105] At 156, the electrical phase delay Φ of the elevated charge Q_1 on the charge terminal T_1 is matched to the complex wave tilt angle Ψ. The phase delay (θ_c) of the helical coil and/or the phase delay (θ_y) of the vertical feed line conductor can be adjusted to make Φ equal to the angle (Ψ) of the wave tilt (W). Based on Equation (31), the angle (Ψ) of the wave tilt can be determined from:

$$W = \frac{E_\rho}{E_z} = \frac{1}{\tan\theta_{i,B}} = \frac{1}{n} = |W|e^{j\Psi}. \tag{66}$$

The electrical phase Φ can then be matched to the angle of the wave tilt. This angular (or phase) relationship is next considered when launching surface waves. For example, the electrical phase delay $\Phi = \theta_c + \theta_y$ can be adjusted by varying the geometrical parameters of the coil 215 (FIG. 7) and/or the length (or height) of the vertical feed line conductor 221 (FIG. 7). By matching $\Phi = \Psi$, an electric field can be established at or beyond the Hankel crossover distance (R_x) with a complex Brewster angle at the boundary interface to excite the surface waveguide mode and launch a traveling wave along the lossy conducting medium 203.

[0106] Next at 159, the load impedance of the charge terminal T_1 is tuned to resonate the equivalent image plane model of the guided surface waveguide probe 200. The depth ($\mathrm{d}/2$) of the conducting image ground plane 139 of FIG. 9A and 9B (or 130 of FIG. 3) can be determined using Equations (52), (53) and (54) and the values of the lossy conducting medium 203 (e.g., the Earth), which can be measured. Using that depth, the phase shift (θ_d) between the image ground plane 139 and the physical boundary 136 of the lossy conducting medium 203 can be determined using $\theta_d = \beta_o\,\mathrm{d}/2$. The impedance ($Z_{in}$) as seen "looking

down" into the lossy conducting medium 203 can then be determined using Equation (65). This resonance relationship can be considered to maximize the launched surface waves.

[0107] Based upon the adjusted parameters of the coil 215 and the length of the vertical feed line conductor 221, the velocity factor, phase delay, and impedance of the coil 215 and vertical feed line conductor 221 can be determined using Equations (45) through (51). In addition, the self-capacitance (C_T) of the charge terminal T_1 can be determined using, e.g., Equation (24). The propagation factor (β_p) of the coil 215 can be determined using Equation (35) and the propagation phase constant (β_w) for the vertical feed line conductor 221 can be determined using Equation (49). Using the self-capacitance and the determined values of the coil 215 and vertical feed line conductor 221, the impedance (Z_{base}) of the guided surface waveguide probe 200 as seen "looking up" into the coil 215 can be determined using Equations (62), (63) and (64).

[0108] The equivalent image plane model of the guided surface waveguide probe 200 can be tuned to resonance by adjusting the load impedance Z_L such that the reactance component X_{base} of Z_{base} cancels out the reactance component X_{in} of Z_{in}, or $X_{base} + X_{in} = 0$. Thus, the impedance at the physical boundary 136 "looking up" into the guided surface waveguide probe 200 is the conjugate of the impedance at the physical boundary 136 "looking down" into the lossy conducting medium 203. The load impedance Z_L can be adjusted by varying the capacitance (C_T) of the charge terminal T_1 without changing the electrical phase delay $\Phi = \theta_c + \theta_y$ of the charge terminal T_1. An iterative approach may be taken to tune the load impedance Z_L for resonance of the equivalent image plane model with respect to the conducting image ground plane 139 (or 130). In this way, the coupling of the electric field to a guided surface waveguide mode along the surface of the lossy conducting medium 203 (e.g., Earth) can be improved and/or maximized.

[0109] This may be better understood by illustrating the situation with a numerical example. Consider a guided surface waveguide probe 200 comprising a top-loaded vertical stub of physical height h_p with a charge terminal T_1 at the top, where the charge terminal T_1 is excited through a helical coil and vertical feed line conductor at an operational frequency (f_o) of 1.85 MHz. With a height (H_1) of 16 feet and the lossy conducting medium 203 (*e.g.*, Earth) having a relative permittivity of $\varepsilon_r = 15$ and a conductivity of $\sigma_1 = 0.010$ mhos/m, several surface wave propagation parameters can be calculated for $f_o = 1.850$ MHz. Under these conditions, the Hankel crossover distance can be found to be $R_x = 54.5$ feet with a physical height of $h_p = 5.5$ feet, which is well below the actual height of the charge terminal T_1. While a charge terminal height of H_1 = 5.5 feet could have been used, the taller probe structure reduced the bound capacitance, permitting a greater percentage of free charge on the charge terminal T_1 providing greater field strength and excitation of the traveling wave.

[0110] The wave length can be determined as:

$$\lambda_o = \frac{c}{f_o} = 162.162 \text{ meters}, \tag{67}$$

where c is the speed of light. The complex index of refraction is:

$$n = \sqrt{\varepsilon_r - jx} = 7.529 - j\ 6.546, \tag{68}$$

from Equation (41), where $x = \sigma_1/\omega\varepsilon_o$ with $\omega = 2\pi f_o$, and the complex Brewster angle is:

$$\theta_{i,B} = \arctan\left(\sqrt{\varepsilon_r - jx}\right) = 85.6 - j\ 3.744°. \tag{69}$$

from Equation (42). Using Equation (66), the wave tilt values can be determined to be:

$$W = \frac{1}{\tan\theta_{i,B}} = \frac{1}{n} = |W|e^{j\Psi} = 0.101e^{j40.614°}. \tag{70}$$

Thus, the helical coil can be adjusted to match $\Phi = \Psi = 40.614°$

[0111] The velocity factor of the vertical feed line conductor (approximated as a uniform cylindrical conductor with a diameter of 0.27 inches) can be given as $V_w \approx 0.93$. Since $h_p \ll \lambda_o$, the propagation phase constant for the vertical feed line conductor can be approximated as:

$$\beta_w = \frac{2\pi}{\lambda_w} = \frac{2\pi}{V_w\lambda_0} = 0.042 \text{ m}^{-1}. \tag{71}$$

From Equation (49) the phase delay of the vertical feed line conductor is:

$$\theta_y = \beta_w h_w \approx \beta_w h_p = 11.640°. \tag{72}$$

By adjusting the phase delay of the helical coil so that $\theta_c = 28.974° = 40.614° - 11.640°$, Φ will equal Ψ to match the guided surface waveguide mode. To illustrate the relationship between Φ and Ψ, FIG. 11 shows a plot of both over a range of frequencies. As both Φ and Ψ are frequency dependent, it can be seen that their respective curves cross over each other at approximately 1.85 MHz.

[0112] For a helical coil having a conductor diameter of 0.0881 inches, a coil diameter (D) of 30 inches and a turn-to-turn spacing (s) of 4 inches, the velocity factor for the coil can be determined using Equation (45) as:

$$V_f = \frac{1}{\sqrt{1+20\left(\frac{D}{s}\right)^{2.5}\left(\frac{D}{\lambda_o}\right)^{0.5}}} = 0.069\ , \tag{73}$$

and the propagation factor from Equation (35) is:

$$\beta_p = \frac{2\pi}{V_f\lambda_0} = 0.564 \text{ m}^{-1}. \tag{74}$$

With $\theta_c = 28.974°$, the axial length of the solenoidal helix (H) can be determined using Equation (46) such that:

$$H = \frac{\theta_c}{\beta_p} = 35.2732 \text{ inches}\ . \tag{75}$$

This height determines the location on the helical coil where the vertical feed line conductor is connected, resulting in a coil with 8.818 turns ($N = H/s$).

[0113] With the traveling wave phase delay of the coil and vertical feed line conductor adjusted to match the wave tilt angle ($\Phi = \theta_c + \theta_y = \Psi$), the load impedance ($Z_L$) of the charge terminal T_1 can be adjusted for standing wave resonance of the equivalent image plane model of the guided surface wave probe 200. From the measured permittivity, conductivity and permeability of the Earth, the radial propagation constant can be determined using Equation (57)

$$\gamma_e = \sqrt{j\omega u_1(\sigma_1 + j\omega\varepsilon_1)} = 0.25 + j\,0.292\ \mathrm{m}^{-1}, \tag{76}$$

And the complex depth of the conducting image ground plane can be approximated from Equation (52) as:

$$\mathrm{d} \approx \frac{2}{\gamma_e} = 3.364 + j\,3.963\ \text{meters}\ , \tag{77}$$

with a corresponding phase shift between the conducting image ground plane and the physical boundary of the Earth given by:

$$\theta_d = \beta_o(\mathrm{d}/2) = 4.015 - j\,4.73°. \tag{78}$$

Using Equation (65), the impedance seen "looking down" into the lossy conducting medium 203 (i.e., Earth) can be determined as:

$$Z_{in} = Z_o \tanh(j\theta_d) = R_{in} + jX_{in} = 31.191 + j\,26.27\ \text{ohms}. \tag{79}$$

[0114] By matching the reactive component (X_{in}) seen "looking down" into the lossy conducting medium 203 with the reactive component (X_{base}) seen "looking up" into the guided surface wave probe 200, the coupling into the guided surface waveguide mode may be maximized. This can be accomplished by adjusting the capacitance of the charge terminal T_1 without changing the traveling wave phase delays of the coil and vertical feed line conductor. For example, by adjusting the charge terminal capacitance (C_T) to 61.8126 pF, the load impedance from Equation (62) is:

$$Z_L = \frac{1}{j\omega C_T} = -j\ 1392\ \text{ohms}, \tag{80}$$

and the reactive components at the boundary are matched.

[0115] Using Equation (51), the impedance of the vertical feed line conductor (having a diameter ($2a$) of 0.27 inches) is given as

$$Z_w = 138\ log\left(\frac{1.123\,V_w\lambda_0}{2\pi a}\right) = 537.534\ \text{ohms}, \tag{81}$$

and the impedance seen "looking up" into the vertical feed line conductor is given by Equation (63) as:

$$Z_2 = Z_W \frac{Z_L + Z_w \tanh(j\theta_y)}{Z_w + Z_L \tanh(j\theta_y)} = -j\ 835.438\ \text{ohms}. \tag{82}$$

Using Equation (47), the characteristic impedance of the helical coil is given as

$$Z_c = \frac{60}{V_f}\left[\ell n\left(\frac{V_f\lambda_0}{D}\right) - 1.027\right] = 1446\ \text{ohms}, \tag{83}$$

and the impedance seen "looking up" into the coil at the base is given by Equation (64) as:

$$Z_{base} = Z_c \frac{Z_2 + Z_c \tanh(j\theta_c)}{Z_c + Z_2 \tanh(j\theta_c)} = -j\ 26.271 \text{ ohms}. \quad (84)$$

When compared to the solution of Equation (79), it can be seen that the reactive components are opposite and approximately equal, and thus are conjugates of each other. Thus, the impedance (Z_{ip}) seen "looking up" into the equivalent image plane model of FIGS. 9A and 9B from the perfectly conducting image ground plane is only resistive or $Z_{ip} = R + j0$.

[0116] When the electric fields produced by a guided surface waveguide probe 200 (FIG. 3) are established by matching the traveling wave phase delay of the feed network to the wave tilt angle and the probe structure is resonated with respect to the perfectly conducting image ground plane at complex depth $z = -d/2$, the fields are substantially mode-matched to a guided surface waveguide mode on the surface of the lossy conducting medium, a guided surface traveling wave is launched along the surface of the lossy conducting medium. As illustrated in FIG. 1, the guided field strength curve 103 of the guided electromagnetic field has a characteristic exponential decay of $e^{-\alpha d}/\sqrt{d}$ and exhibits a distinctive knee 109 on the log-log scale.

[0117] In summary, both analytically and experimentally, the *traveling wave* component on the structure of the guided surface waveguide probe 200 has a phase delay (Φ) at its upper terminal that matches the angle (Ψ) of the wave tilt of the surface traveling wave ($\Phi = \Psi$). Under this condition, the surface waveguide may be considered to be "mode-matched". Furthermore, the resonant *standing wave* component on the structure of the guided surface waveguide probe 200 has a V_{MAX} at the charge terminal T_1 and a V_{MIN} down at the image plane 139 (FIG. 8B) where $Z_{ip} = R_{ip} + j\ 0$ at a complex depth of $z = -\mathrm{d}/2$, not at the connection at the physical boundary 136 of the lossy conducting medium 203 (FIG. 8B). Lastly, the charge terminal T_1 is of sufficient height H_1 of FIG. 3 ($h \geq R_x \tan\psi_{i,B}$) so that electromagnetic waves incident onto the lossy conducting medium 203 at the complex Brewster angle do so out at a distance ($\geq R_x$) where the $1/\sqrt{r}$ term is predominant. Receive circuits can be utilized with one or more guided surface waveguide probes to facilitate wireless transmission and/or power delivery systems.

[0118] Referring back to FIG. 3, operation of a guided surface waveguide probe 200 may be controlled to adjust for variations in operational conditions associated with the guided surface waveguide probe 200. For example, an adaptive probe control system 230 can be used to control the feed network 209 and/or the charge terminal T_1 to control the operation of the guided surface waveguide probe 200. Operational conditions can include, but are not limited to, variations in the characteristics of the lossy conducting medium 203 (*e.g.*, conductivity σ and relative permittivity ε_r), variations in field strength and/or variations

in loading of the guided surface waveguide probe 200. As can be seen from Equations (31), (41) and (42), the index of refraction (n), the complex Brewster angle ($\theta_{i,B}$), and the wave tilt ($|W|e^{j\Psi}$) can be affected by changes in soil conductivity and permittivity resulting from, *e.g.*, weather conditions.

[0119] Equipment such as, *e.g.*, conductivity measurement probes, permittivity sensors, ground parameter meters, field meters, current monitors and/or load receivers can be used to monitor for changes in the operational conditions and provide information about current operational conditions to the adaptive probe control system 230. The probe control system 230 can then make one or more adjustments to the guided surface waveguide probe 200 to maintain specified operational conditions for the guided surface waveguide probe 200. For instance, as the moisture and temperature vary, the conductivity of the soil will also vary. Conductivity measurement probes and/or permittivity sensors may be located at multiple locations around the guided surface waveguide probe 200. Generally, it would be desirable to monitor the conductivity and/or permittivity at or about the Hankel crossover distance R_x for the operational frequency. Conductivity measurement probes and/or permittivity sensors may be located at multiple locations (*e.g.*, in each quadrant) around the guided surface waveguide probe 200.

[0120] The conductivity measurement probes and/or permittivity sensors can be configured to evaluate the conductivity and/or permittivity on a periodic basis and communicate the information to the probe control system 230. The information may be communicated to the probe control system 230 through a network such as, but not limited to, a LAN, WLAN, cellular network, or other appropriate wired or wireless communication network. Based upon the monitored conductivity and/or permittivity, the probe control system 230 may evaluate the variation in the index of refraction (n), the complex Brewster angle ($\theta_{i,B}$), and/or the wave tilt ($|W|e^{j\Psi}$) and adjust the guided surface waveguide probe 200 to maintain the phase delay (Φ) of the feed network 209 equal to the wave tilt angle (Ψ) and/or maintain resonance of the equivalent image plane model of the guided surface waveguide probe 200. This can be accomplished by adjusting, *e.g.*, θ_y, θ_c and/or C_T. For instance, the probe control system 230 can adjust the self-capacitance of the charge terminal T_1 and/or the phase delay (θ_y, θ_c) applied to the charge terminal T_1 to maintain the electrical launching efficiency of the guided surface wave at or near its maximum. For example, the self-capacitance of the charge terminal T_1 can be varied by changing the size of the terminal. The charge distribution can also be improved by increasing the size of the charge terminal T_1, which can reduce the chance of an electrical discharge from the charge terminal T_1. In other embodiments, the charge terminal T_1 can include a variable inductance that can be adjusted to change the load impedance Z_L. The phase applied to the charge terminal T_1 can

be adjusted by varying the tap position on the coil 215 (FIG. 7), and/or by including a plurality of predefined taps along the coil 215 and switching between the different predefined tap locations to maximize the launching efficiency.

[0121] Field or field strength (FS) meters may also be distributed about the guided surface waveguide probe 200 to measure field strength of fields associated with the guided surface wave. The field or FS meters can be configured to detect the field strength and/or changes in the field strength (*e.g.*, electric field strength) and communicate that information to the probe control system 230. The information may be communicated to the probe control system 230 through a network such as, but not limited to, a LAN, WLAN, cellular network, or other appropriate communication network. As the load and/or environmental conditions change or vary during operation, the guided surface waveguide probe 200 may be adjusted to maintain specified field strength(s) at the FS meter locations to ensure appropriate power transmission to the receivers and the loads they supply.

[0122] For example, the phase delay ($\Phi = \theta_y + \theta_c$) applied to the charge terminal T_1 can be adjusted to match the wave tilt angle (Ψ). By adjusting one or both phase delays, the guided surface waveguide probe 200 can be adjusted to ensure the wave tilt corresponds to the complex Brewster angle. This can be accomplished by adjusting a tap position on the coil 215 (FIG. 7) to change the phase delay supplied to the charge terminal T_1. The voltage level supplied to the charge terminal T_1 can also be increased or decreased to adjust the electric field strength. This may be accomplished by adjusting the output voltage of the excitation source 212 or by adjusting or reconfiguring the feed network 209. For instance, the position of the tap 227 (FIG. 7) for the AC source 212 can be adjusted to increase the voltage seen by the charge terminal T_1. Maintaining field strength levels within predefined ranges can improve coupling by the receivers, reduce ground current losses, and avoid interference with transmissions from other guided surface waveguide probes 200.

[0123] The probe control system 230 can be implemented with hardware, firmware, software executed by hardware, or a combination thereof. For example, the probe control system 230 can include processing circuitry including a processor and a memory, both of which can be coupled to a local interface such as, for example, a data bus with an accompanying control/address bus as can be appreciated by those with ordinary skill in the art. A probe control application may be executed by the processor to adjust the operation of the guided surface waveguide probe 200 based upon monitored conditions. The probe control system 230 can also include one or more network interfaces for communicating with the various monitoring devices. Communications can be through a network such as, but not limited to, a LAN, WLAN, cellular network, or other appropriate communication network. The

probe control system 230 may comprise, for example, a computer system such as a server, desktop computer, laptop, or other system with like capability.

[0124] Referring back to the example of FIG. 5A, the complex angle trigonometry is shown for the ray optic interpretation of the incident electric field (E) of the charge terminal T_1 with a complex Brewster angle ($\theta_{i,B}$) at the Hankel crossover distance (R_x). Recall that, for a lossy conducting medium, the Brewster angle is complex and specified by equation (38). Electrically, the geometric parameters are related by the electrical effective height (h_{eff}) of the charge terminal T_1 by equation (39). Since both the physical height (h_p) and the Hankel crossover distance (R_x) are real quantities, the angle of the desired guided surface wave tilt at the Hankel crossover distance (W_{Rx}) is equal to the phase (Φ) of the complex effective height (h_{eff}). With the charge terminal T_1 positioned at the physical height h_p and excited with a charge having the appropriate phase Φ, the resulting electric field is incident with the lossy conducting medium boundary interface at the Hankel crossover distance R_x, and at the Brewster angle. Under these conditions, the guided surface waveguide mode can be excited without reflection or substantially negligible reflection.

[0125] However, Equation (39) means that the physical height of the guided surface waveguide probe 200 can be relatively small. While this will excite the guided surface waveguide mode, this can result in an unduly large bound charge with little free charge. To compensate, the charge terminal T_1 can be raised to an appropriate elevation to increase the amount of free charge. As one example rule of thumb, the charge terminal T_1 can be positioned at an elevation of about 4-5 times (or more) the effective diameter of the charge terminal T_1. FIG. 6 illustrates the effect of raising the charge terminal T_1 above the physical height (h_p) shown in FIG. 5A. The increased elevation causes the distance at which the wave tilt is incident with the lossy conductive medium to move beyond the Hankel crossover point 121 (FIG. 5A). To improve coupling in the guided surface waveguide mode, and thus provide for a greater launching efficiency of the guided surface wave, a lower compensation terminal T_2 can be used to adjust the total effective height (h_{TE}) of the charge terminal T_1 such that the wave tilt at the Hankel crossover distance is at the Brewster angle.

[0126] Referring to FIG. 12, shown is an example of a guided surface waveguide probe 200c that includes an elevated charge terminal T_1 and a lower compensation terminal T_2 that are arranged along a vertical axis z that is normal to a plane presented by the lossy conducting medium 203. In this respect, the charge terminal T_1 is placed directly above the compensation terminal T_2 although it is possible that some other arrangement of two or more charge and/or compensation terminals T_N can be used. The guided surface waveguide probe 200c is disposed above a lossy conducting medium 203 according to an embodiment of the present disclosure. The lossy conducting medium 203 makes up Region 1 with a

second medium 206 that makes up Region 2 sharing a boundary interface with the lossy conducting medium 203.

[0127] The guided surface waveguide probe 200c includes a feed network 209 that couples an excitation source 212 to the charge terminal T_1 and the compensation terminal T_2. According to various embodiments, charges Q_1 and Q_2 can be imposed on the respective charge and compensation terminals T_1 and T_2, depending on the voltages applied to terminals T_1 and T_2 at any given instant. I_1 is the conduction current feeding the charge Q_1 on the charge terminal T_1 via the terminal lead, and I_2 is the conduction current feeding the charge Q_2 on the compensation terminal T_2 via the terminal lead.

[0128] According to the embodiment of FIG. 12, the charge terminal T_1 is positioned over the lossy conducting medium 203 at a physical height H_1, and the compensation terminal T_2 is positioned directly below T_1 along the vertical axis z at a physical height H_2, where H_2 is less than H_1. The height h of the transmission structure may be calculated as $h = H_1 - H_2$. The charge terminal T_1 has an isolated (or self) capacitance C_1, and the compensation terminal T_2 has an isolated (or self) capacitance C_2. A mutual capacitance C_M can also exist between the terminals T_1 and T_2 depending on the distance there between. During operation, charges Q_1 and Q_2 are imposed on the charge terminal T_1 and the compensation terminal T_2, respectively, depending on the voltages applied to the charge terminal T_1 and the compensation terminal T_2 at any given instant.

[0129] Referring next to FIG. 13, shown is a ray optics interpretation of the effects produced by the elevated charge Q_1 on charge terminal T_1 and compensation terminal T_2 of FIG. 12. With the charge terminal T_1 elevated to a height where the ray intersects with the lossy conductive medium at the Brewster angle at a distance greater than the Hankel crossover point 121 as illustrated by line 163, the compensation terminal T_2 can be used to adjust h_{TE} by compensating for the increased height. The effect of the compensation terminal T_2 is to reduce the electrical effective height of the guided surface waveguide probe (or effectively raise the lossy medium interface) such that the wave tilt at the Hankel crossover distance is at the Brewster angle as illustrated by line 166.

[0130] The total effective height can be written as the superposition of an upper effective height (h_{UE}) associated with the charge terminal T_1 and a lower effective height (h_{LE}) associated with the compensation terminal T_2 such that

$$h_{TE} = h_{UE} + h_{LE} = h_p e^{j(\beta h_p + \Phi_U)} + h_d e^{j(\beta h_d + \Phi_L)} = R_x \times W, \quad (85)$$

where Φ_U is the phase delay applied to the upper charge terminal T_1, Φ_L is the phase delay applied to the lower compensation terminal T_2, $\beta = 2\pi/\lambda_p$ is the propagation factor from Equation (35), h_p is the physical height of the charge terminal T_1 and h_d is the physical height of the compensation terminal T_2. If extra lead lengths are taken into consideration,

they can be accounted for by adding the charge terminal lead length z to the physical height h_p of the charge terminal T_1 and the compensation terminal lead length y to the physical height h_d of the compensation terminal T_2 as shown in

$$h_{TE} = (h_p + z)e^{j(\beta(h_p+z)+\Phi_U)} + (h_d + y)e^{j(\beta(h_d+y)+\Phi_L)} = R_x \times W. \quad (86)$$

The lower effective height can be used to adjust the total effective height (h_{TE}) to equal the complex effective height (h_{eff}) of FIG. 5A.

[0131] Equations (85) or (86) can be used to determine the physical height of the lower disk of the compensation terminal T_2 and the phase angles to feed the terminals in order to obtain the desired wave tilt at the Hankel crossover distance. For example, Equation (86) can be rewritten as the phase shift applied to the charge terminal T_1 as a function of the compensation terminal height (h_d) to give

$$\Phi_U(h_d) = -\beta(h_p + z) - j\ln\left(\frac{R_x \times W - (h_d+y)e^{j(\beta h_d + \beta y + \Phi_L)}}{(h_p+z)}\right). \quad (87)$$

[0132] To determine the positioning of the compensation terminal T_2, the relationships discussed above can be utilized. First, the total effective height (h_{TE}) is the superposition of the complex effective height (h_{UE}) of the upper charge terminal T_1 and the complex effective height (h_{LE}) of the lower compensation terminal T_2 as expressed in Equation (86). Next, the tangent of the angle of incidence can be expressed geometrically as

$$\tan\psi_E = \frac{h_{TE}}{R_x}, \quad (88)$$

which is equal to the definition of the wave tilt, W. Finally, given the desired Hankel crossover distance R_x, the h_{TE} can be adjusted to make the wave tilt of the incident ray match the complex Brewster angle at the Hankel crossover point 121. This can be accomplished by adjusting h_p, Φ_U, and/or h_d.

[0133] These concepts may be better understood when discussed in the context of an example of a guided surface waveguide probe. Referring to FIG. 14, shown is a graphical representation of an example of a guided surface waveguide probe 200d including an upper charge terminal T_1 (*e.g.*, a sphere at height h_T) and a lower compensation terminal T_2 (*e.g.*, a disk at height h_d) that are positioned along a vertical axis z that is substantially normal to the plane presented by the lossy conducting medium 203. During operation, charges Q_1 and Q_2 are imposed on the charge and compensation terminals T_1 and T_2, respectively, depending on the voltages applied to the terminals T_1 and T_2 at any given instant.

[0134] An AC source 212 acts as the excitation source for the charge terminal T_1, which is coupled to the guided surface waveguide probe 200d through a feed network 209 comprising a coil 215 such as, *e.g.*, a helical coil. The AC source 212 can be connected across a lower portion of the coil 215 through a tap 227, as shown in FIG. 14, or can be inductively coupled to the coil 215 by way of a primary coil. The coil 215 can be coupled to a

ground stake 218 at a first end and the charge terminal T_1 at a second end. In some implementations, the connection to the charge terminal T_1 can be adjusted using a tap 224 at the second end of the coil 215. The compensation terminal T_2 is positioned above and substantially parallel with the lossy conducting medium 203 (*e.g.*, the ground or Earth), and energized through a tap 233 coupled to the coil 215. An ammeter 236 located between the coil 215 and ground stake 218 can be used to provide an indication of the magnitude of the current flow (I_0) at the base of the guided surface waveguide probe. Alternatively, a current clamp may be used around the conductor coupled to the ground stake 218 to obtain an indication of the magnitude of the current flow (I_0).

[0135] In the example of FIG. 14, the coil 215 is coupled to a ground stake 218 at a first end and the charge terminal T_1 at a second end via a vertical feed line conductor 221. In some implementations, the connection to the charge terminal T_1 can be adjusted using a tap 224 at the second end of the coil 215 as shown in FIG. 14. The coil 215 can be energized at an operating frequency by the AC source 212 through a tap 227 at a lower portion of the coil 215. In other implementations, the AC source 212 can be inductively coupled to the coil 215 through a primary coil. The compensation terminal T_2 is energized through a tap 233 coupled to the coil 215. An ammeter 236 located between the coil 215 and ground stake 218 can be used to provide an indication of the magnitude of the current flow at the base of the guided surface waveguide probe 200d. Alternatively, a current clamp may be used around the conductor coupled to the ground stake 218 to obtain an indication of the magnitude of the current flow. The compensation terminal T_2 is positioned above and substantially parallel with the lossy conducting medium 203 (*e.g.*, the ground).

[0136] In the example of FIG. 14, the connection to the charge terminal T_1 located on the coil 215 above the connection point of tap 233 for the compensation terminal T_2. Such an adjustment allows an increased voltage (and thus a higher charge Q_1) to be applied to the upper charge terminal T_1. In other embodiments, the connection points for the charge terminal T_1 and the compensation terminal T_2 can be reversed. It is possible to adjust the total effective height (h_{TE}) of the guided surface waveguide probe 200d to excite an electric field having a guided surface wave tilt at the Hankel crossover distance R_x. The Hankel crossover distance can also be found by equating the magnitudes of equations (20b) and (21) for $-j\gamma\rho$, and solving for R_x as illustrated by FIG. 4. The index of refraction (n), the complex Brewster angle ($\theta_{i,B}$ and $\psi_{i,B}$), the wave tilt ($|W|e^{j\Psi}$) and the complex effective height ($h_{eff} = h_p e^{j\Phi}$) can be determined as described with respect to Equations (41) – (44) above.

[0137] With the selected charge terminal T_1 configuration, a spherical diameter (or the effective spherical diameter) can be determined. For example, if the charge terminal T_1 is not

configured as a sphere, then the terminal configuration may be modeled as a spherical capacitance having an effective spherical diameter. The size of the charge terminal T_1 can be chosen to provide a sufficiently large surface for the charge Q_1 imposed on the terminals. In general, it is desirable to make the charge terminal T_1 as large as practical. The size of the charge terminal T_1 should be large enough to avoid ionization of the surrounding air, which can result in electrical discharge or sparking around the charge terminal. To reduce the amount of bound charge on the charge terminal T_1, the desired elevation to provide free charge on the charge terminal T_1 for launching a guided surface wave should be at least 4-5 times the effective spherical diameter above the lossy conductive medium (*e.g.*, the Earth). The compensation terminal T_2 can be used to adjust the total effective height (h_{TE}) of the guided surface waveguide probe 200d to excite an electric field having a guided surface wave tilt at R_x. The compensation terminal T_2 can be positioned below the charge terminal T_1 at $h_d = h_T - h_p$, where h_T is the total physical height of the charge terminal T_1. With the position of the compensation terminal T_2 fixed and the phase delay Φ_U applied to the upper charge terminal T_1, the phase delay Φ_L applied to the lower compensation terminal T_2 can be determined using the relationships of Equation (86), such that:

$$\Phi_U(h_d) = -\beta(h_d + y) - j\ln\left(\frac{R_x \times W - (h_p+z)e^{j(\beta h_p+\beta z+\Phi_L)}}{(h_d+y)}\right). \quad (89)$$

In alternative embodiments, the compensation terminal T_2 can be positioned at a height h_d where $\mathrm{Im}\{\Phi_L\} = 0$. This is graphically illustrated in FIG. 15A, which shows plots 172 and 175 of the imaginary and real parts of Φ_U, respectively. The compensation terminal T_2 is positioned at a height h_d where $\mathrm{Im}\{\Phi_U\} = 0$, as graphically illustrated in plot 172. At this fixed height, the coil phase Φ_U can be determined from $\mathrm{Re}\{\Phi_U\}$, as graphically illustrated in plot 175.

[0138] With the AC source 212 coupled to the coil 215 (*e.g.*, at the 50Ω point to maximize coupling), the position of tap 233 may be adjusted for parallel resonance of the compensation terminal T_2 with at least a portion of the coil at the frequency of operation. FIG. 15B shows a schematic diagram of the general electrical hookup of FIG. 14 in which V_1 is the voltage applied to the lower portion of the coil 215 from the AC source 212 through tap 227, V_2 is the voltage at tap 224 that is supplied to the upper charge terminal T_1, and V_3 is the voltage applied to the lower compensation terminal T_2 through tap 233. The resistances R_p and R_d represent the ground return resistances of the charge terminal T_1 and compensation terminal T_2, respectively. The charge and compensation terminals T_1 and T_2 may be configured as spheres, cylinders, toroids, rings, hoods, or any other combination of capacitive structures. The size of the charge and compensation terminals T_1 and T_2 can be chosen to provide a sufficiently large surface for the charges Q_1 and Q_2 imposed on the

terminals. In general, it is desirable to make the charge terminal T_1 as large as practical. The size of the charge terminal T_1 should be large enough to avoid ionization of the surrounding air, which can result in electrical discharge or sparking around the charge terminal. The self-capacitance C_p and C_d of the charge and compensation terminals T_1 and T_2 respectively, can be determined using, for example, equation (24).

[0139] As can be seen in FIG. 15B, a resonant circuit is formed by at least a portion of the inductance of the coil 215, the self-capacitance C_d of the compensation terminal T_2, and the ground return resistance R_d associated with the compensation terminal T_2. The parallel resonance can be established by adjusting the voltage V_3 applied to the compensation terminal T_2 (*e.g.*, by adjusting a tap 233 position on the coil 215) or by adjusting the height and/or size of the compensation terminal T_2 to adjust C_d. The position of the coil tap 233 can be adjusted for parallel resonance, which will result in the ground current through the ground stake 218 and through the ammeter 236 reaching a maximum point. After parallel resonance of the compensation terminal T_2 has been established, the position of the tap 227 for the AC source 212 can be adjusted to the 50Ω point on the coil 215.

[0140] Voltage V_2 from the coil 215 can be applied to the charge terminal T_1, and the position of tap 224 can be adjusted such that the phase (Φ) of the total effective height (h_{TE}) approximately equals the angle of the guided surface wave tilt (W_{Rx}) at the Hankel crossover distance (R_x). The position of the coil tap 224 can be adjusted until this operating point is reached, which results in the ground current through the ammeter 236 increasing to a maximum. At this point, the resultant fields excited by the guided surface waveguide probe 200d are substantially mode-matched to a guided surface waveguide mode on the surface of the lossy conducting medium 203, resulting in the launching of a guided surface wave along the surface of the lossy conducting medium 203. This can be verified by measuring field strength along a radial extending from the guided surface waveguide probe 200.

[0141] Resonance of the circuit including the compensation terminal T_2 may change with the attachment of the charge terminal T_1 and/or with adjustment of the voltage applied to the charge terminal T_1 through tap 224. While adjusting the compensation terminal circuit for resonance aids the subsequent adjustment of the charge terminal connection, it is not necessary to establish the guided surface wave tilt (W_{Rx}) at the Hankel crossover distance (R_x). The system may be further adjusted to improve coupling by iteratively adjusting the position of the tap 227 for the AC source 212 to be at the 50Ω point on the coil 215 and adjusting the position of tap 233 to maximize the ground current through the ammeter 236. Resonance of the circuit including the compensation terminal T_2 may drift as the positions of taps 227 and 233 are adjusted, or when other components are attached to the coil 215.

[0142] In other implementations, the voltage V_2 from the coil 215 can be applied to the charge terminal T_1, and the position of tap 233 can be adjusted such that the phase (Φ) of the total effective height (h_{TE}) approximately equals the angle (Ψ) of the guided surface wave tilt at R_x. The position of the coil tap 224 can be adjusted until the operating point is reached, resulting in the ground current through the ammeter 236 substantially reaching a maximum. The resultant fields are substantially mode-matched to a guided surface waveguide mode on the surface of the lossy conducting medium 203, and a guided surface wave is launched along the surface of the lossy conducting medium 203. This can be verified by measuring field strength along a radial extending from the guided surface waveguide probe 200. The system may be further adjusted to improve coupling by iteratively adjusting the position of the tap 227 for the AC source 212 to be at the 50Ω point on the coil 215 and adjusting the position of tap 224 and/or 233 to maximize the ground current through the ammeter 236.

[0143] Referring back to FIG. 12, operation of a guided surface waveguide probe 200 may be controlled to adjust for variations in operational conditions associated with the guided surface waveguide probe 200. For example, a probe control system 230 can be used to control the feed network 209 and/or positioning of the charge terminal T_1 and/or compensation terminal T_2 to control the operation of the guided surface waveguide probe 200. Operational conditions can include, but are not limited to, variations in the characteristics of the lossy conducting medium 203 (*e.g.*, conductivity σ and relative permittivity ε_r), variations in field strength and/or variations in loading of the guided surface waveguide probe 200. As can be seen from Equations (41) – (44), the index of refraction (n), the complex Brewster angle ($\theta_{i,B}$ and $\psi_{i,B}$) , the wave tilt ($|W|e^{j\Psi}$) and the complex effective height ($h_{eff} = h_p e^{j\Phi}$) can be affected by changes in soil conductivity and permittivity resulting from, *e.g.*, weather conditions.

[0144] Equipment such as, *e.g.*, conductivity measurement probes, permittivity sensors, ground parameter meters, field meters, current monitors and/or load receivers can be used to monitor for changes in the operational conditions and provide information about current operational conditions to the probe control system 230. The probe control system 230 can then make one or more adjustments to the guided surface waveguide probe 200 to maintain specified operational conditions for the guided surface waveguide probe 200. For instance, as the moisture and temperature vary, the conductivity of the soil will also vary. Conductivity measurement probes and/or permittivity sensors may be located at multiple locations around the guided surface waveguide probe 200. Generally, it would be desirable to monitor the conductivity and/or permittivity at or about the Hankel crossover distance R_x for the operational frequency. Conductivity measurement probes and/or permittivity sensors may be

located at multiple locations (*e.g.*, in each quadrant) around the guided surface waveguide probe 200.

[0145] With reference then to FIG. 16, shown is an example of a guided surface waveguide probe 200e that includes a charge terminal T_1 and a charge terminal T_2 that are arranged along a vertical axis z. The guided surface waveguide probe 200e is disposed above a lossy conducting medium 203, which makes up Region 1. In addition, a second medium 206 shares a boundary interface with the lossy conducting medium 203 and makes up Region 2. The charge terminals T_1 and T_2 are positioned over the lossy conducting medium 203. The charge terminal T_1 is positioned at height H_1, and the charge terminal T_2 is positioned directly below T_1 along the vertical axis z at height H_2, where H_2 is less than H_1. The height h of the transmission structure presented by the guided surface waveguide probe 200e is $h = H_1 - H_2$. The guided surface waveguide probe 200e includes a feed network 209 that couples an excitation source 212 to the charge terminals T_1 and T_2.

[0146] The charge terminals T_1 and/or T_2 include a conductive mass that can hold an electrical charge, which may be sized to hold as much charge as practically possible. The charge terminal T_1 has a self-capacitance C_1, and the charge terminal T_2 has a self-capacitance C_2, which can be determined using, for example, equation (24). By virtue of the placement of the charge terminal T_1 directly above the charge terminal T_2, a mutual capacitance C_M is created between the charge terminals T_1 and T_2. Note that the charge terminals T_1 and T_2 need not be identical, but each can have a separate size and shape, and can include different conducting materials. Ultimately, the field strength of a guided surface wave launched by a guided surface waveguide probe 200e is directly proportional to the quantity of charge on the terminal T_1. The charge Q_1 is, in turn, proportional to the self-capacitance C_1 associated with the charge terminal T_1 since $Q_1 = C_1V$, where V is the voltage imposed on the charge terminal T_1.

[0147] When properly adjusted to operate at a predefined operating frequency, the guided surface waveguide probe 200e generates a guided surface wave along the surface of the lossy conducting medium 203. The excitation source 212 can generate electrical energy at the predefined frequency that is applied to the guided surface waveguide probe 200e to excite the structure. When the electromagnetic fields generated by the guided surface waveguide probe 200e are substantially mode-matched with the lossy conducting medium 203, the electromagnetic fields substantially synthesize a wave front incident at a complex Brewster angle that results in little or no reflection. Thus, the surface waveguide probe 200e does not produce a radiated wave, but launches a guided surface traveling wave along the surface of a lossy conducting medium 203. The energy from the excitation source 212 can

be transmitted as Zenneck surface currents to one or more receivers that are located within an effective transmission range of the guided surface waveguide probe 200e.

[0148] One can determine asymptotes of the radial Zenneck surface current $J_\rho(\rho)$ on the surface of the lossy conducting medium 203 to be $J_1(\rho)$ close-in and $J_2(\rho)$ far-out, where

$$\text{Close-in } (\rho < \lambda/8): J_\rho(\rho) \sim J_1 = \frac{I_1+I_2}{2\pi\rho} + \frac{E_\rho^{QS}(Q_1)+E_\rho^{QS}(Q_2)}{Z_\rho}, \text{ and} \quad (90)$$

$$\text{Far-out } (\rho >> \lambda/8): J_\rho(\rho) \sim J_2 = \frac{j\gamma\omega Q_1}{4} \times \sqrt{\frac{2\gamma}{\pi}} \times \frac{e^{-(\alpha+j\beta)\rho}}{\sqrt{\rho}}. \quad (91)$$

where I_1 is the conduction current feeding the charge Q_1 on the first charge terminal T_1, and I_2 is the conduction current feeding the charge Q_2 on the second charge terminal T_2. The charge Q_1 on the upper charge terminal T_1 is determined by $Q_1 = C_1V_1$, where C_1 is the isolated capacitance of the charge terminal T_1. Note that there is a third component to J_1 set forth above given by $\left(E_\rho^{Q_1}\right)/Z_\rho$, which follows from the Leontovich boundary condition and is the radial current contribution in the lossy conducting medium 203 pumped by the quasi-static field of the elevated oscillating charge on the first charge terminal Q_1. The quantity $Z_\rho = j\omega\mu_o/\gamma_e$ is the radial impedance of the lossy conducting medium, where $\gamma_e = (j\omega\mu_1\sigma_1 - \omega^2\mu_1\varepsilon_1)^{1/2}$.

[0149] The asymptotes representing the radial current close-in and far-out as set forth by equations (90) and (91) are complex quantities. According to various embodiments, a physical surface current $\mathbf{J}(\boldsymbol{\rho})$, is synthesized to match as close as possible the current asymptotes in *magnitude* and *phase*. That is to say close-in, $|\mathbf{J}(\boldsymbol{\rho})|$ is to be tangent to $|J_1|$, and far-out $|\mathbf{J}(\boldsymbol{\rho})|$ is to be tangent to $|J_2|$. Also, according to the various embodiments, the phase of $\mathbf{J}(\boldsymbol{\rho})$ should transition from the phase of J_1 close-in to the phase of J_2 far-out.

[0150] In order to match the guided surface wave mode at the site of transmission to launch a guided surface wave, the phase of the surface current $|J_2|$far-out should differ from the phase of the surface current $|J_1|$ close-in by the propagation phase corresponding to $e^{-j\beta(\rho_2-\rho_1)}$ plus a constant of approximately 45 degrees or 225 degrees. This is because there are two roots for $\sqrt{\gamma}$, one near π/4 and one near 5π/4. The properly adjusted synthetic radial surface current is

$$J_\rho(\rho, \phi, 0) = \frac{I_o\gamma}{4} H_1^{(2)}(-j\gamma\rho). \quad (92)$$

Note that this is consistent with equation (17). By Maxwell's equations, such a $\mathbf{J}(\boldsymbol{\rho})$ surface current automatically creates fields that conform to

$$H_\phi = \frac{-\gamma I_o}{4} e^{-u_2 z} H_1^{(2)}(-j\gamma\rho), \quad (93)$$

$$E_\rho = \frac{-\gamma I_o}{4}\left(\frac{u_2}{j\omega\varepsilon_o}\right) e^{-u_2 z} H_1^{(2)}(-j\gamma\rho), \text{ and} \quad (94)$$

$$E_z = \frac{-\gamma I_o}{4}\left(\frac{-\gamma}{\omega\varepsilon_o}\right) e^{-u_2 z} H_0^{(2)}(-j\gamma\rho). \quad (95)$$

Thus, the difference in phase between the surface current $|J_2|$ far-out and the surface current $|J_1|$ close-in for the guided surface wave mode that is to be matched is due to the characteristics of the Hankel functions in equations (93)-(95), which are consistent with equations (1)-(3). It is of significance to recognize that the fields expressed by equations (1)-(6) and (17) and equations (92)-(95) have the nature of *a transmission line mode* bound to a lossy interface, *not radiation fields* that are associated with groundwave propagation.

[0151] In order to obtain the appropriate voltage magnitudes and phases for a given design of a guided surface waveguide probe 200e at a given location, an iterative approach may be used. Specifically, analysis may be performed of a given excitation and configuration of a guided surface waveguide probe 200e taking into account the feed currents to the terminals T_1 and T_2, the charges on the charge terminals T_1 and T_2, and their images in the lossy conducting medium 203 in order to determine the radial surface current density generated. This process may be performed iteratively until an optimal configuration and excitation for a given guided surface waveguide probe 200e is determined based on desired parameters. To aid in determining whether a given guided surface waveguide probe 200e is operating at an optimal level, a guided field strength curve 103 (FIG. 1) may be generated using equations (1)-(12) based on values for the conductivity of Region 1 (σ_1) and the permittivity of Region 1 (ε_1) at the location of the guided surface waveguide probe 200e. Such a guided field strength curve 103 can provide a benchmark for operation such that measured field strengths can be compared with the magnitudes indicated by the guided field strength curve 103 to determine if optimal transmission has been achieved.

[0152] In order to arrive at an optimized condition, various parameters associated with the guided surface waveguide probe 200e may be adjusted. One parameter that may be varied to adjust the guided surface waveguide probe 200e is the height of one or both of the charge terminals T_1 and/or T_2 relative to the surface of the lossy conducting medium 203. In addition, the distance or spacing between the charge terminals T_1 and T_2 may also be adjusted. In doing so, one may minimize or otherwise alter the mutual capacitance C_M or any bound capacitances between the charge terminals T_1 and T_2 and the lossy conducting medium 203 as can be appreciated. The size of the respective charge terminals T_1 and/or T_2 can also be adjusted. By changing the size of the charge terminals T_1 and/or T_2, one will alter the respective self-capacitances C_1 and/or C_2, and the mutual capacitance C_M as can be appreciated.

[0153] Still further, another parameter that can be adjusted is the feed network 209 associated with the guided surface waveguide probe 200e. This may be accomplished by adjusting the size of the inductive and/or capacitive reactances that make up the feed network 209. For example, where such inductive reactances comprise coils, the number of

turns on such coils may be adjusted. Ultimately, the adjustments to the feed network 209 can be made to alter the electrical length of the feed network 209, thereby affecting the voltage magnitudes and phases on the charge terminals T_1 and T_2.

[0154] Note that the iterations of transmission performed by making the various adjustments may be implemented by using computer models or by adjusting physical structures as can be appreciated. By making the above adjustments, one can create corresponding "close-in" surface current J_1 and "far-out" surface current J_2 that approximate the same currents $\mathbf{J}(\rho)$ of the guided surface wave mode specified in Equations (90) and (91) set forth above. In doing so, the resulting electromagnetic fields would be substantially or approximately mode-matched to a guided surface wave mode on the surface of the lossy conducting medium 203.

[0155] While not shown in the example of FIG. 16, operation of the guided surface waveguide probe 200e may be controlled to adjust for variations in operational conditions associated with the guided surface waveguide probe 200. For example, a probe control system 230 shown in FIG. 12 can be used to control the feed network 209 and/or positioning and/or size of the charge terminals T_1 and/or T_2 to control the operation of the guided surface waveguide probe 200e. Operational conditions can include, but are not limited to, variations in the characteristics of the lossy conducting medium 203 (*e.g.*, conductivity σ and relative permittivity ε_r), variations in field strength and/or variations in loading of the guided surface waveguide probe 200e.

[0156] Referring now to FIG. 17, shown is an example of the guided surface waveguide probe 200e of FIG. 16, denoted herein as guided surface waveguide probe 200f. The guided surface waveguide probe 200f includes the charge terminals T_1 and T_2 that are positioned along a vertical axis z that is substantially normal to the plane presented by the lossy conducting medium 203 (e.g., the Earth). The second medium 206 is above the lossy conducting medium 203. The charge terminal T_1 has a self-capacitance C_1, and the charge terminal T_2 has a self-capacitance C_2. During operation, charges Q_1 and Q_2 are imposed on the charge terminals T_1 and T_2, respectively, depending on the voltages applied to the charge terminals T_1 and T_2 at any given instant. A mutual capacitance C_M may exist between the charge terminals T_1 and T_2 depending on the distance there between. In addition, bound capacitances may exist between the respective charge terminals T_1 and T_2 and the lossy conducting medium 203 depending on the heights of the respective charge terminals T_1 and T_2 with respect to the lossy conducting medium 203.

[0157] The guided surface waveguide probe 200f includes a feed network 209 that comprises an inductive impedance comprising a coil L_{1a} having a pair of leads that are coupled to respective ones of the charge terminals T_1 and T_2. In one embodiment, the coil

L_{1a} is specified to have an electrical length that is one-half (½) of the wavelength at the operating frequency of the guided surface waveguide probe 200f.

[0158] While the electrical length of the coil L_{1a} is specified as approximately one-half (1/2) the wavelength at the operating frequency, it is understood that the coil L_{1a} may be specified with an electrical length at other values. According to one embodiment, the fact that the coil L_{1a} has an electrical length of approximately one-half the wavelength at the operating frequency provides for an advantage in that a maximum voltage differential is created on the charge terminals T_1 and T_2. Nonetheless, the length or diameter of the coil L_{1a} may be increased or decreased when adjusting the guided surface waveguide probe 200f to obtain optimal excitation of a guided surface wave mode. Adjustment of the coil length may be provided by taps located at one or both ends of the coil. In other embodiments, it may be the case that the inductive impedance is specified to have an electrical length that is significantly less than or greater than ½ the wavelength at the operating frequency of the guided surface waveguide probe 200f.

[0159] The excitation source 212 can be coupled to the feed network 209 by way of magnetic coupling. Specifically, the excitation source 212 is coupled to a coil L_P that is inductively coupled to the coil L_{1a}. This may be done by link coupling, a tapped coil, a variable reactance, or other coupling approach as can be appreciated. To this end, the coil L_P acts as a primary, and the coil L_{1a} acts as a secondary as can be appreciated.

[0160] In order to adjust the guided surface waveguide probe 200f for the transmission of a desired guided surface wave, the heights of the respective charge terminals T_1 and T_2 may be altered with respect to the lossy conducting medium 203 and with respect to each other. Also, the sizes of the charge terminals T_1 and T_2 may be altered. In addition, the size of the coil L_{1a} may be altered by adding or eliminating turns or by changing some other dimension of the coil L_{1a}. The coil L_{1a} can also include one or more taps for adjusting the electrical length as shown in FIG. 17. The position of a tap connected to either charge terminal T_1 or T_2 can also be adjusted.

[0161] Referring next to FIGS. 18A, 18B, 18C and 19, shown are examples of generalized receive circuits for using the surface-guided waves in wireless power delivery systems. FIGS. 18A and 18B-18C include a linear probe 303 and a tuned resonator 306, respectively. FIG. 19 is a magnetic coil 309 according to various embodiments of the present disclosure. According to various embodiments, each one of the linear probe 303, the tuned resonator 306, and the magnetic coil 309 may be employed to receive power transmitted in the form of a guided surface wave on the surface of a lossy conducting medium 203 according to various embodiments. As mentioned above, in one embodiment the lossy conducting medium 203 comprises a terrestrial medium (or Earth).

[0162] With specific reference to FIG. 18A, the open-circuit terminal voltage at the output terminals 312 of the linear probe 303 depends upon the effective height of the linear probe 303. To this end, the terminal point voltage may be calculated as

$$V_T = \int_0^{h_e} E_{inc} \cdot dl, \tag{96}$$

where E_{inc} is the strength of the incident electric field induced on the linear probe 303 in Volts per meter, dl is an element of integration along the direction of the linear probe 303, and h_e is the effective height of the linear probe 303. An electrical load 315 is coupled to the output terminals 312 through an impedance matching network 318.

[0163] When the linear probe 303 is subjected to a guided surface wave as described above, a voltage is developed across the output terminals 312 that may be applied to the electrical load 315 through a conjugate impedance matching network 318 as the case may be. In order to facilitate the flow of power to the electrical load 315, the electrical load 315 should be substantially impedance matched to the linear probe 303 as will be described below.

[0164] Referring to FIG. 18B, a ground current excited coil 306a possessing a phase shift equal to the wave tilt of the guided surface wave includes a charge terminal T_R that is elevated (or suspended) above the lossy conducting medium 203. The charge terminal T_R has a self-capacitance C_R. In addition, there may also be a bound capacitance (not shown) between the charge terminal T_R and the lossy conducting medium 203 depending on the height of the charge terminal T_R above the lossy conducting medium 203. The bound capacitance should preferably be minimized as much as is practicable, although this may not be entirely necessary in every instance.

[0165] The tuned resonator 306a also includes a receiver network comprising a coil L_R having a phase shift Φ. One end of the coil L_R is coupled to the charge terminal T_R, and the other end of the coil L_R is coupled to the lossy conducting medium 203. The receiver network can include a vertical supply line conductor that couples the coil L_R to the charge terminal T_R. To this end, the coil L_R (which may also be referred to as tuned resonator L_R-C_R) comprises a series-adjusted resonator as the charge terminal C_R and the coil L_R are situated in series. The phase delay of the coil L_R can be adjusted by changing the size and/or height of the charge terminal T_R, and/or adjusting the size of the coil L_R so that the phase Φ of the structure is made substantially equal to the angle of the wave tilt Ψ. The phase delay of the vertical supply line can also be adjusted by, e.g., changing length of the conductor.

[0166] For example, the reactance presented by the self-capacitance C_R is calculated as $1/j\omega C_R$. Note that the total capacitance of the structure 306a may also include capacitance between the charge terminal T_R and the lossy conducting medium 203, where the total capacitance of the structure 306a may be calculated from both the self-capacitance

C_R and any bound capacitance as can be appreciated. According to one embodiment, the charge terminal T_R may be raised to a height so as to substantially reduce or eliminate any bound capacitance. The existence of a bound capacitance may be determined from capacitance measurements between the charge terminal T_R and the lossy conducting medium 203 as previously discussed.

[0167] The inductive reactance presented by a discrete-element coil L_R may be calculated as $j\omega L$, where L is the lumped-element inductance of the coil L_R. If the coil L_R is a distributed element, its equivalent terminal-point inductive reactance may be determined by conventional approaches. To tune the structure 306a, one would make adjustments so that the phase delay is equal to the wave tilt for the purpose of mode-matching to the surface waveguide at the frequency of operation. Under this condition, the receiving structure may be considered to be "mode-matched" with the surface waveguide. A transformer link around the structure and/or an impedance matching network 324 may be inserted between the probe and the electrical load 327 in order to couple power to the load. Inserting the impedance matching network 324 between the probe terminals 321 and the electrical load 327 can effect a conjugate-match condition for maximum power transfer to the electrical load 327.

[0168] When placed in the presence of surface currents at the operating frequencies power will be delivered from the surface guided wave to the electrical load 327. To this end, an electrical load 327 may be coupled to the structure 306a by way of magnetic coupling, capacitive coupling, or conductive (direct tap) coupling. The elements of the coupling network may be lumped components or distributed elements as can be appreciated.

[0169] In the embodiment shown in FIG. 18B, magnetic coupling is employed where a coil L_S is positioned as a secondary relative to the coil L_R that acts as a transformer primary. The coil L_S may be link-coupled to the coil L_R by geometrically winding it around the same core structure and adjusting the coupled magnetic flux as can be appreciated. In addition, while the receiving structure 306a comprises a series-tuned resonator, a parallel-tuned resonator or even a distributed-element resonator of the appropriate phase delay may also be used.

[0170] While a receiving structure immersed in an electromagnetic field may couple energy from the field, it can be appreciated that polarization-matched structures work best by maximizing the coupling, and conventional rules for probe-coupling to waveguide modes should be observed. For example, a TE_{20} (transverse electric mode) waveguide probe may be optimal for extracting energy from a conventional waveguide excited in the TE_{20} mode. Similarly, in these cases, a mode-matched and phase-matched receiving structure can be optimized for coupling power from a surface-guided wave. The guided surface wave excited

by a guided surface waveguide probe 200 on the surface of the lossy conducting medium 203 can be considered a waveguide mode of an open waveguide. Excluding waveguide losses, the source energy can be completely recovered. Useful receiving structures may be E-field coupled, H-field coupled, or surface-current excited.

[0171] The receiving structure can be adjusted to increase or maximize coupling with the guided surface wave based upon the local characteristics of the lossy conducting medium 203 in the vicinity of the receiving structure. To accomplish this, the phase delay (Φ) of the receiving structure can be adjusted to match the angle (Ψ) of the wave tilt of the surface traveling wave at the receiving structure. If configured appropriately, the receiving structure may then be tuned for resonance with respect to the perfectly conducting image ground plane at complex depth $z = -d/2$.

[0172] For example, consider a receiving structure comprising the tuned resonator 306a of FIG. 18B, including a coil L_R and a vertical supply line connected between the coil L_R and a charge terminal T_R. With the charge terminal T_R positioned at a defined height above the lossy conducting medium 203, the total phase shift Φ of the coil L_R and vertical supply line can be matched with the angle (Ψ) of the wave tilt at the location of the tuned resonator 306a. From Equation (22), it can be seen that the wave tilt asymptotically passes to

$$W = |W|e^{j\Psi} = \frac{E_\rho}{E_z} \xrightarrow[\rho\to\infty]{} \frac{1}{\sqrt{\varepsilon_r - j\frac{\sigma_1}{\omega\varepsilon_o}}}, \tag{97}$$

where ε_r comprises the relative permittivity and σ_1 is the conductivity of the lossy conducting medium 203 at the location of the receiving structure, ε_o is the permittivity of free space, and $\omega = 2\pi f$, where f is the frequency of excitation. Thus, the wave tilt angle (Ψ) can be determined from Equation (97).

[0173] The total phase shift ($\Phi = \theta_c + \theta_y$) of the tuned resonator 306a includes both the phase delay (θ_c) through the coil L_R and the phase delay of the vertical supply line (θ_y). The spatial phase delay along the conductor length l_w of the vertical supply line can be given by $\theta_y = \beta_w l_w$, where β_w is the propagation phase constant for the vertical supply line conductor. The phase delay due to the coil (or helical delay line) is $\theta_c = \beta_p l_C$, with a physical length of l_C and a propagation factor of

$$\beta_p = \frac{2\pi}{\lambda_p} = \frac{2\pi}{V_f \lambda_0}, \tag{98}$$

where V_f is the velocity factor on the structure, λ_0 is the wavelength at the supplied frequency, and λ_p is the propagation wavelength resulting from the velocity factor V_f. One or both of the phase delays ($\theta_c + \theta_y$) can be adjusted to match the phase shift Φ to the angle (Ψ) of the wave tilt. For example, a tap position may be adjusted on the coil L_R of FIG. 18B to adjust the coil phase delay (θ_c) to match the total phase shift to the wave tilt angle ($\Phi = \Psi$).

For example, a portion of the coil can be bypassed by the tap connection as illustrated in FIG. 18B. The vertical supply line conductor can also be connected to the coil L_R via a tap, whose position on the coil may be adjusted to match the total phase shift to the angle of the wave tilt.

[0174] Once the phase delay (Φ) of the tuned resonator 306a has been adjusted, the impedance of the charge terminal T_R can then be adjusted to tune to resonance with respect to the perfectly conducting image ground plane at complex depth $z = -d/2$. This can be accomplished by adjusting the capacitance of the charge terminal T_1 without changing the traveling wave phase delays of the coil L_R and vertical supply line. The adjustments are similar to those described with respect to FIGS. 9A and 9B.

[0175] The impedance seen "looking down" into the lossy conducting medium 203 to the complex image plane is given by:

$$Z_{in} = R_{in} + jX_{in} = Z_o \tanh\left(j\beta_o(\mathrm{d}/2)\right), \tag{99}$$

where $\beta_o = \omega\sqrt{\mu_o\varepsilon_o}$. For vertically polarized sources over the Earth, the depth of the complex image plane can be given by:

$$\mathrm{d}/2 \approx 1/\sqrt{j\omega\mu_1\sigma_1 - \omega^2\mu_1\varepsilon_1}\,, \tag{100}$$

where μ_1 is the permeability of the lossy conducting medium 203 and $\varepsilon_1 = \varepsilon_r\varepsilon_o$.

[0176] At the base of the tuned resonator 306a, the impedance seen "looking up" into the receiving structure is $Z_{\uparrow} = Z_{base}$ as illustrated in FIG. 9A. With a terminal impedance of:

$$Z_R = \frac{1}{j\omega C_R}\,, \tag{101}$$

where C_R is the self-capacitance of the charge terminal T_R, the impedance seen "looking up" into the vertical supply line conductor of the tuned resonator 306a is given by:

$$Z_2 = Z_W \frac{Z_R + Z_W \tanh(j\beta_w h_w)}{Z_w + Z_R \tanh(j\beta_w h_w)} = Z_W \frac{Z_R + Z_W \tanh(j\theta_y)}{Z_w + Z_R \tanh(j\theta_y)}\,, \tag{102}$$

and the impedance seen "looking up" into the coil L_R of the tuned resonator 306a is given by:

$$Z_{base} = R_{base} + jX_{base} = Z_R \frac{Z_2 + Z_R \tanh(j\beta_p H)}{Z_R + Z_2 \tanh(j\beta_p H)} = Z_c \frac{Z_2 + Z_R \tanh(j\theta_c)}{Z_R + Z_2 \tanh(j\theta_c)}\,. \tag{103}$$

By matching the reactive component (X_{in}) seen "looking down" into the lossy conducting medium 203 with the reactive component (X_{base}) seen "looking up" into the tuned resonator 306a, the coupling into the guided surface waveguide mode may be maximized.

[0177] Referring next to FIG. 18C, shown is an example of a tuned resonator 306b that does not include a charge terminal T_R at the top of the receiving structure. In this embodiment, the tuned resonator 306b does not include a vertical supply line coupled between the coil L_R and the charge terminal T_R. Thus, the total phase shift (Φ) of the tuned resonator 306b includes only the phase delay (θ_c) through the coil L_R. As with the tuned resonator 306a of FIG. 18B, the coil phase delay θ_c can be adjusted to match the angle (Ψ)

of the wave tilt determined from Equation (97), which results in $\Phi = \Psi$. While power extraction is possible with the receiving structure coupled into the surface waveguide mode, it is difficult to adjust the receiving structure to maximize coupling with the guided surface wave without the variable reactive load provided by the charge terminal T_R.

[0178] Referring to FIG. 18D, shown is a flow chart 180 illustrating an example of adjusting a receiving structure to substantially mode-match to a guided surface waveguide mode on the surface of the lossy conducting medium 203. Beginning with 181, if the receiving structure includes a charge terminal T_R (e.g., of the tuned resonator 306a of FIG. 18B), then the charge terminal T_R is positioned at a defined height above a lossy conducting medium 203 at 184. As the surface guided wave has been established by a guided surface waveguide probe 200, the physical height (h_p) of the charge terminal T_R may be below that of the effective height. The physical height may be selected to reduce or minimize the bound charge on the charge terminal T_R (e.g., four times the spherical diameter of the charge terminal). If the receiving structure does not include a charge terminal T_R (e.g., of the tuned resonator 306b of FIG. 18C), then the flow proceeds to 187.

[0179] At 187, the electrical phase delay Φ of the receiving structure is matched to the complex wave tilt angle Ψ defined by the local characteristics of the lossy conducting medium 203. The phase delay (θ_c) of the helical coil and/or the phase delay (θ_y) of the vertical supply line can be adjusted to make Φ equal to the angle (Ψ) of the wave tilt (W). The angle (Ψ) of the wave tilt can be determined from Equation (86). The electrical phase Φ can then be matched to the angle of the wave tilt. For example, the electrical phase delay $\Phi = \theta_c + \theta_y$ can be adjusted by varying the geometrical parameters of the coil L_R and/or the length (or height) of the vertical supply line conductor.

[0180] Next at 190, the load impedance of the charge terminal T_R can be tuned to resonate the equivalent image plane model of the tuned resonator 306a. The depth ($\mathrm{d}/2$) of the conducting image ground plane 139 (FIG. 9A) below the receiving structure can be determined using Equation (100) and the values of the lossy conducting medium 203 (e.g., the Earth) at the receiving structure, which can be locally measured. Using that complex depth, the phase shift (θ_d) between the image ground plane 139 and the physical boundary 136 (FIG. 9A) of the lossy conducting medium 203 can be determined using $\theta_d = \beta_o \, \mathrm{d}/2$. The impedance ($Z_{in}$) as seen "looking down" into the lossy conducting medium 203 can then be determined using Equation (99). This resonance relationship can be considered to maximize coupling with the guided surface waves.

[0181] Based upon the adjusted parameters of the coil L_R and the length of the vertical supply line conductor, the velocity factor, phase delay, and impedance of the coil L_R and vertical supply line can be determined. In addition, the self-capacitance (C_R) of the charge

terminal T_R can be determined using, e.g., Equation (24). The propagation factor (β_p) of the coil L_R can be determined using Equation (98), and the propagation phase constant (β_w) for the vertical supply line can be determined using Equation (49). Using the self-capacitance and the determined values of the coil L_R and vertical supply line, the impedance (Z_{base}) of the tuned resonator 306a as seen "looking up" into the coil L_R can be determined using Equations (101), (102), and (103).

[0182] The equivalent image plane model of FIG. 9A also applies to the tuned resonator 306a of FIG. 18B. The tuned resonator 306a can be tuned to resonance with respect to the complex image plane by adjusting the load impedance Z_R of the charge terminal T_R such that the reactance component X_{base} of Z_{base} cancels out the reactance component of X_{in} of Z_{in}, or $X_{base} + X_{in} = 0$. Thus, the impedance at the physical boundary 136 (FIG. 9A) "looking up" into the coil of the tuned resonator 306a is the conjugate of the impedance at the physical boundary 136 "looking down" into the lossy conducting medium 203. The load impedance Z_R can be adjusted by varying the capacitance (C_R) of the charge terminal T_R without changing the electrical phase delay $\Phi = \theta_c + \theta_y$ seen by the charge terminal T_R. An iterative approach may be taken to tune the load impedance Z_R for resonance of the equivalent image plane model with respect to the conducting image ground plane 139. In this way, the coupling of the electric field to a guided surface waveguide mode along the surface of the lossy conducting medium 203 (e.g., Earth) can be improved and/or maximized.

[0183] Referring to FIG. 19, the magnetic coil 309 comprises a receive circuit that is coupled through an impedance matching network 333 to an electrical load 336. In order to facilitate reception and/or extraction of electrical power from a guided surface wave, the magnetic coil 309 may be positioned so that the magnetic flux of the guided surface wave, H_φ, passes through the magnetic coil 309, thereby inducing a current in the magnetic coil 309 and producing a terminal point voltage at its output terminals 330. The magnetic flux of the guided surface wave coupled to a single turn coil is expressed by

$$\mathcal{F} = \iint_{A_{CS}} \mu_r \mu_o \vec{H} \cdot \hat{n} dA \tag{104}$$

where $\mathcal{F}$ is the coupled magnetic flux, μ_r is the effective relative permeability of the core of the magnetic coil 309, μ_o is the permeability of free space, $\vec{H}$ is the incident magnetic field strength vector, $\hat{n}$ is a unit vector normal to the cross-sectional area of the turns, and A_{CS} is the area enclosed by each loop. For an N-turn magnetic coil 309 oriented for maximum coupling to an incident magnetic field that is uniform over the cross-sectional area of the magnetic coil 309, the open-circuit induced voltage appearing at the output terminals 330 of the magnetic coil 309 is

$$V = -N\frac{d\mathcal{F}}{dt} \approx -j\omega\mu_r\mu_0 NHA_{CS}, \quad (105)$$

where the variables are defined above. The magnetic coil 309 may be tuned to the guided surface wave frequency either as a distributed resonator or with an external capacitor across its output terminals 330, as the case may be, and then impedance-matched to an external electrical load 336 through a conjugate impedance matching network 333.

[0184] Assuming that the resulting circuit presented by the magnetic coil 309 and the electrical load 336 are properly adjusted and conjugate impedance matched, via impedance matching network 333, then the current induced in the magnetic coil 309 may be employed to optimally power the electrical load 336. The receive circuit presented by the magnetic coil 309 provides an advantage in that it does not have to be physically connected to the ground.

[0185] With reference to FIGS. 18A, 18B, 18C and 19, the receive circuits presented by the linear probe 303, the mode-matched structure 306, and the magnetic coil 309 each facilitate receiving electrical power transmitted from any one of the embodiments of guided surface waveguide probes 200 described above. To this end, the energy received may be used to supply power to an electrical load 315/327/336 via a conjugate matching network as can be appreciated. This contrasts with the signals that may be received in a receiver that were transmitted in the form of a *radiated* electromagnetic field. Such signals have very low available power, and receivers of such signals do not load the transmitters.

[0186] It is also characteristic of the present guided surface waves generated using the guided surface waveguide probes 200 described above that the receive circuits presented by the linear probe 303, the mode-matched structure 306, and the magnetic coil 309 will load the excitation source 212 (e.g., FIGS. 3, 12 and 16) that is applied to the guided surface waveguide probe 200, thereby generating the guided surface wave to which such receive circuits are subjected. This reflects the fact that the guided surface wave generated by a given guided surface waveguide probe 200 described above comprises a transmission line mode. By way of contrast, a power source that drives a radiating antenna that generates a radiated electromagnetic wave is not loaded by the receivers, regardless of the number of receivers employed.

[0187] Thus, together one or more guided surface waveguide probes 200 and one or more receive circuits in the form of the linear probe 303, the tuned mode-matched structure 306, and/or the magnetic coil 309 can make up a wireless distribution system. Given that the distance of transmission of a guided surface wave using a guided surface waveguide probe 200 as set forth above depends upon the frequency, it is possible that wireless power distribution can be achieved across wide areas and even globally.

[0188] The conventional wireless-power transmission/distribution systems extensively investigated today include “energy harvesting” from radiation fields and also sensor coupling

to inductive or reactive near-fields. In contrast, the present wireless-power system does not waste power in the form of radiation which, if not intercepted, is lost forever. Nor is the presently disclosed wireless-power system limited to extremely short ranges as with conventional mutual-reactance coupled near-field systems. The wireless-power system disclosed herein probe-couples to the novel surface-guided transmission line mode, which is equivalent to delivering power to a load by a wave-guide or a load directly wired to the distant power generator. Not counting the power required to maintain transmission field strength plus that dissipated in the surface waveguide, which at extremely low frequencies is insignificant relative to the transmission losses in conventional high-tension power lines at 60 Hz, all of the generator power goes only to the desired electrical load. When the electrical load demand is terminated, the source power generation is relatively idle.

[0189] Referring next to FIGS. 20A-E, shown are examples of various schematic symbols that are used with reference to the discussion that follows. With specific reference to FIG. 20A, shown is a symbol that represents any one of the guided surface waveguide probes 200a, 200b, 200c, 200e, 200d, or 200f; or any variations thereof. In the following drawings and discussion, a depiction of this symbol will be referred to as a guided surface waveguide probe P. For the sake of simplicity in the following discussion, any reference to the guided surface waveguide probe P is a reference to any one of the guided surface waveguide probes 200a, 200b, 200c, 200e, 200d, or 200f; or variations thereof.

[0190] Similarly, with reference to FIG. 20B, shown is a symbol that represents a guided surface wave receive structure that may comprise any one of the linear probe 303 (FIG. 18A), the tuned resonator 306 (FIGS. 18B-18C), or the magnetic coil 309 (FIG. 19). In the following drawings and discussion, a depiction of this symbol will be referred to as a guided surface wave receive structure R. For the sake of simplicity in the following discussion, any reference to the guided surface wave receive structure R is a reference to any one of the linear probe 303, the tuned resonator 306, or the magnetic coil 309; or variations thereof.

[0191] Further, with reference to FIG. 20C, shown is a symbol that specifically represents the linear probe 303 (FIG. 18A). In the following drawings and discussion, a depiction of this symbol will be referred to as a guided surface wave receive structure R_P. For the sake of simplicity in the following discussion, any reference to the guided surface wave receive structure R_P is a reference to the linear probe 303 or variations thereof.

[0192] Further, with reference to FIG. 20D, shown is a symbol that specifically represents the tuned resonator 306 (FIGS. 18B-18C). In the following drawings and discussion, a depiction of this symbol will be referred to as a guided surface wave receive structure R_R. For the sake of simplicity in the following discussion, any reference to the

guided surface wave receive structure R_R is a reference to the tuned resonator 306 or variations thereof.

[0193] Further, with reference to FIG. 20E, shown is a symbol that specifically represents the magnetic coil 309 (FIG. 19). In the following drawings and discussion, a depiction of this symbol will be referred to as a guided surface wave receive structure R_M. For the sake of simplicity in the following discussion, any reference to the guided surface wave receive structure R_M is a reference to the magnetic coil 309 or variations thereof.

[0194] With reference to FIGS. 21-27, disclosed are various embodiments for locating a position using guided surface waves launched from a guided surface wave waveguide probe P. A navigation device detects multiple guided surface waves launched from multiple guided surface wave waveguide probes P. By analyzing the time difference on arrival of the guided surface waves, the time each of the guided surface waves spent traveling from the corresponding guided surface wave waveguide probe P to the location of the navigation device, the difference in the intensity of the guided surface waves at the location of the navigation device compared to the original intensity of the guided surface waves, the phase shift between the guided surface waves measured at the location of the navigation device, or some combination of these approaches, the location of the navigation device on the Earth may be determined. Further, in some embodiments, the navigation device may be powered by one or more of the guided surface waves. Moreover, the guide surface waves may be used for time synchronization to improve the accuracy of the navigation device and/or other devices.

[0195] The range of the guided surface waves is dependent on the frequency of the guided surface waves. For examples, guided surface waves with a frequency of approximately 20kHz or less are capable of travelling around the earth. At these frequencies, the various embodiments of the present disclosure may be used for global positioning and navigation. Higher frequencies will go shorter distances, such as hundreds or tens of miles, limiting the various embodiments to regional usage for position and navigation. Note that the frequency of the guided surface wave may also determine whether the guided surface wave travels at a uniform speed around the entire Earth. Specifically, the lower the frequency, the more likely that the guided surface wave will be uniform around its circumference. However, at higher frequencies, local terrain or water may cause a difference in the speed of propagation. Such effects should be taken into account in the various embodiments described herein if they are significant.

[0196] With specific reference to FIG. 21, shown is a navigation unit 400 according to various embodiments. The navigation unit 400 includes a receiver 403, an antenna mount 406, and a computing device 409. The receiver 403 is connected to the antenna mount 406,

which is in turn connected to the computing device 409. In some embodiments, the navigation unit 400 may include a display. In such embodiments, the display may comprise, for example, one or more devices such as liquid crystal display (LCD) displays, gas plasma-based flat panel displays, organic light emitting diode (OLED) displays, electrophoretic ink (E ink) displays, LCD projectors, or other types of display devices, *etc*.

[0197] In some embodiments, all or portions of the navigation unit 400 may be enclosed in an external case that protects the various components of the navigation unit 400. For example, in some embodiments, the navigation unit 400 may be a portable or handheld unit, with the receiver 403, the antenna mount 406, and the computing device 409 enclosed within a single shell. Such embodiments may include a mobile computing device, such as a tablet computer, a cellular phone, a smart phone, a personal digital assistant (PDA), and/or similar mobile computing device. Such embodiments may also include a dedicated navigation unit, such as personal navigation devices, handheld navigation devices, or navigation devices that can be mounted to the dashboard of a bus, automobile, motor boat, or similar vehicle. In other embodiments, the receiver 403 may be remote or external to the computing device 409 and connected to the computing device via the antenna mount 406. Such embodiments may include, for example, vehicular navigation units 400, such as those found on ships or in airplanes.

[0198] The receiver 403 may correspond to one or more structures capable of receiving a guided surface wave. The receiver 403 may include, for example, a linear probe, a tuned resonator, a magnetic coil, and/or similar structures for receiving a guided surface wave, as previously described above. In some embodiments, the receiver 403 may represent a plurality of receivers 403, each of which is tuned to receive a guided surface wave on a different frequency from the other receivers 403. In various embodiments, the receiver 403 may be configured to be tuned to receive multiple guided surface waves on different frequencies simultaneously. In some embodiments, the receiver 403 may be configured to alternate frequencies in order to detect, receive, and/or measure a guided surface wave on a first frequency and then switch to a second frequency to detect a second guided surface wave on a second frequency. The antenna mount 406 may correspond to any physical structure capable of connecting the receiver 403 to the computing device 409.

[0199] The computing device 409 can also include at least one processor circuit having a processor 413 and a memory 416, both of which are coupled to a local interface 419. The local interface 419 may comprise, for example, a data bus with an accompanying address/control bus or other bus structure as can be appreciated. Stored in the memory 416 are both data and several components that are executable by the processor 413. In particular, stored in the memory 416 and executable by the processor 413 is a multilateration

application 423, and potentially other applications. Also stored in the memory 416 may be a data store 426, which may store map data 429, inertial data 431, and/or potentially other data. In addition, an operating system may be stored in the memory 416 and executable by the processor 413.

[0200] The map data 429 represents one or more geographies within which the navigation unit 400 may be navigating or in which geolocation may be occurring. Map data 429 may include global data, or data related to particular regions or locales, such as a hemisphere, continent, ocean, sea, lake, country, state/province, city, and/or portions thereof. Map data 429 may also include one or more coordinate systems for identifying a location on the globe, or within a particular region or locale. Such coordinate systems may include latitude and longitude lines, the Universal Transverse Mercator (UTM) coordinate system, the Universal Polar Stereographic (UPS) coordinate system, a grid system, and/or other coordinate systems.

[0201] The map data 429 can include relevant data necessary to disambiguate between locations on the globe. This can include a list of cellular networks in various countries or regions. This can include a list of radio or television broadcast stations in various countries or regions. In some instances, this can include a list of media access control (MAC) addresses for wireless network access points at various locations. In various instances, this can also include data related to specific ground stations located around the globe. Such data can include the location of the ground station, a base frequency of a primary guided surface wave launched from a guided surface waveguide probe at the ground station, and the frequencies at which overlaid guided surface waves are launched from one or more other guided surface waveguide probes at the ground station. The data can also include the initial phase at which the various guided surface waves are launched from the ground station.

[0202] The inertial data 431 represents navigational data describing the current and historical trajectories of the navigation unit 400. Inertial data 431 may represent, for example, a current speed, a current altitude, and/or a current heading of the navigation unit 400 or an object to which the navigation unit 400 is attached, as well as other navigation data. Inertial data 431 may also include historical data, such as an initial or starting location, past speeds and corresponding headings, past altitudes, and/or other navigation data.

[0203] The multilateration application 423 is executed to identify the location of the navigation unit 400 based on one or more guided surface waves received by the navigation unit 400. For example, the multilateration application 423 can determine which overlaid guided surface waves are reaching the navigation unit 400 in order to determine which wavelength of a base guided surface wave the navigation unit 400 is currently within. The multilateration application 423 can then determine the position of the navigation unit 400

within the wavelength from the phase of the base guided surface wave at the location of the navigation unit 400. Based on the position, the multilateration application 423 can calculate the distance from the ground station that includes the guided surface waveguide probe that launched the base guided surface wave.

[0204] It is understood that there may be other applications that are stored in the memory 416 and are executable by the processor 413 as can be appreciated. These other applications may, for example, be executed to determine the intensity of guided surface waves detected by the navigation unit 400 with the receiver 403. Where any component discussed herein is implemented in the form of software, any one of a number of programming languages may be employed such as, for example, C, C++, C#, Objective C, Java®, JavaScript®, Perl, PHP, Visual Basic®, Python®, Ruby, Flash®, or other programming languages.

[0205] A number of software components are stored in the memory 416 and are executable by the processor 413. In this respect, the term "executable" means a program file that is in a form that can ultimately be run by the processor 413. Examples of executable programs may be, for example, a compiled program that can be translated into machine code in a format that can be loaded into a random access portion of the memory 416 and run by the processor 413, source code that may be expressed in proper format such as object code that is capable of being loaded into a random access portion of the memory 416 and executed by the processor 413, or source code that may be interpreted by another executable program to generate instructions in a random access portion of the memory 416 to be executed by the processor 413, *etc*. An executable program may be stored in any portion or component of the memory 416 including, for example, random access memory (RAM), read-only memory (ROM), hard drive, solid-state drive, USB flash drive, memory card, optical disc such as compact disc (CD) or digital versatile disc (DVD), floppy disk, magnetic tape, or other memory components.

[0206] The memory 416 is defined herein as including both volatile and nonvolatile memory and data storage components. Volatile components are those that do not retain data values upon loss of power. Nonvolatile components are those that retain data upon a loss of power. Thus, the memory 416 may comprise, for example, random access memory (RAM), read-only memory (ROM), hard disk drives, solid-state drives, USB flash drives, memory cards accessed via a memory card reader, floppy disks accessed via an associated floppy disk drive, optical discs accessed via an optical disc drive, magnetic tapes accessed via an appropriate tape drive, and/or other memory components, or a combination of any two or more of these memory components. In addition, the RAM may comprise, for example, static random access memory (SRAM), dynamic random access memory (DRAM), or

magnetic random access memory (MRAM) and other such devices. The ROM may comprise, for example, a programmable read-only memory (PROM), an erasable programmable read-only memory (EPROM), an electrically erasable programmable read-only memory (EEPROM), or other like memory device.

[0207] Also, the processor 413 may represent multiple processors 413 and/or multiple processor cores and the memory 416 may represent multiple memories 416 that operate in parallel processing circuits, respectively. In such a case, the local interface 419 may be an appropriate network that facilitates communication between any two of the multiple processors 413, between any processor 413 and any of the memories 416, or between any two of the memories 416, *etc*. The local interface 419 may comprise additional systems designed to coordinate this communication, including, for example, performing load balancing. The processor 413 may be of electrical or of some other available construction.

[0208] Although the multilateration application 423, and other various systems described herein may be embodied in software or code executed by general purpose hardware as discussed above, as an alternative the same may also be embodied in dedicated hardware or a combination of software/general purpose hardware and dedicated hardware. If embodied in dedicated hardware, each can be implemented as a circuit or state machine that employs any one of or a combination of a number of technologies. These technologies may include, but are not limited to, discrete logic circuits having logic gates for implementing various logic functions upon an application of one or more data signals, application specific integrated circuits (ASICs) having appropriate logic gates, field-programmable gate arrays (FPGAs), or other components, *etc.* Such technologies are generally well known by those skilled in the art and, consequently, are not described in detail herein.

[0209] Moving on to FIG. 22, shown is an illustration of some of the principals underlying geolocation using guided surface waves. As illustrated, a ground station 500 launches a base guided surface wave corresponding to a standing guided surface wave. Although the base guided surface wave traverses the Earth and reflects from the antipode of the ground station 500 to create a standing wave, the base guided surface wave is illustrated herein as having a range equal to that of the bas knee 503 for illustrative purposes. The ground station 500 also launches a number of overlaid guided surface waves at higher frequencies, which travel shorter distances before suddenly dissipating at the respective overlaid knees 506a, 506b, 506c, and 506d. Generally, the frequency of the overlaid guided surface waves will be chosen such that the overlaid knees 506a, 506b, 506c, and 506d are separated by a distance equal to one wavelength of the base guided surface wave.

[0210] In some embodiments, the ground station 500 can include a number of guided surface waveguide probes P, each of which is configured to continuously launch a guided surface wave. As an illustrative example, if the ground station 500 were to launch a base guided surface wave and four overlaid guided surface waves, then the ground station 500 could include a first guided surface waveguide probe that launches the based guided surface wave to create a standing wave and four additional guided surface waveguide probes, each of which is configured to continuously launch a respective one of the four overlaid guided surface waves.

[0211] In other embodiments, the ground station 500 can include a single guided surface waveguide probe P. In such an embodiment, the single guided surface waveguide probe P can be configured to launch the base guided surface wave and each of the overlaid guided surface waves. For example, the single guided surface waveguide probe P may first launch the based guided surface wave, then reconfigure itself (or be reconfigured) to launch a first overlaid guided surface wave at a first frequency at a later specified time. The single guided surface waveguide probe could then continue to launch additional overlaid guided surface waves before cycling back to relaunch the base guided surface wave, continuing the cycle.

[0212] Proceeding next to FIG. 23, shown is another illustration of some of the principals underlying geolocation using guided surface waves. Here, the overlaid knees 506a, 506b, 506c, and 506d of the overlaid guided surface waves occur one wavelength of the base guided surface wave apart. Between the ground station 500 (FIG. 22) and the first overlaid knee 506a is a distance equal to a first wavelength 509a of the base guided surface wave of the base guided surface wave. The distance between the first overlaid knee 506a and the second overlaid knee 506b is a distance equal to a second wavelength 509b of the base guided surface wave. The distance between the second overlaid knee 506b and the third overlaid knee 506c is equal to a third wavelength 509c of the base guided surface wave. The distance between the third overlaid knee 506c and a fourth overlaid knee 506d is equal to a fourth wavelength 509d of the base guided surface wave.

[0213] If the navigation unit 400 (FIG. 21) can determine its location based on which of the overlaid guided surface waves it can receive. For example, if the navigation unit 400 determined that it could receive the overlaid guided surface waves corresponding to the third overlaid knee 506c, but not the guided surface wave corresponding to the second overlaid knee 506b, the navigation unit 400 could determine that its position is somewhere between the second overlaid knee 506b and the third overlaid knee 506c. By determining the phase of the base guided surface wave, the navigation unit 400 could determine where it was between the second overlaid knee 506b and the third overlaid knee 506c.

[0214] Referring next to FIG. 24, shown is a graphical representation of a determination of a location of the navigation unit 400 (FIG. 21) by the multilateration application 423 (FIG. 21). Here, a first ground station 500a launches a first base guided surface wave and several overlaid guided surface waves. The navigation unit 400 receives the first base guided surface wave at a point along a first circumference of a first circle 513a. A second ground station 500b launches a second based guided surface wave and several overlaid guided surface waves. The navigation unit 400 receives the second based guided surface wave at a point somewhere along a second circumference of a second circle 513b.

[0215] The navigation unit 400 also receives some of the overlaid guided surface waves launched from the first ground station 500a and some of the overlaid guided surface waves launched from the second ground station 500b. The navigation unit 400 can use the overlaid guided surface waves that are received to determine the distance of the navigation unit 400 from each ground station. For example, if the navigation unit 400 were to receive a second overlaid guided surface wave launched from the first ground station 500a with a second overlaid knee 506b, but not a first overlaid guided surface wave launched from the first ground station 500a, then the navigation unit 400 could determine how far it is from the first ground station 500a. This would correspond to a radius for the first circumference of the first circle 513a. Similarly, if the navigation unit 400 were to receive a third overlaid guided surface wave launched from the second ground station 500b with a third overlaid knee 509b, but not a first or a second overlaid guided surface wave launched from the second ground station 500b, the then the navigation unit 400 could determine how far it is from the second ground station 500b. This would correspond to a radius for the second circumference of the second circle 513b. The guided surface waveguide probes P that generate the base and overlaid guided surface waves may comprise the same guided surface waveguide probe P that transmits at multiple frequencies, or it may comprise a plurality of probes that are located in very close proximity to a single point.

[0216] The navigation unit 400 can then identify its potential location as being at any intersection 516 of the first circumference of the first circle 513a and the second circumference of the second circle 513b. The navigation unit 400 can then use additional information to disambiguate between potential locations based on other data. For example, if a third ground station were launching guided surface waves, the navigation unit 400 could isolate its location to the intersection 516 matching the distance of the navigation unit 400 from the third ground station. As another example, the navigation unit 400 could use inertial data 431 or other historical data to identify which intersection 516 corresponds to the current location of the navigation unit 400. In some instances, the navigation unit 400 could use environment data (*e.g.* available cellular networks, available Wi-Fi networks, available radio

or television broadcast signals, or similar data) to identify which intersection 516 corresponds to the current location of the navigation unit 400.

[0217] Moving on to FIG. 25 shown is a flowchart that provides one example of the operation of a portion of the multilateration application 423 according to various embodiments. It is understood that the flowchart of FIG. 25 provides merely an example of the many different types of functional arrangements that may be employed to implement the operation of the portion of the multilateration application 423 as described herein. As an alternative, the flowchart of FIG. 25 may be viewed as depicting an example of elements of a method implemented in the computing device 409 (FIG. 21) according to one or more embodiments.

[0218] Beginning with box 603, the multilateration application 423 determines whether the navigation unit 400 is receiving guided surface waves from a minimum number of distinct ground stations and, therefore, a minimum number of distinct probes. For example, some embodiments of the invention may require that the navigation unit 400 receive guided surface waves launched from at least two different ground stations, while other embodiments may require that the navigation unit 400 receive guided surface waves launched from additional ground stations for increased accuracy. If the navigation unit 400 is receiving guided surface waves from the requisite number of ground stations, then execution proceeds to box 606. Otherwise, execution ends.

[0219] Moving on to box 606, the multilateration application 423 identifies each base guided surface wave it is receiving and the corresponding ground station 500 (FIG. 24) that launched it. For example, the multilateration application 423 may identify all of the guided surface waves that the navigation unit 400 is currently receiving and reference map data 429 (FIG. 21) to determine which of the guided surface waves are base guided surface waves and which ground station 500 corresponds to each base guided surface wave received.

[0220] Proceeding to box 609, the multilateration application 423 identifies the overlaid guided surface waves it is receiving from each ground station 500 (FIG. 24). For example, the multilateration application 423 may identify all guided surface waves it is currently receiving and then reference map data 429 to determine which of the guided surface waves are overlaid guided surface waves and the corresponding ground station 500 that launched each one.

[0221] Referring next to box 613, the multilateration application 423 causes the navigation unit 400 to determine or otherwise measure the phase of each base guided surface wave that the navigation unit 400 is receiving at its current location.

[0222] Moving on to box 616, the multilateration application 423 calculates a distance from each ground station 500 to the navigation unit 400. For each ground station, the

multilateration application 423 first determines the wavelength of the corresponding base guided surface wave on which the navigation unit 400 is located. The multilateration application 423 then uses the phase of the base guided surface wave to determine where on the wavelength the navigation unit 400 is located. The multilateration application 423 then can reference map data 429 to determine the distance of the navigation unit 400 from the ground station 500 or the multilateration application 423 can calculate the distance from the ground station 500 according to the following equation:

$$D=Nw \qquad (106)$$

where "D" equals the distance between the navigation unit 400 and the ground station 500, "N" equals the number of wavelengths of the base guided surface wave that are between the navigation unit 400 and the ground station 500, and "w" equals the wavelength of the base guided surface wave launched by the ground station 500. It should be noted that "N" is a decimal number that can include fractional portions of wavelengths. For example, "N" could equal values such as 2.3, 4.9, 6, or 10 depending on the distance in wavelengths between the navigation unit 400 and the ground station 500.

[0223] The multilateration application 423 can determine the number of whole wavelengths between the navigation unit 400 and a ground station 500 based on which overlaid guided surface waves launched by the ground station 500 are received by the navigation unit 400. As previously discussed, a ground station 500 can launch a number of overlaid guided surface waves, each of which has a range equal to a whole number of wavelengths of the based guided surface wave. For example, if the multilateration application 423 determines that is receiving the overlaid guided surface waves with a range of three and four wavelengths of the base guided surface wave, respectively, but is not receiving any overlaid guided surface waves with a range or one or two wavelengths of the base guided surface wave, then the navigation unit 400 is more than two, but less than three, whole wavelengths of the base guided surface wave away from the ground station 500.

[0224] Proceeding next to box 619, the multilateration application 423 calculates, plots, or otherwise generates a circumference of a circle 503 (FIG. 22) around each of the ground stations 500 or antipodes of the ground stations 500 in order to identify the location 506 of the navigation unit 400. The circumference of the circle may, for example, be calculated by creating a circle with a center equivalent to the location of the ground station 500 with a radius equal to the calculated distance to the location of the ground station 500. In instances, the circle may not correspond to a perfect circle, but may instead represent a shape that is substantially circular. The location of the ground station 500 may be previously known and stored in the memory 416 (FIG. 21) of the navigation device 400 or may be determined using various approaches.

[0225] Referring next to box 623, the multilateration application 423 identifies each intersection 516 where each circumference of each circle intersects every other circumference of every other circle. This intersection 516 represents a possible location of the navigation unit 400 relative to each of the ground stations 500.

[0226] Moving on to box 626, the multilateration application 423 disambiguates between multiple intersections 516 to determine the current location of the navigation unit 400. For example, the multilateration application 423 could use inertial data 431 to disambiguate between multiple locations. For example, if the inertial data 431 indicated that the navigation unit 400 began its current journey in New York City, had been travelling at a speed of 500 miles-per-hour, and had been travelling for 1 hour, then the multilateration application 423 would know that it is located on a circumference of a circle with a radius of 500 miles and centered on New York City. Whichever intersection 516 identified at box 623 fell along that circumference would correspond to the current location of the navigation unit 400. Similarly, if one intersection 516 determined at box 623 were located within North America and the other intersection 516 determined at box 623 were located in Asia, the multilateration application 423 could identify the North American intersection 516 as the current location of the navigation unit 400.

[0227] As another example, the multilateration application 423 could make use of external data sources to disambiguate between multiple locations. As an example, one location determined at box 623 could be located within North America and the other location determined at box 623 could be located in Asia. If the navigation unit 400 were able to receive signals from a North American cellular phone provider, the multilateration application 423 could determine that the North American position identified at box 623 was the correct current location of the navigation unit 400. Similar determinations could be made based on whether the navigation unit 400 was receiving broadcasts of particular radio stations (*e.g.* an AM or FM radio station located in North America versus an AM or FM radio station located in Asia), wireless network signals (*e.g.* from a network access point with a MAC address previously identified as being located in North America), television stations, or other signals.

[0228] After disambiguating the current location of the navigation unit 400, execution subsequently ends.

[0229] The flowchart of FIG. 25 shows the functionality and operation of an implementation of portions of the multilateration application 423. If embodied in software, each block may represent a module, segment, or portion of code that comprises program instructions to implement the specified logical function(s). The program instructions may be embodied in the form of source code that comprises human-readable statements written in a programming language or machine code that comprises numerical instructions recognizable

by a suitable execution system such as a processor 413 (FIG. 21) in a computer system or other system. The machine code may be converted from the source code, *etc*. If embodied in hardware, each block may represent a circuit or a number of interconnected circuits to implement the specified logical function(s).

[0230] Although the flowchart of FIG. 25 shows a specific order of execution, it is understood that the order of execution may differ from that which is depicted. For example, the order of execution of two or more blocks may be scrambled relative to the order shown. Also, two or more blocks shown in succession in FIG. 25 may be executed concurrently or with partial concurrence. Further, in some embodiments, one or more of the blocks shown in FIG. 25 may be skipped or omitted. In addition, any number of counters, state variables, warning semaphores, or messages might be added to the logical flow described herein, for purposes of enhanced utility, accounting, performance measurement, or providing troubleshooting aids, *etc*. It is understood that all such variations are within the scope of the present disclosure.

[0231] Also, any logic or application described herein, including the multilateration application 423, that comprises software or code can be embodied in any non-transitory computer-readable medium for use by or in connection with an instruction execution system such as, for example, a processor 413 in a computer system or other system. In this sense, the logic may comprise, for example, statements including instructions and declarations that can be fetched from the computer-readable medium and executed by the instruction execution system. In the context of the present disclosure, a "computer-readable medium" can be any medium that can contain, store, or maintain the logic or application described herein for use by or in connection with the instruction execution system.

[0232] The computer-readable medium can comprise any one of many physical media such as, for example, magnetic, optical, or semiconductor media. More specific examples of a suitable computer-readable medium would include, but are not limited to, magnetic tapes, magnetic floppy diskettes, magnetic hard drives, memory cards, solid-state drives, USB flash drives, or optical discs. Also, the computer-readable medium may be a random access memory (RAM) including, for example, static random access memory (SRAM) and dynamic random access memory (DRAM), or magnetic random access memory (MRAM). In addition, the computer-readable medium may be a read-only memory (ROM), a programmable read-only memory (PROM), an erasable programmable read-only memory (EPROM), an electrically erasable programmable read-only memory (EEPROM), or other type of memory device.

[0233] Further, any logic or application described herein, including the multilateration application 423, may be implemented and structured in a variety of ways. For example, one

or more applications described may be implemented as modules or components of a single application. Additionally, it is understood that terms such as "application," "service," "system," "engine," "module," and so on may be interchangeable and are not intended to be limiting.

[0234] Disjunctive language such as the phrase "at least one of X, Y, or Z," unless specifically stated otherwise, is otherwise understood with the context as used in general to present that an item, term, etc., may be either X, Y, or Z, or any combination thereof (*e.g.*, X, Y, and/or Z). Thus, such disjunctive language is not generally intended to, and should not, imply that certain embodiments require at least one of X, at least one of Y, or at least one of Z to each be present.

[0235] Example embodiments of the present disclosure are provided in the following clauses. These clauses provide several examples of various embodiments of the present disclosure. However, the description provided in these clauses does not exclude alternative implementations or embodiments. Rather, these clauses are intended to provide an illustration of potential embodiments of the present disclosure.

[0236] Clause 1. An apparatus, comprising: a charge terminal elevated over a lossy conducting medium; a receiver network coupled between the charge terminal and the lossy conducting medium, the receiver network having a phase delay (Φ) that matches a wave tilt angle (Ψ) associated with the guided surface wave, the wave tilt angle (Ψ) based at least in part upon characteristics of the lossy conducting medium in a vicinity of the receiving structure; a processor; a memory; and an application stored in the memory and executable by the processor, wherein the application causes the apparatus to perform at least the following actions when executed by the processor: identify a wavelength and a phase of a base guided surface wave launched from a ground station and received by the receiver network; identify a range of an overlaid guided surface wave launched from the ground station and received by the receiver network, wherein the range of the overlaid guided surface wave is measured as a number of wavelengths of the base guided surface wave; calculate a distance of the receiver network from the ground station based at least in part on the phase of the base guided surface wave and the range of the overlaid guided surface wave; and determine a location of the receiver network based at least in part on the distance of the receiver network from the ground station.

[0237] Clause 2. The apparatus of clause 1, wherein the application, when executed by the processor, further causes the apparatus to at least: identify a second wavelength and a second phase of a second base guided surface wave launched from a second ground station and received by the receiver network; identify a second range of a second overlaid guided surface wave launched from the second ground station and received by the receiver network, wherein the second range of the second overlaid guided surface wave is measured

as a second number of wavelengths of the second based guided surface wave; calculate a second distance of the receiver network from the second ground station based at least in part on the second phase of the second base guided surface wave and the second range of the second overlaid guided surface wave; and causing the apparatus to determine the location of the receiver network is further based at least in part on the second distance of the receiver network from the second ground station.

[0238] Clause 3. The apparatus of clause 1 or 2, wherein the application, when executed by the processor, further causes the apparatus to at least identify an approximate position of the receiver network based at least in part on inertial data associated with the apparatus, wherein the inertial data is stored in the memory of the apparatus; and wherein causing the apparatus to determine the location of the receiver network is further based at least in part on the approximate position of the receiver network.

[0239] Clause 4. The apparatus of clause 1 or 2, wherein the application, when executed by the processor, further causes the apparatus to at least identify an approximate position of the receiver network is based at least in part on an identity of a cellular network tower within range of the receiver network; and wherein causing the apparatus to determine the location of the receiver network is further based at least in part on the approximate position of the receiver network.

[0240] Clause 5. The apparatus of clause 1 or 2, wherein the application, when executed by the processor, further causes the apparatus to at least identify an approximate position of the receiver network based at least in part on an identity of a radio transmission tower within range of the receiver network; and wherein causing the apparatus to determine the location of the receiver network is further based at least in part on the approximate position of the receiver network.

[0241] Clause 6. The apparatus of clauses 1-5, wherein the charge terminal is height adjustable such that a change in a height of the charge terminal causes a change in the phase delay (Φ).

[0242] Clause 7. The apparatus of clauses 1-6, wherein the overlaid guided surface wave has a higher frequency than the base guided surface wave.

[0243] Clause 8. A method, comprising: receiving a base guided surface wave launched from a ground station; identifying a wavelength and a phase of the base guided surface wave; receiving an overlaid guided surface wave launched from the ground station; identifying a range of the overlaid guided surface wave, wherein the range of the overlaid guided surface wave is measured as a number of wavelengths of the base guided surface wave; calculating a distance from the ground station based at least in part on the phase of

the base guided surface wave and the range of the overlaid guided surface wave; and determining a current location based at least in part on the distance from the ground station.

[0244] Clause 9. The method of clause 8, further comprising: receiving a second based guided surface wave launched from a second ground station; identifying a second wavelength and a second phase of the second base guided surface wave; receiving a second overlaid guided surface wave launched from a second ground station; identifying a second range of the second overlaid guided surface wave launched, wherein the second range of the second overlaid guided surface wave is measured as a second number of wavelengths of the second based guided surface wave; calculating a second distance from the second ground station based at least in part on the second phase of the second base guided surface wave and the second range of the second overlaid guided surface wave; and wherein determining the location is further based at least in part on the second distance from the second ground station.

[0245] Clause 10. The method of clause 8 or 9, further comprising identifying an approximate position based at least in part on inertial data, wherein determining the current location is further based at least in part on the approximate position.

[0246] Clause 11. The method of clause 8 or 9, further comprising identifying an approximate position based at least in part on an identity of a cellular network tower, wherein determining the current location is further based at least in part on the approximate position.

[0247] Clause 12. The method of clause 8 or 9, further comprising: receiving a broadcast transmission; identifying an approximate position based at least in part on an identity of the broadcast transmission; and wherein determining the current location is further based at least in part on the approximate position.

[0248] Clause 13. The method of clauses 8 or 9, further comprising: receiving a signal from a wireless network; identifying a media access control (MAC) address associated with an access point for the wireless network; identifying an approximate position based at least in part on the MAC address; and wherein determining the current location is further based at least in part on the approximate position.

[0249] Clause 14. The method of clauses 8-13, wherein the overlaid guided surface wave has a higher frequency than the base guided surface wave.

[0250] Clause 15. A system, comprising: a guided surface wave receive structure configured to obtain electrical energy from a guided surface wave traveling along a terrestrial medium; a processor; a memory; and an application stored in the memory that, when executed by the processor, causes the apparatus to at least: identify a wavelength and a phase of a base guided surface wave launched from a ground station and received by the guided surface wave receive structure; identify a range of an overlaid guided surface wave

launched from the ground station and received by the guided surface wave receive structure, wherein the range of the overlaid guided surface wave is measured as a number of wavelengths of the base guided surface wave; calculate a distance of the guided surface wave receive structure from the ground station based at least in part on the phase of the base guided surface wave and the range of the overlaid guided surface wave; and determine a location of the guided surface wave receive structure based at least in part on the distance of the guided surface wave receive structure from the ground station.

[0251] Clause 16. The system of claim 15, wherein the application, when executed by the processor, further causes the system to at least: identify a second wavelength and a second phase of a second base guided surface wave launched from a second ground station and received by the guided surface wave receive structure; identify a second range of a second overlaid guided surface wave launched from the second ground station and received by the guided surface wave receive structure, wherein the second range of the second overlaid guided surface wave is measured as a second number of wavelengths of the second based guided surface wave; calculate a second distance of the guided surface wave receive structure from the second ground station based at least in part on the second phase of the second base guided surface wave and the second range of the second overlaid guided surface wave; and causing the apparatus to determine the location of the guided surface wave receive structure is further based at least in part on the second distance of the guided surface wave receive structure from the second ground station.

[0252] Clause 17. The system of clause 15 or 16, wherein the application, when executed by the processor, further causes the system to at least identify an approximate position of guided surface wave receive structure based at least in part on inertial data associated with the system, wherein the inertial data is stored in the memory of the system; and wherein causing the system to determine the location of the guided surface wave receive structure is further based at least in part on the approximate position of the guided surface wave receive structure.

[0253] Clause 18. The system of clause 15 or 16, wherein the application, when executed by the processor, further causes the system to at least identify an approximate position of the guided surface wave receive structure based at least in part on inertial data associated with the system, wherein the inertial data is stored in the memory of the system; and wherein causing the system to determine the location of the guided surface wave receive structure is further based at least in part on the approximate position of the guided surface wave receive structure.

[0254] Clause 19. The system of clause 15 or 16, wherein the application, when executed by the processor, further causes the system to at least identify an approximate

position of the guided surface wave receive structure based at least in part on an identity of a radio transmission tower within range of the guided surface wave receive structure; and wherein causing the apparatus to determine the location of the guided surface wave receive structure is further based at least in part on the approximate position of the guided surface wave receive structure.

[0255] Clause 20. The system of clauses 15-19, wherein the overlaid guided surface wave has a higher frequency than the base guided surface wave.

[0256] It should be emphasized that the above-described embodiments of the present disclosure are merely possible examples of implementations set forth for a clear understanding of the principles of the disclosure. Many variations and modifications can be made to the above-described embodiment(s) without departing substantially from the spirit and principles of the disclosure. All such modifications and variations are intended to be included herein within the scope of this disclosure and protected by the following claims. In addition, all optional and preferred features and modifications of the described embodiments and dependent claims are usable in all aspects of the disclosure taught herein. Furthermore, the individual features of the dependent claims, as well as all optional and preferred features and modifications of the described embodiments are combinable and interchangeable with one another where applicable. To this end, the various embodiments described above disclose elements that can optionally be combined in a variety of ways depending on the desired implementation.

CLAIMS

Therefore, the following is claimed:

1. An apparatus, comprising:

a charge terminal elevated over a lossy conducting medium;

a receiver network coupled between the charge terminal and the lossy conducting medium, the receiver network having a phase delay (Φ) that matches a wave tilt angle (Ψ) associated with the guided surface wave, the wave tilt angle (Ψ) based at least in part upon characteristics of the lossy conducting medium in a vicinity of the receiving structure;

a processor;

a memory; and

an application stored in the memory and executable by the processor, wherein the application causes the apparatus to perform at least the following actions when executed by the processor:

identify a wavelength and a phase of a base guided surface wave launched from a ground station and received by the receiver network;

identify a range of an overlaid guided surface wave launched from the ground station and received by the receiver network, wherein the range of the overlaid guided surface wave is measured as a number of wavelengths of the base guided surface wave;

calculate a distance of the receiver network from the ground station based at least in part on the phase of the base guided surface wave and the range of the overlaid guided surface wave; and

determine a location of the receiver network based at least in part on the distance of the receiver network from the ground station.

2. The apparatus of claim 1, wherein the application, when executed by the processor, further causes the apparatus to at least:

identify a second wavelength and a second phase of a second base guided surface wave launched from a second ground station and received by the receiver network;

identify a second range of a second overlaid guided surface wave launched from the second ground station and received by the receiver network, wherein the second range of the second overlaid guided surface wave is measured as a second number of wavelengths of the second based guided surface wave;

calculate a second distance of the receiver network from the second ground station based at least in part on the second phase of the second base guided surface wave and the second range of the second overlaid guided surface wave; and

causing the apparatus to determine the location of the receiver network is further based at least in part on the second distance of the receiver network from the second ground station.

3. The apparatus of claim 1 or 2, wherein the application, when executed by the processor, further causes the apparatus to at least identify an approximate position of the receiver network based at least in part on inertial data associated with the apparatus, wherein the inertial data is stored in the memory of the apparatus; and

wherein causing the apparatus to determine the location of the receiver network is further based at least in part on the approximate position of the receiver network.

4. The apparatus of claim 1 or 2, wherein the application, when executed by the processor, further causes the apparatus to at least identify an approximate position of the receiver network is based at least in part on an identity of a cellular network tower within range of the receiver network; and

wherein causing the apparatus to determine the location of the receiver network is further based at least in part on the approximate position of the receiver network.

5. The apparatus of claim 1 or 2, wherein the application, when executed by the processor, further causes the apparatus to at least identify an approximate position of the receiver network based at least in part on an identity of a radio transmission tower within range of the receiver network; and

wherein causing the apparatus to determine the location of the receiver network is further based at least in part on the approximate position of the receiver network.

6. The apparatus of claims 1-5, wherein the charge terminal is height adjustable such that a change in a height of the charge terminal causes a change in the phase delay (Φ).

7. The apparatus of claims 1-6, wherein the overlaid guided surface wave has a higher frequency than the base guided surface wave.

8. A method, comprising:

receiving a base guided surface wave launched from a ground station;

identifying a wavelength and a phase of the base guided surface wave;

receiving an overlaid guided surface wave launched from the ground station;

identifying a range of the overlaid guided surface wave, wherein the range of the overlaid guided surface wave is measured as a number of wavelengths of the base guided surface wave;

calculating a distance from the ground station based at least in part on the phase of the base guided surface wave and the range of the overlaid guided surface wave; and

determining a current location based at least in part on the distance from the ground station.

9. The method of claim 8, further comprising:

receiving a second based guided surface wave launched from a second ground station;

identifying a second wavelength and a second phase of the second base guided surface wave;

receiving a second overlaid guided surface wave launched from a second ground station;

identifying a second range of the second overlaid guided surface wave launched, wherein the second range of the second overlaid guided surface wave is measured as a second number of wavelengths of the second based guided surface wave;

calculating a second distance from the second ground station based at least in part on the second phase of the second base guided surface wave and the second range of the second overlaid guided surface wave; and

wherein determining the location is further based at least in part on the second distance from the second ground station.

10. The method of claim 8 or 9, further comprising identifying an approximate position based at least in part on inertial data, wherein determining the current location is further based at least in part on the approximate position.

11. The method of claim 8 or 9, further comprising identifying an approximate position based at least in part on an identity of a cellular network tower, wherein determining the current location is further based at least in part on the approximate position.

12. The method of claim 8 or 9, further comprising:

receiving a broadcast transmission;

identifying an approximate position based at least in part on an identity of the broadcast transmission; and

wherein determining the current location is further based at least in part on the approximate position.

13. The method of claim 8 or 9, further comprising:

receiving a signal from a wireless network;

identifying a media access control (MAC) address associated with an access point for the wireless network; and

identifying an approximate position based at least in part on the MAC address.

14. The method of claims 10-13, wherein determining the current location is further based at least in part on the approximate position.

15. The method of claims 8-14, wherein the overlaid guided surface wave has a higher frequency than the base guided surface wave.

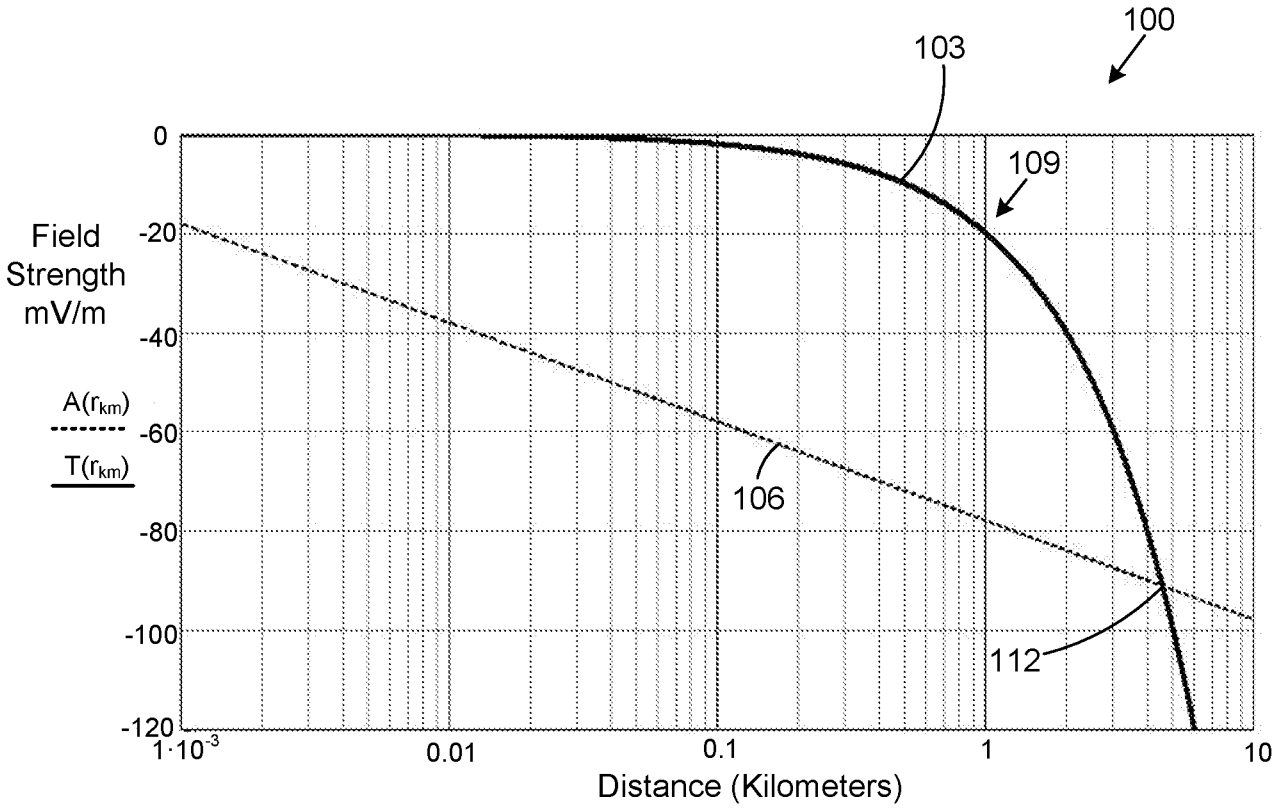

100
103
109
106
112
0
-20
-40
-60
-80
-100
-120
Field Strength mV/m
A(r_km)
T(r_km)
1·10^-3
0.01
0.1
1
10
Distance (Kilometers)

FIG. 1

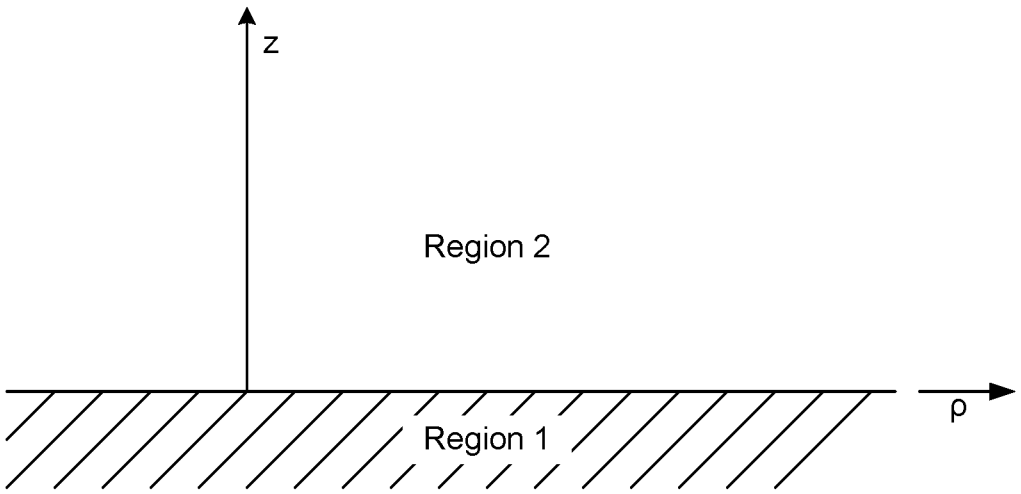

z
Region 2
Region 1
ρ

FIG. 2

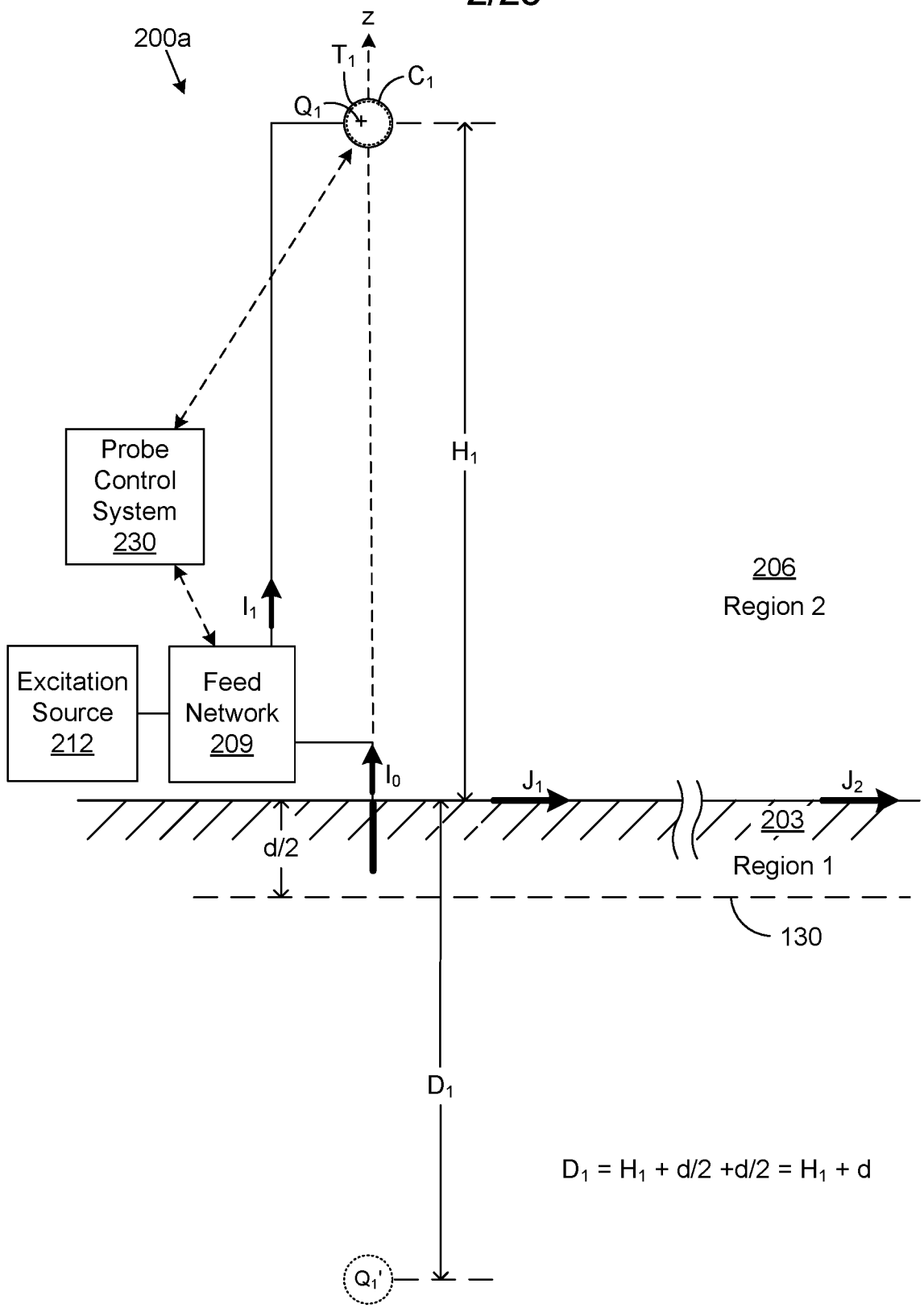

200a
z
T1
C1
Q1
H1
Probe Control System 230
206
Region 2
I1
Excitation Source 212
Feed Network 209
I0
J1
J2
203
Region 1
d/2
130
D1
D1 = H1 + d/2 +d/2 = H1 + d
Q1'

FIG. 3

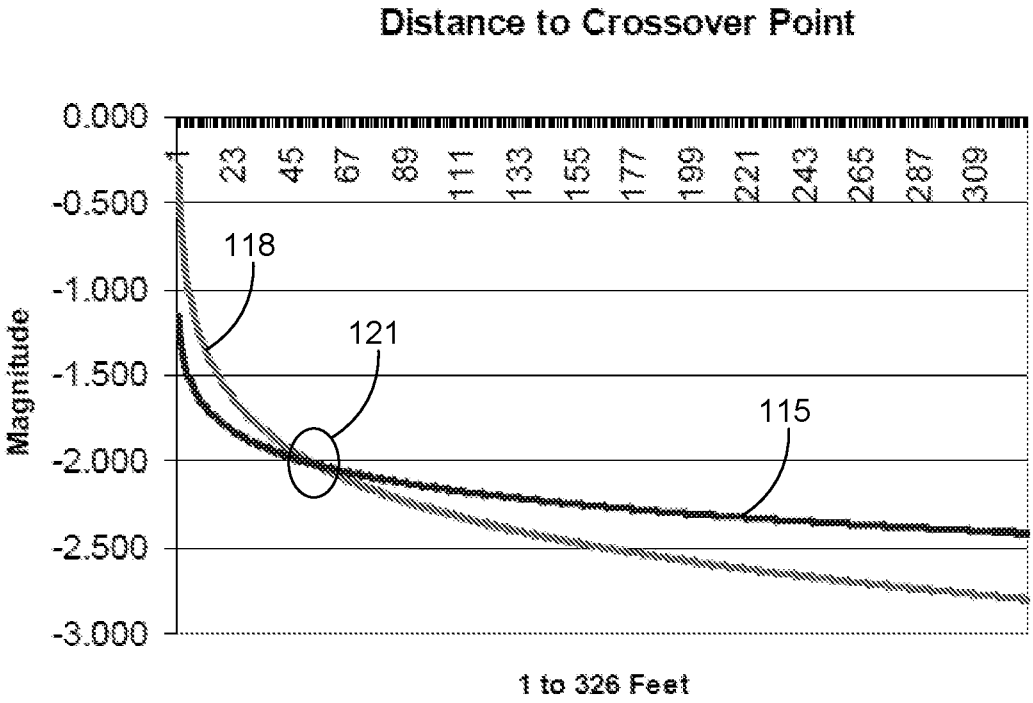

Distance to Crossover Point
0.000
-0.500
-1.000
-1.500
-2.000
-2.500
-3.000
Magnitude
1
23
45
67
89
111
133
155
177
199
221
243
265
287
309
118
121
115
1 to 326 Feet

FIG. 4

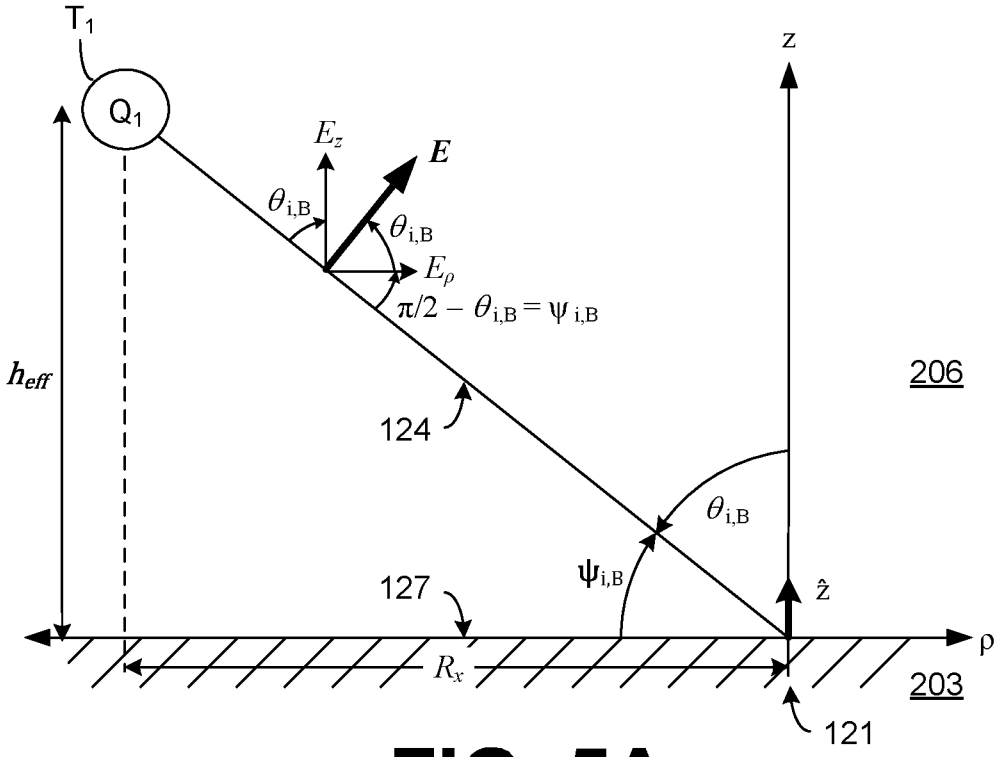

T1
Q1
Ez
E
θi,B
θi,B
Eρ
π/2 − θi,B = ψ i,B
heff
124
206
θi,B
ψi,B
127
z
ẑ
ρ
Rx
203
121

FIG. 5A

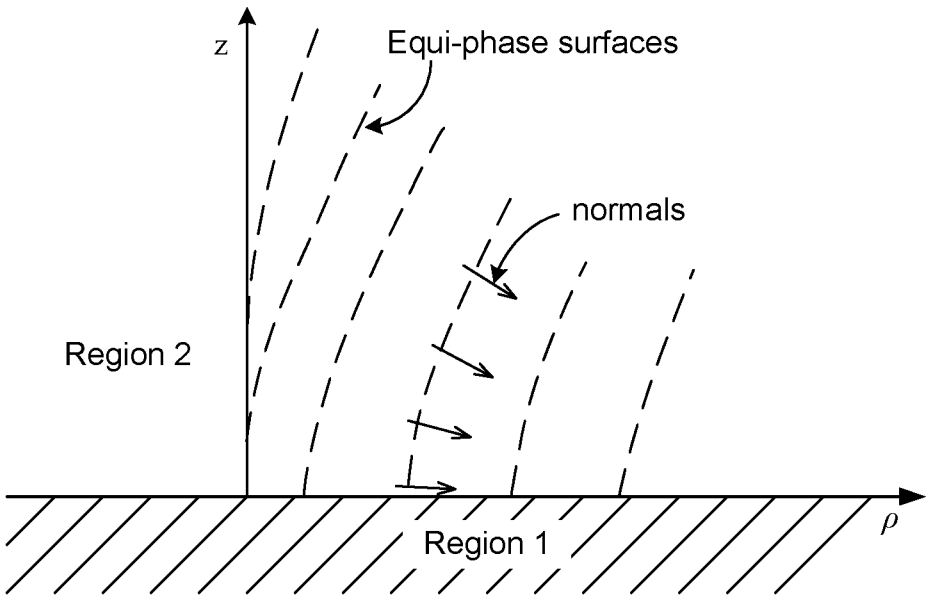

z
Equi-phase surfaces
normals
Region 2
Region 1
ρ

FIG. 5B

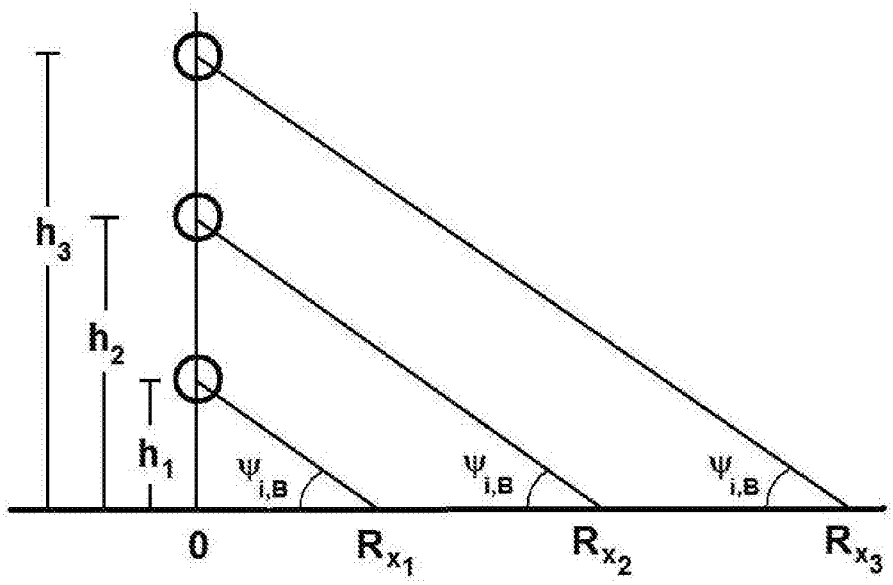

h3
h2
h1
ψi,B
ψi,B
ψi,B
0
Rx1
Rx2
Rx3

FIG. 6

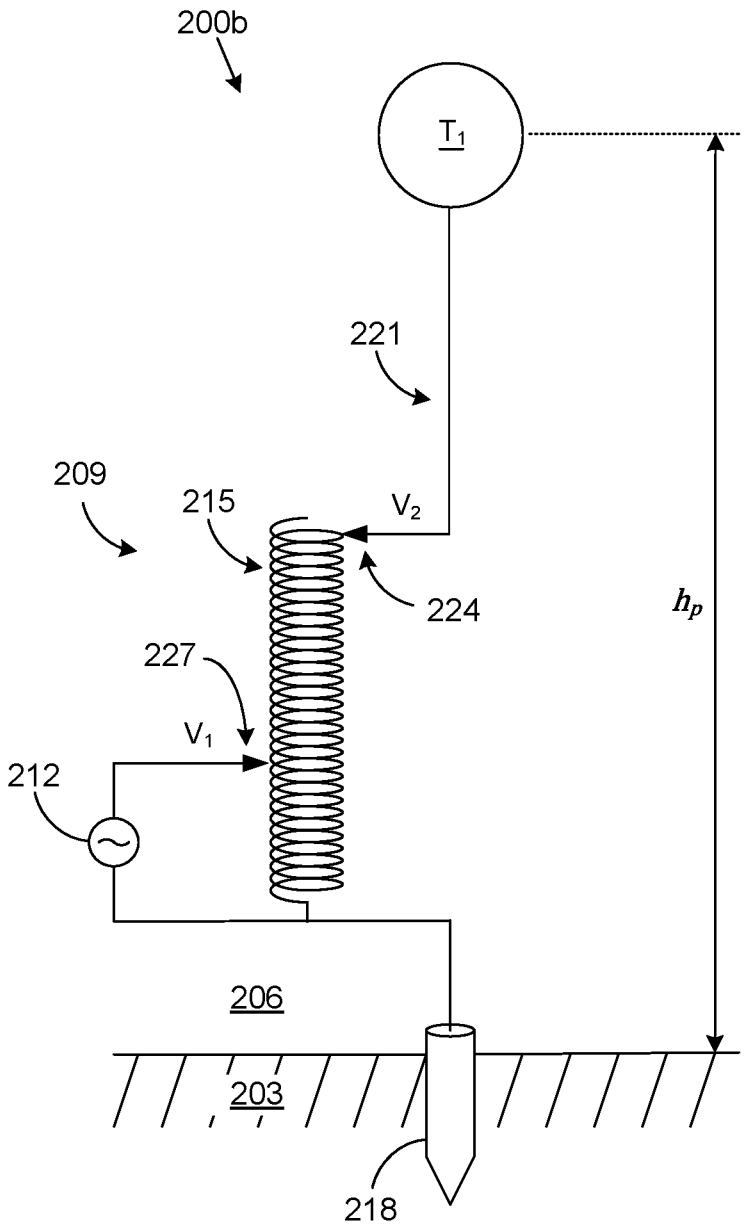


FIG. 7

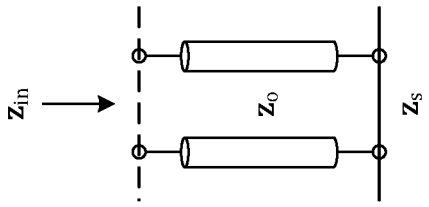


FIG. 8C

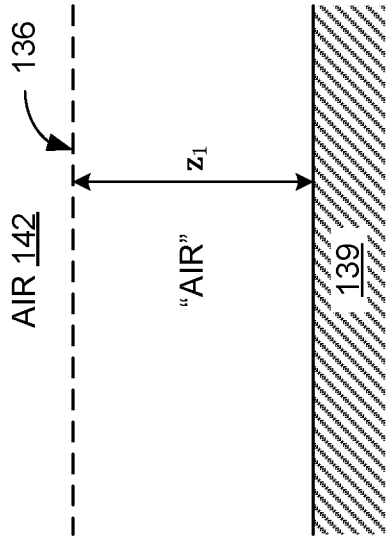


FIG. 8B

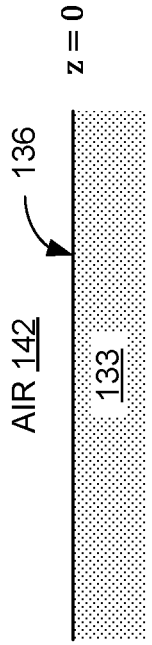


FIG. 8A

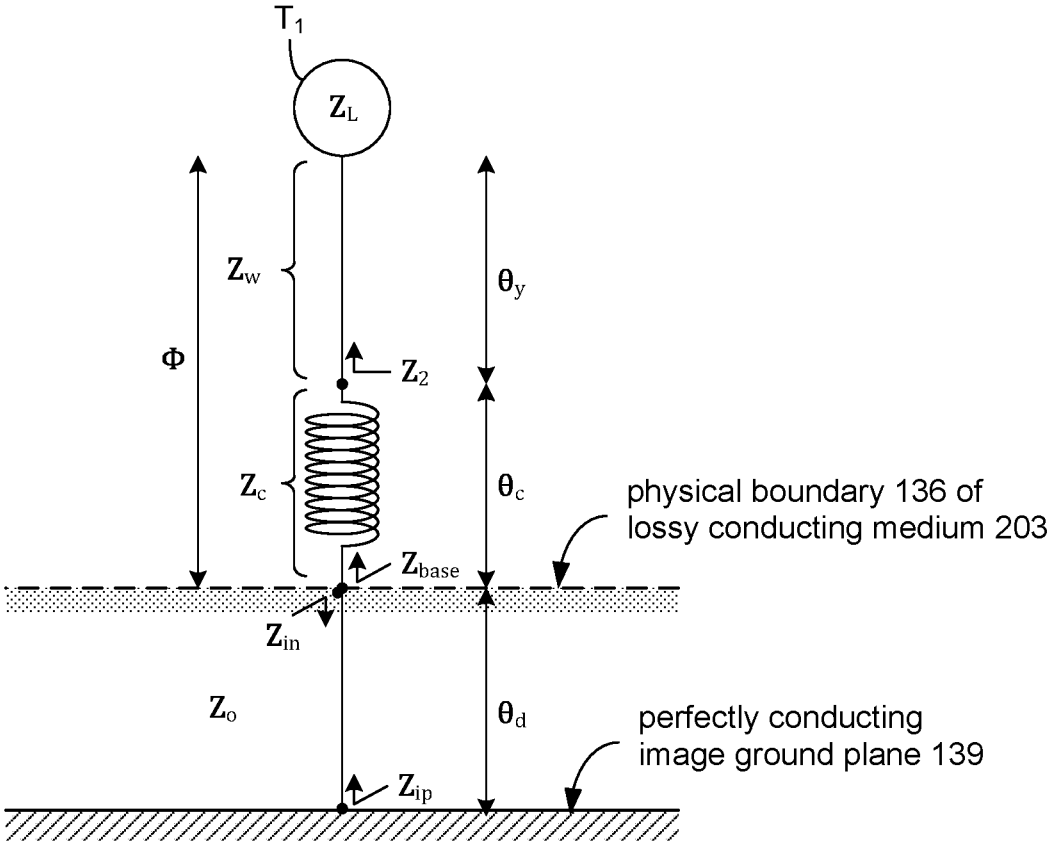

T1
ZL
Zw
θy
Φ
Z2
Zc
θc
physical boundary 136 of lossy conducting medium 203
Zbase
Zin
Zo
θd
perfectly conducting image ground plane 139
Zip

FIG. 9A

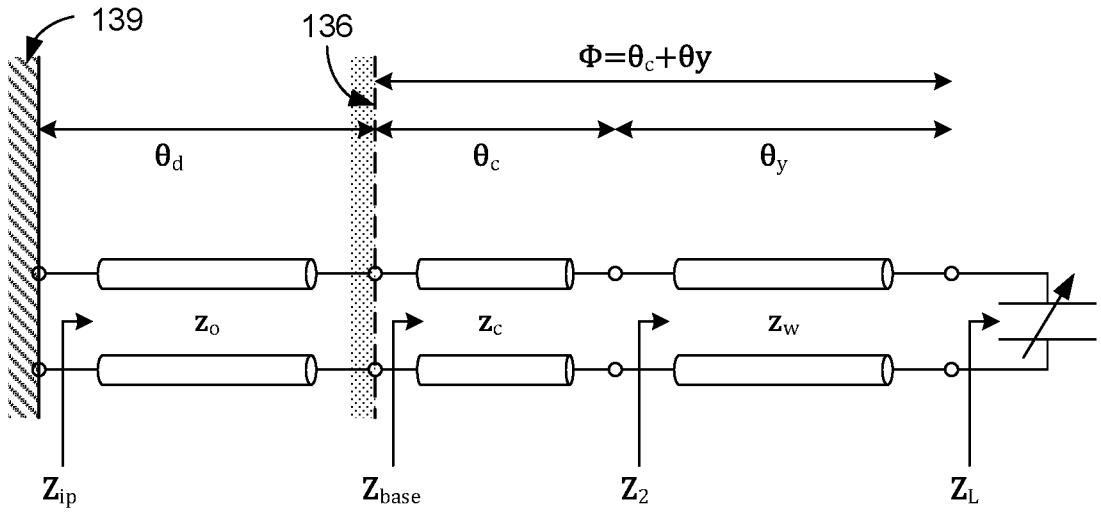

139
136
Φ=θc+θy
θd
θc
θy
zo
zc
zw
Zip
Zbase
Z2
ZL

FIG. 9B

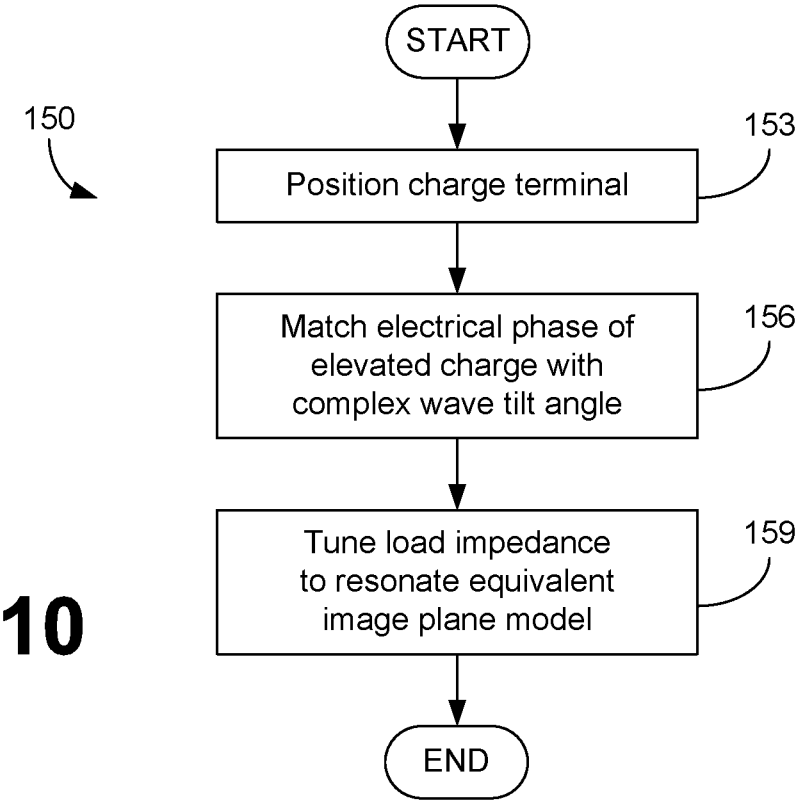

START
150
153
Position charge terminal
156
Match electrical phase of elevated charge with complex wave tilt angle
159
Tune load impedance to resonate equivalent image plane model
END

FIG. 10

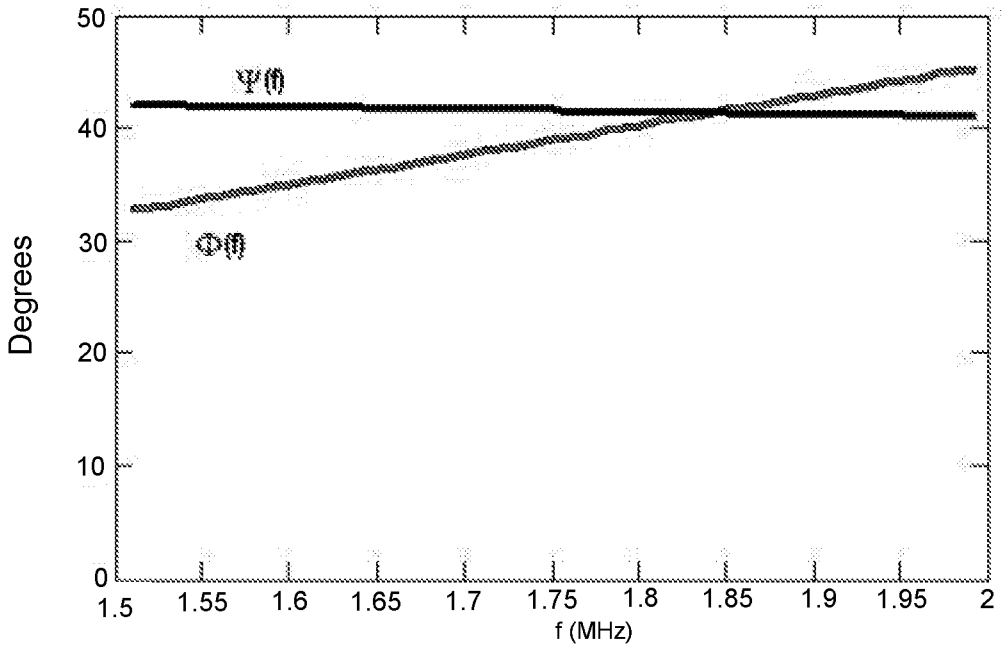

50
40
30
20
10
0
Degrees
Ψ(f)
Φ(f)
1.5
1.55
1.6
1.65
1.7
1.75
1.8
1.85
1.9
1.95
2
f (MHz)

FIG. 11

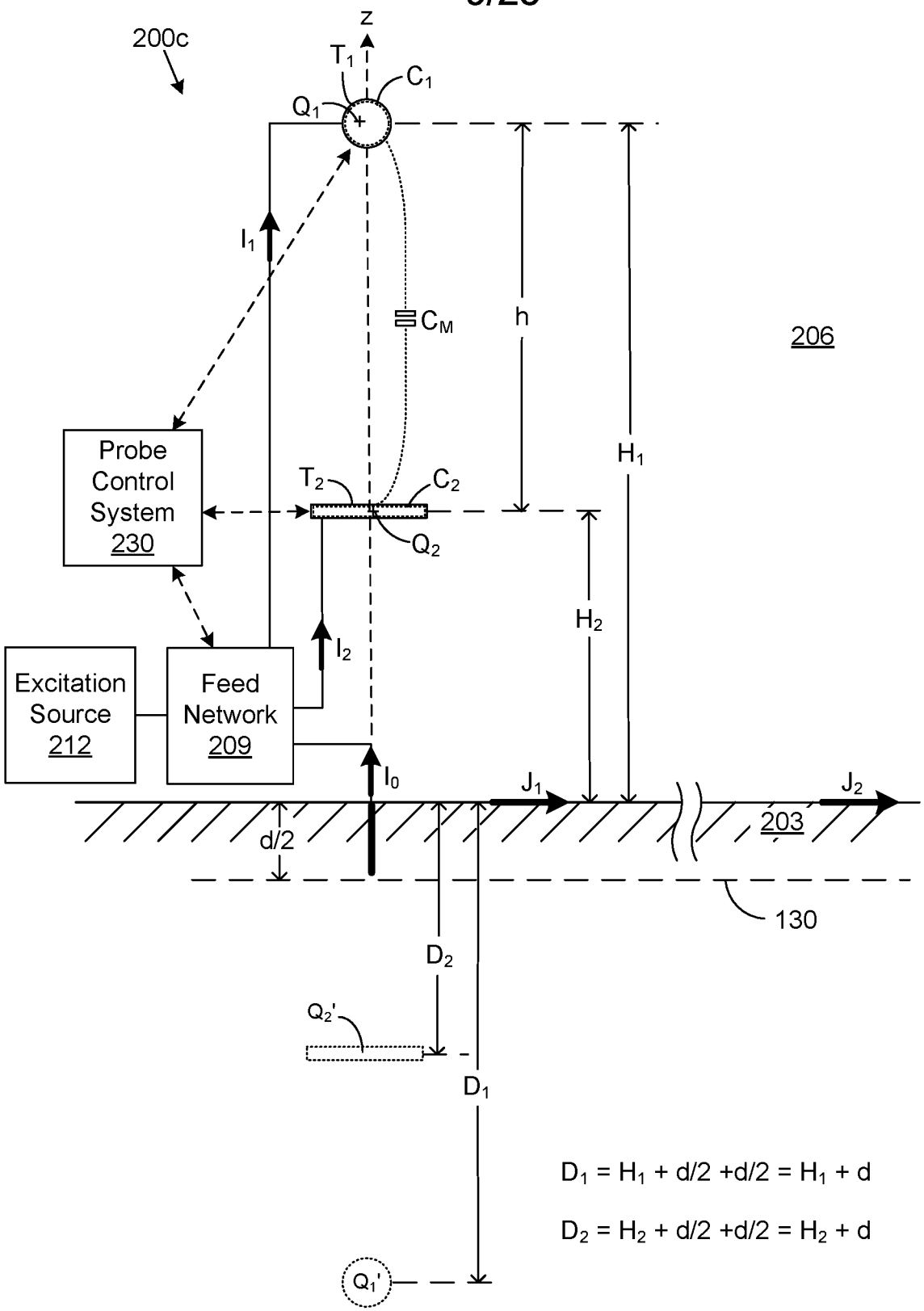

200c
z
T1
C1
Q1
I1
CM
h
206
H1
Probe Control System 230
T2
C2
Q2
H2
I2
Excitation Source 212
Feed Network 209
I0
J1
J2
203
d/2
130
D2
Q2'
D1
Q1'
D1 = H1 + d/2 +d/2 = H1 + d
D2 = H2 + d/2 +d/2 = H2 + d

FIG. 12

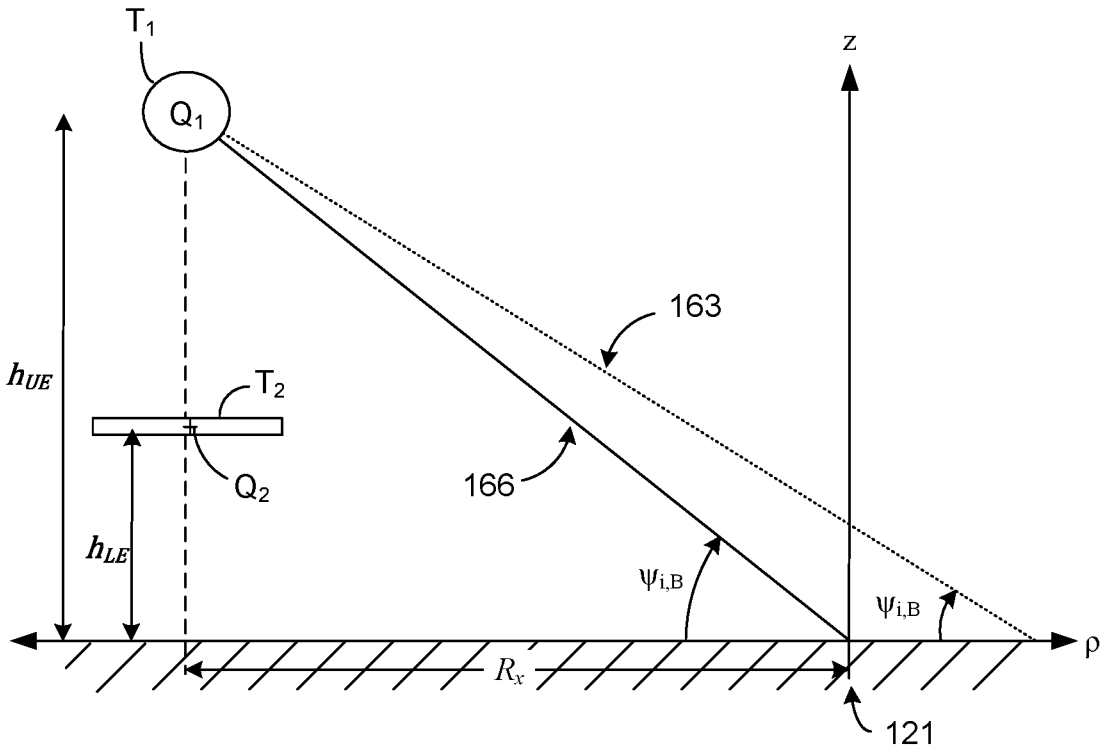


FIG. 13

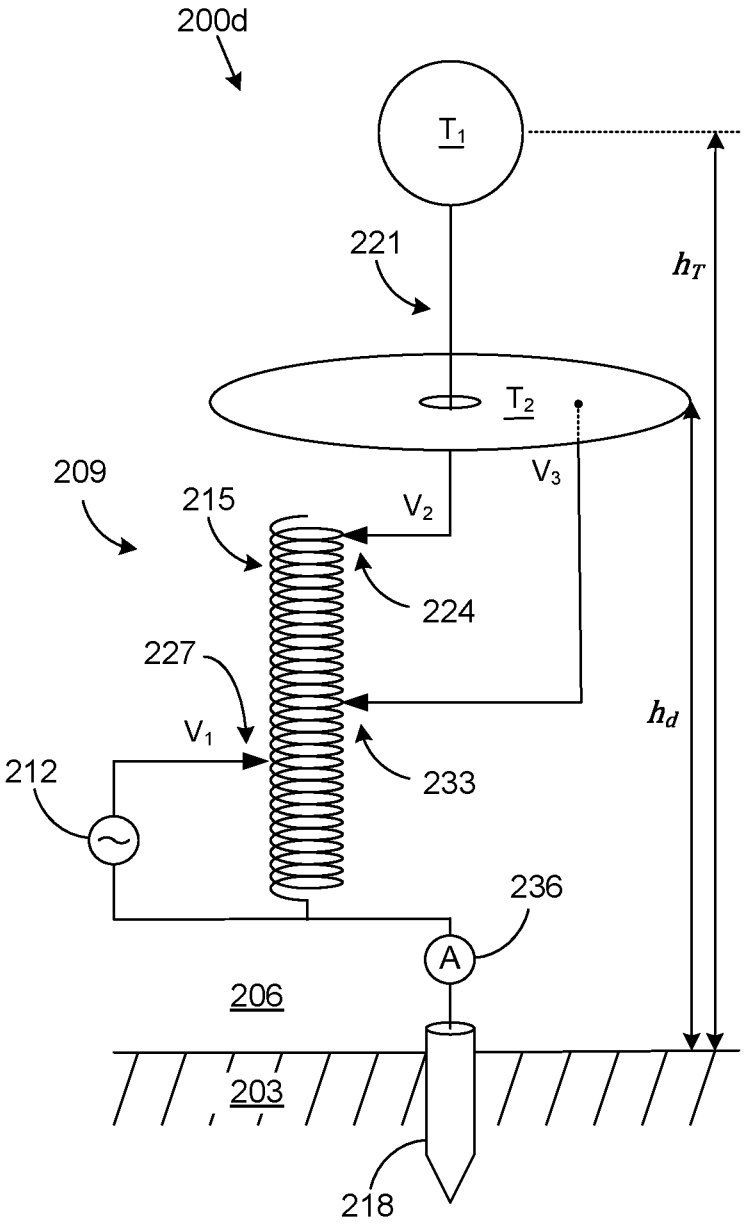

200d
T1
221
h_T
T2
V3
209
215
V2
224
227
V1
h_d
212
233
236
A
206
203
218

FIG. 14

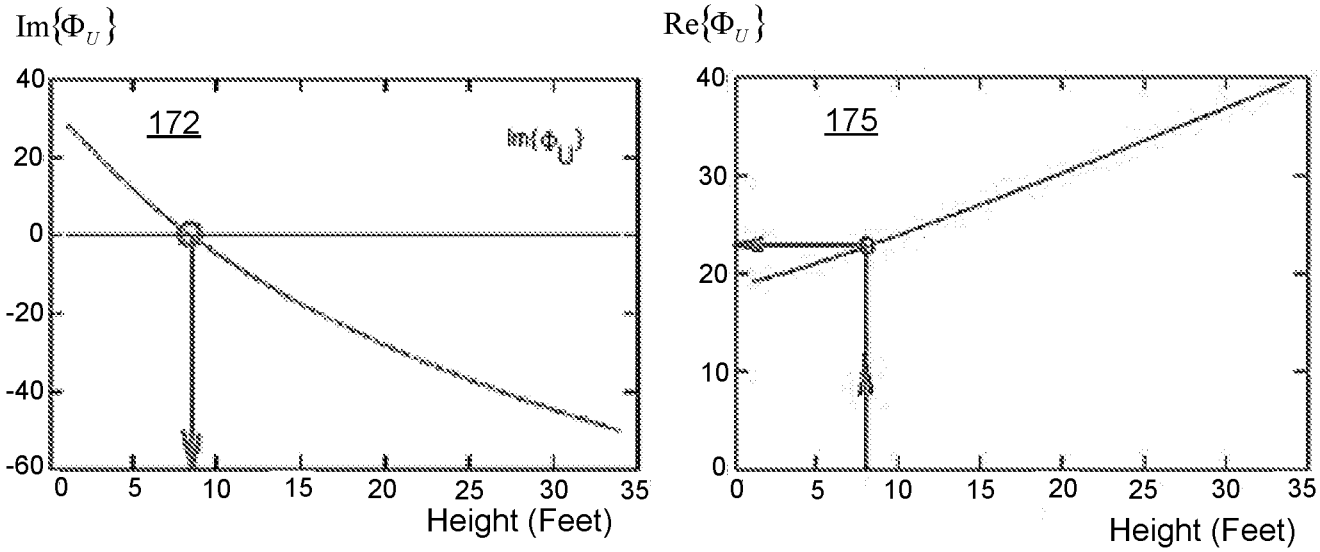


FIG. 15A

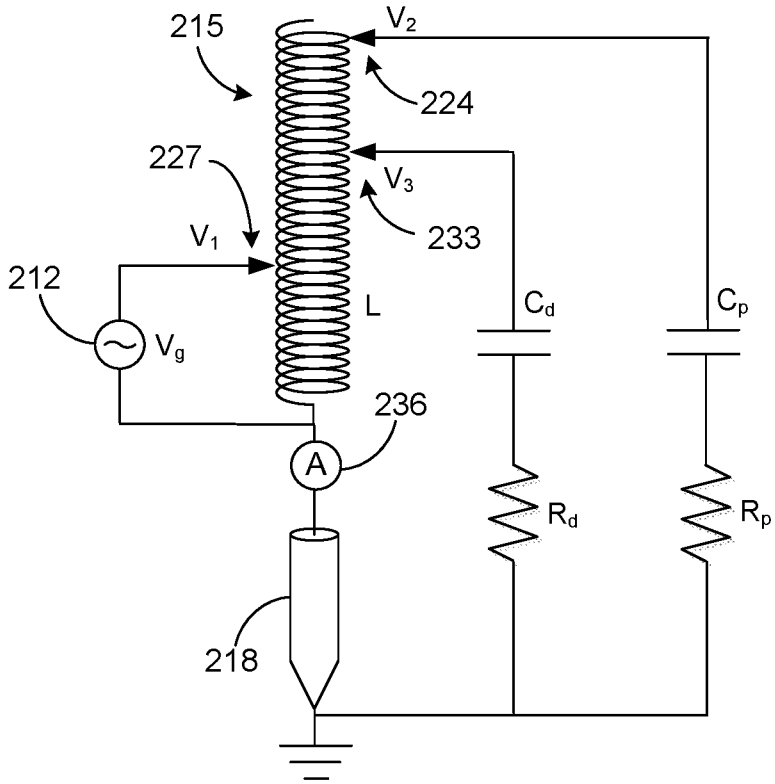


FIG. 15B

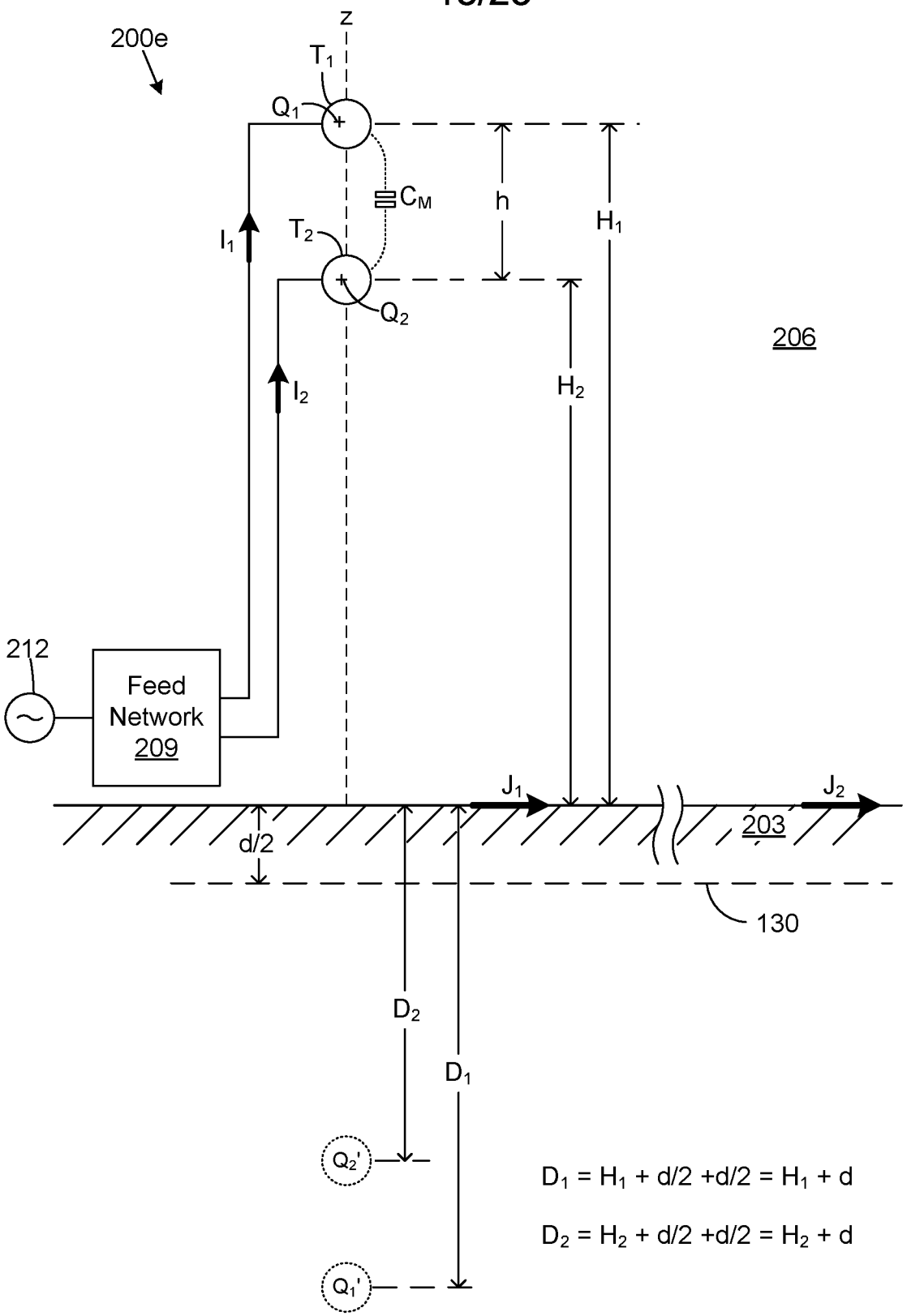

200e
z
T1
Q1
CM
h
H1
I1
T2
Q2
206
I2
H2
212
Feed
Network
209
J1
J2
203
d/2
130
D2
D1
Q2'
Q1'
D1 = H1 + d/2 +d/2 = H1 + d
D2 = H2 + d/2 +d/2 = H2 + d

FIG. 16

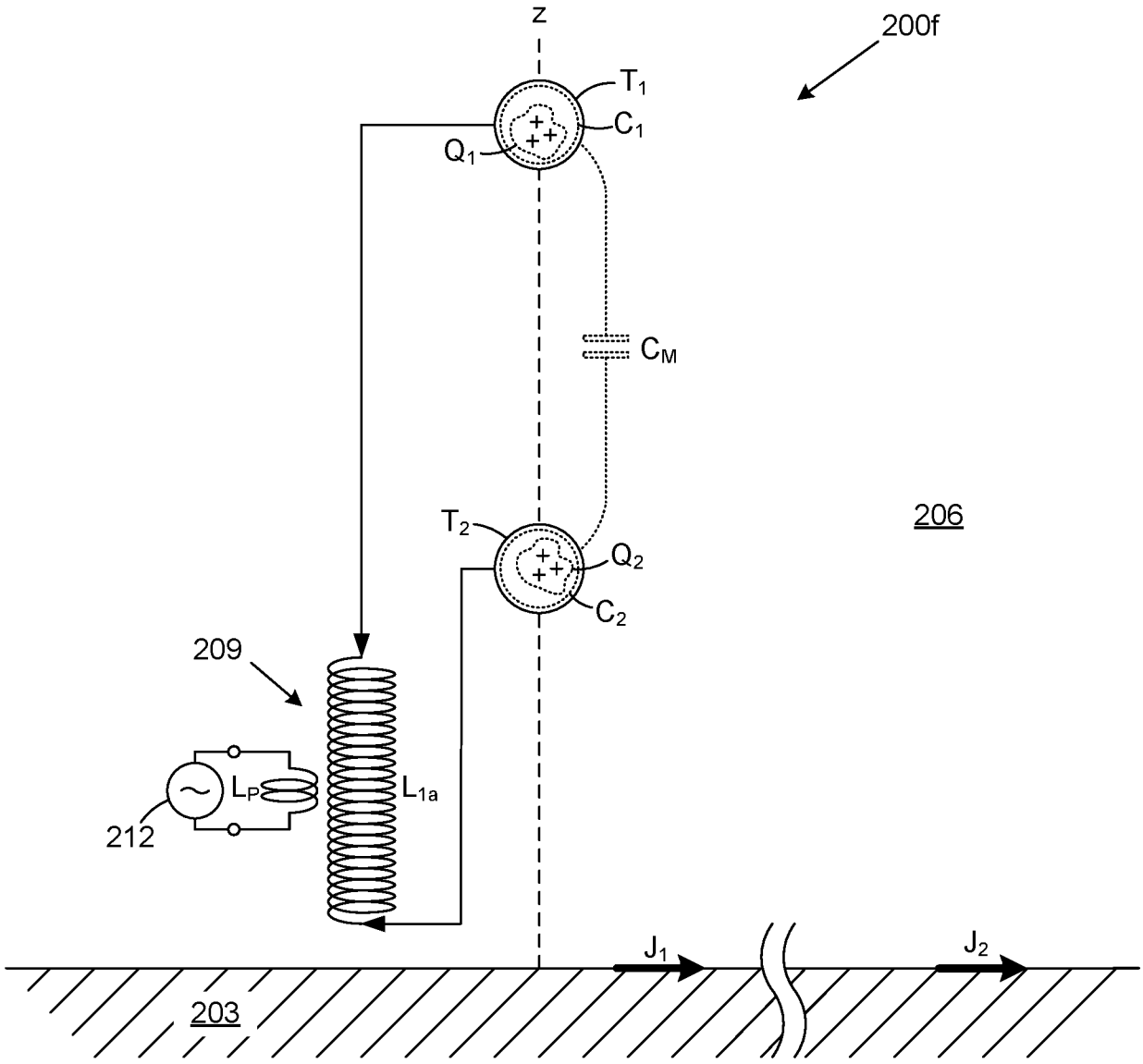


FIG. 17

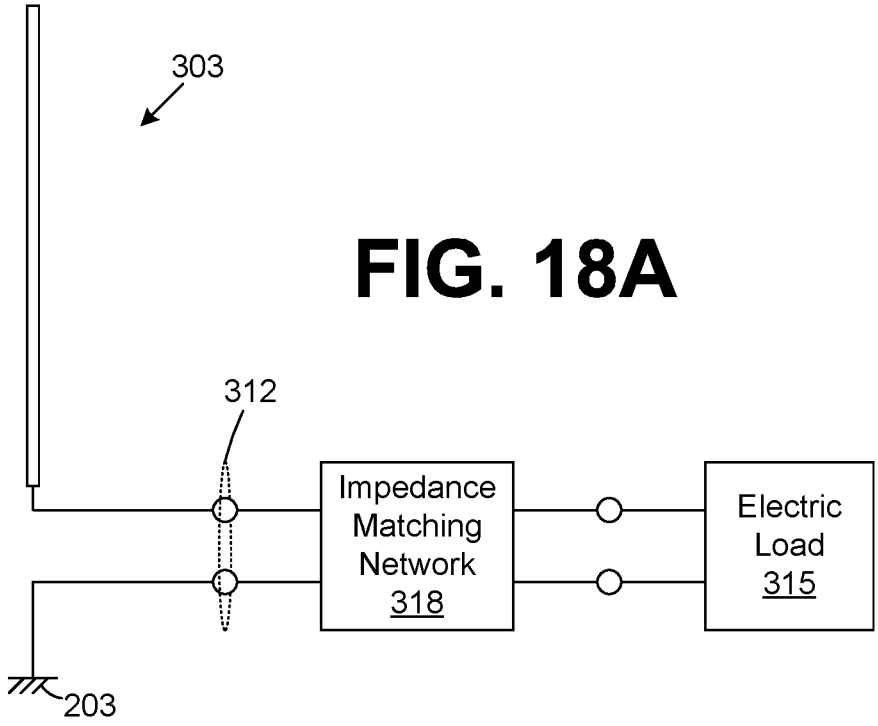


FIG. 18A

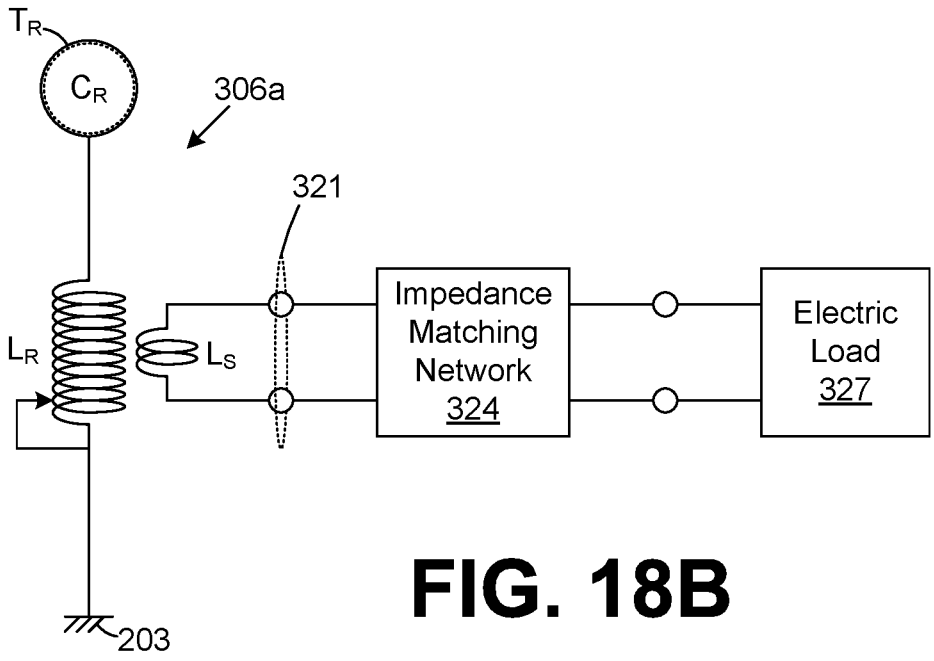


FIG. 18B

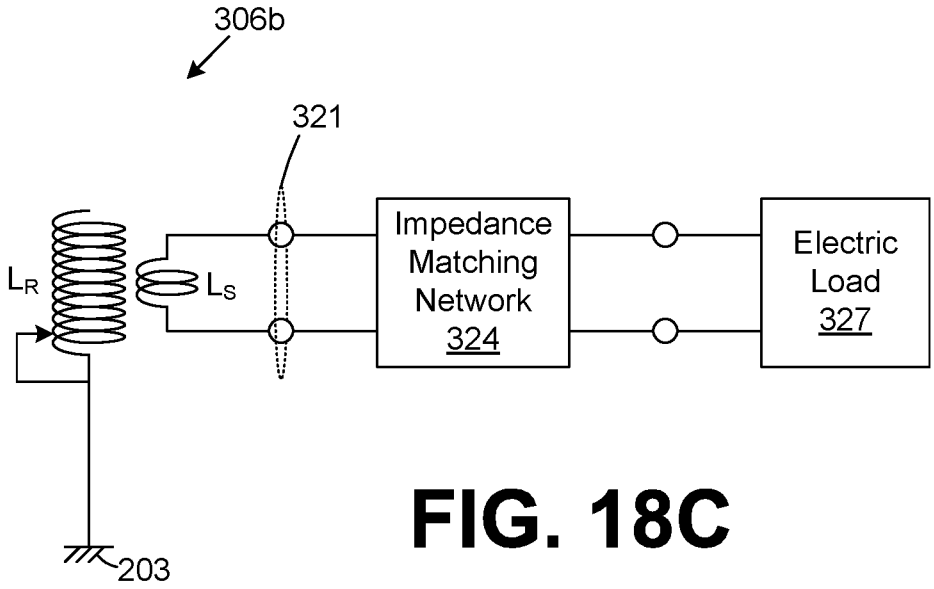


FIG. 18C

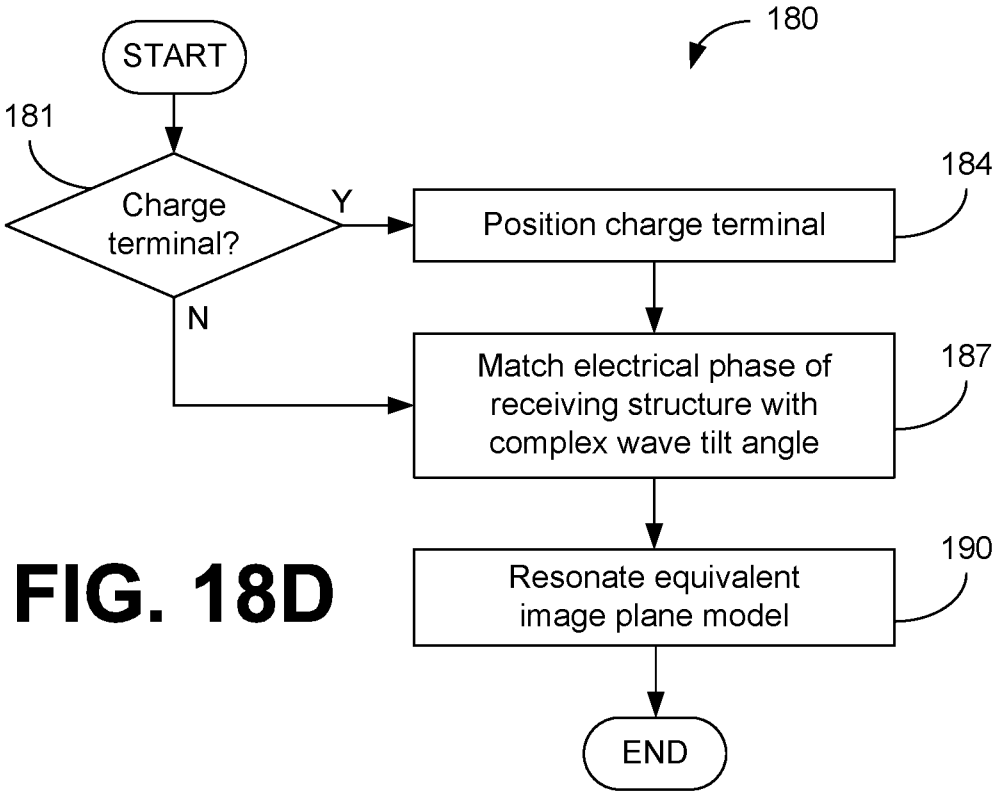


FIG. 18D

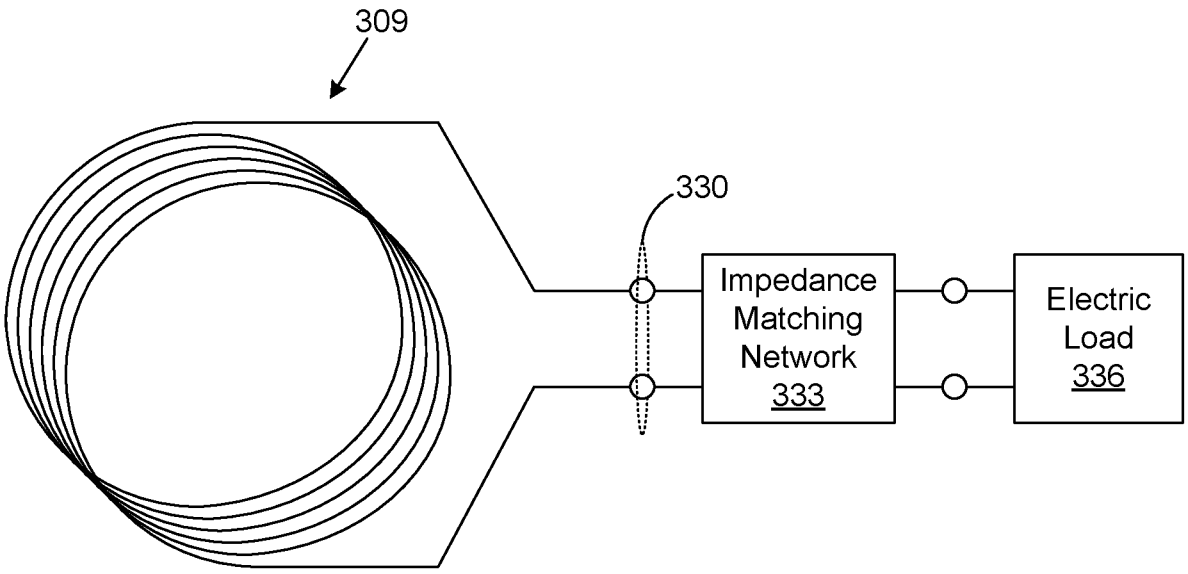


FIG. 19

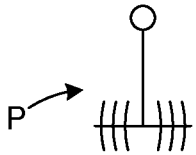


FIG. 20A

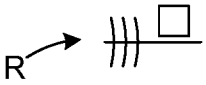


FIG. 20B

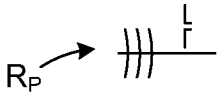


FIG. 20C

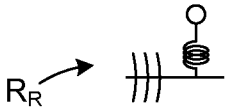


FIG. 20D

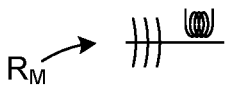


FIG. 20E

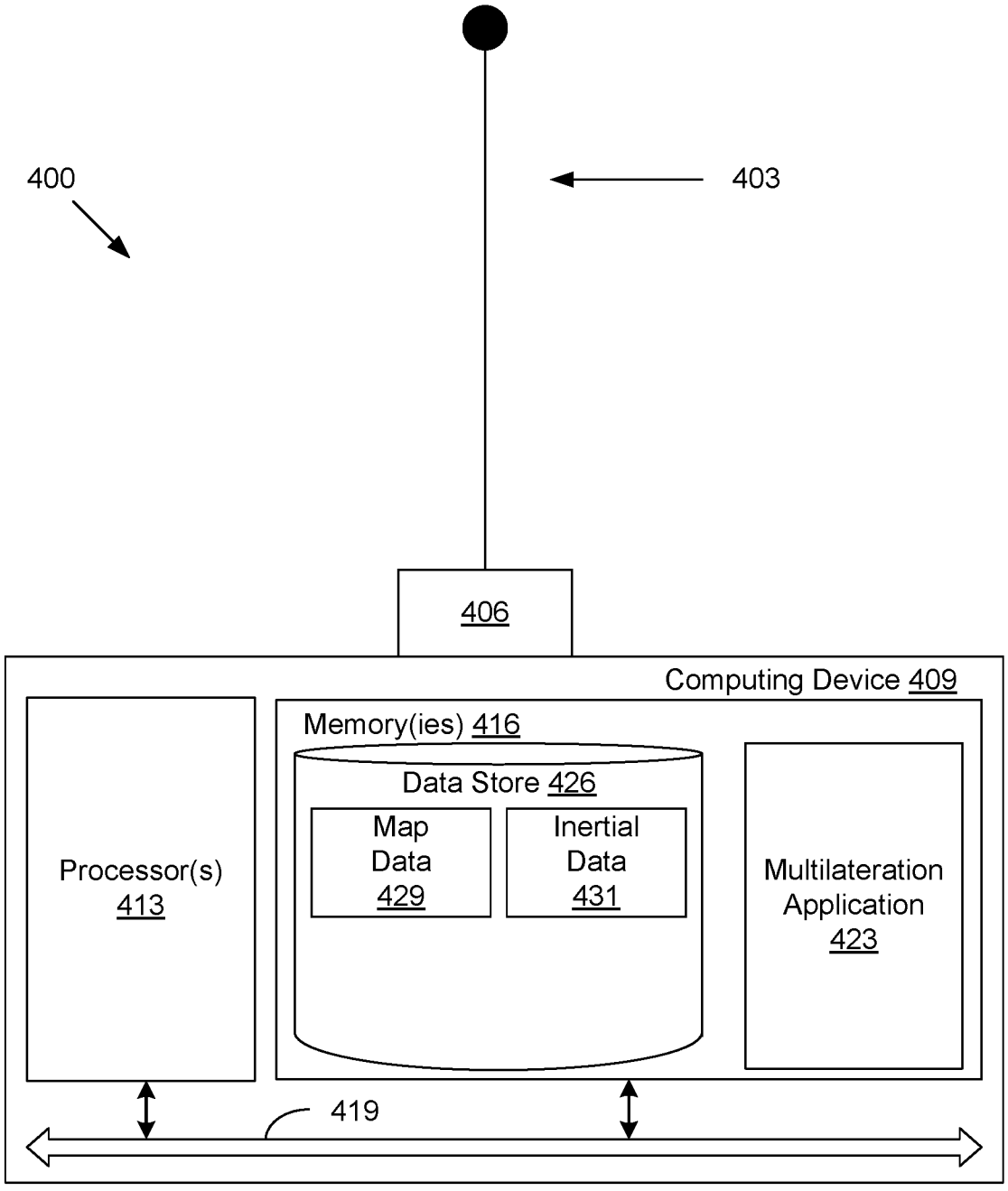

400
403
406
Computing Device 409
Memory(ies) 416
Data Store 426
Map Data 429
Inertial Data 431
Processor(s) 413
Multilateration Application 423
419

FIG. 21

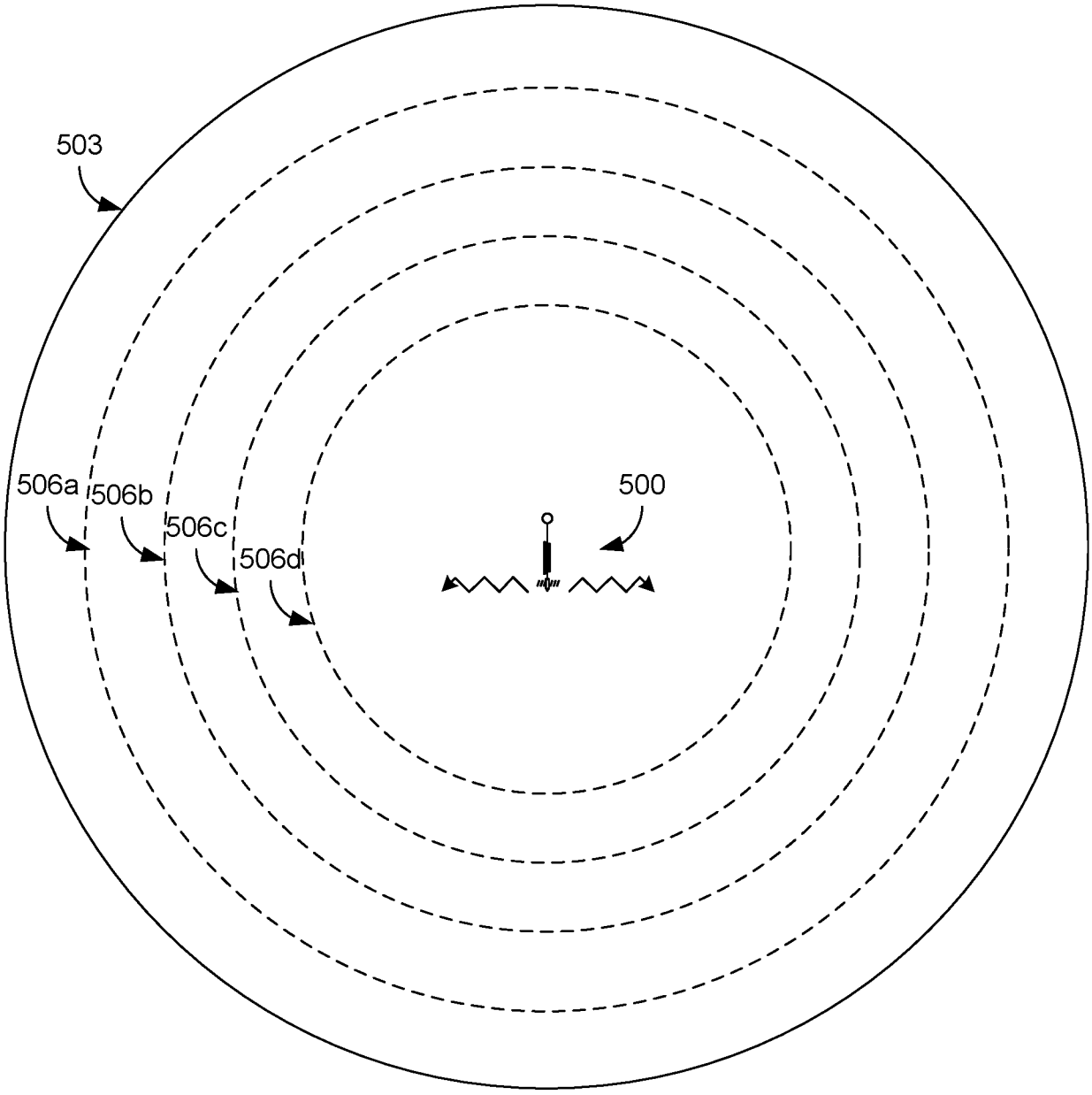


FIG. 22

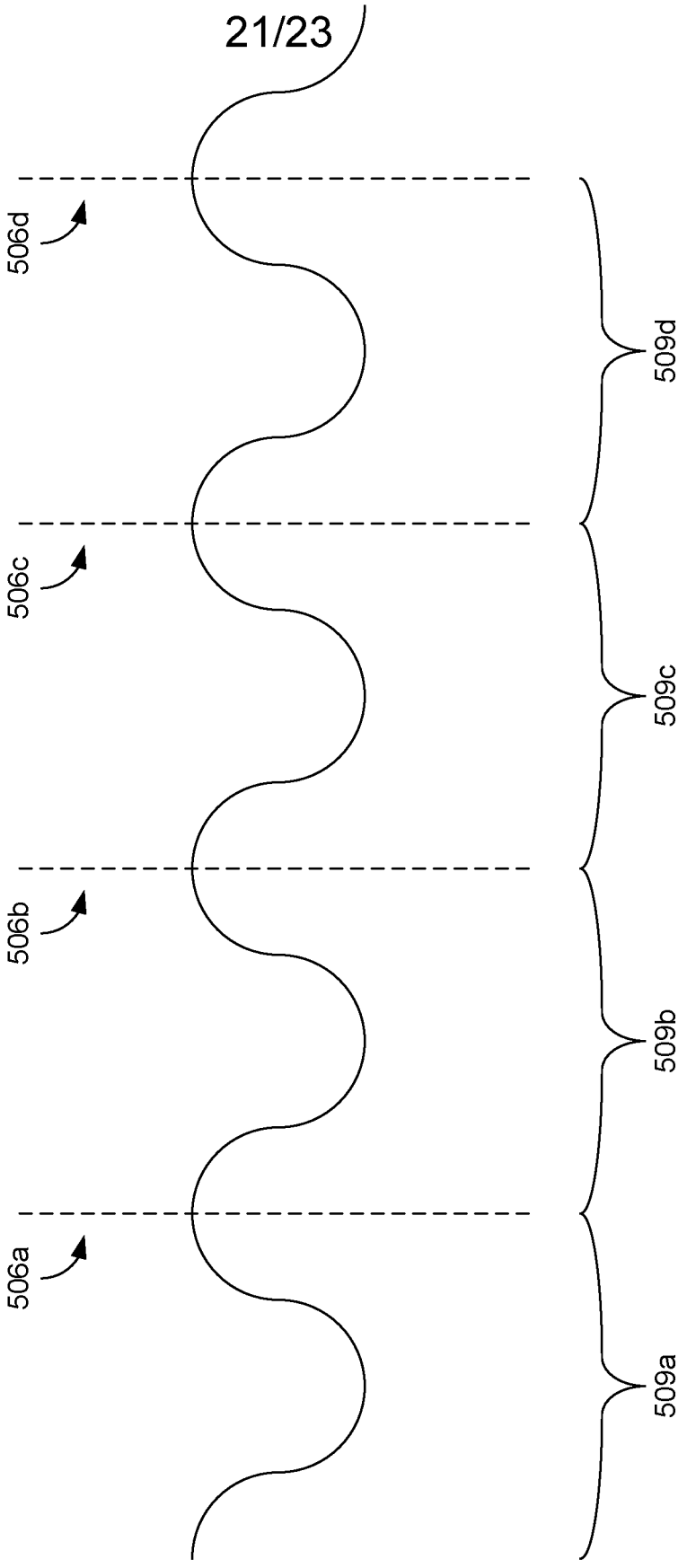


FIG. 23

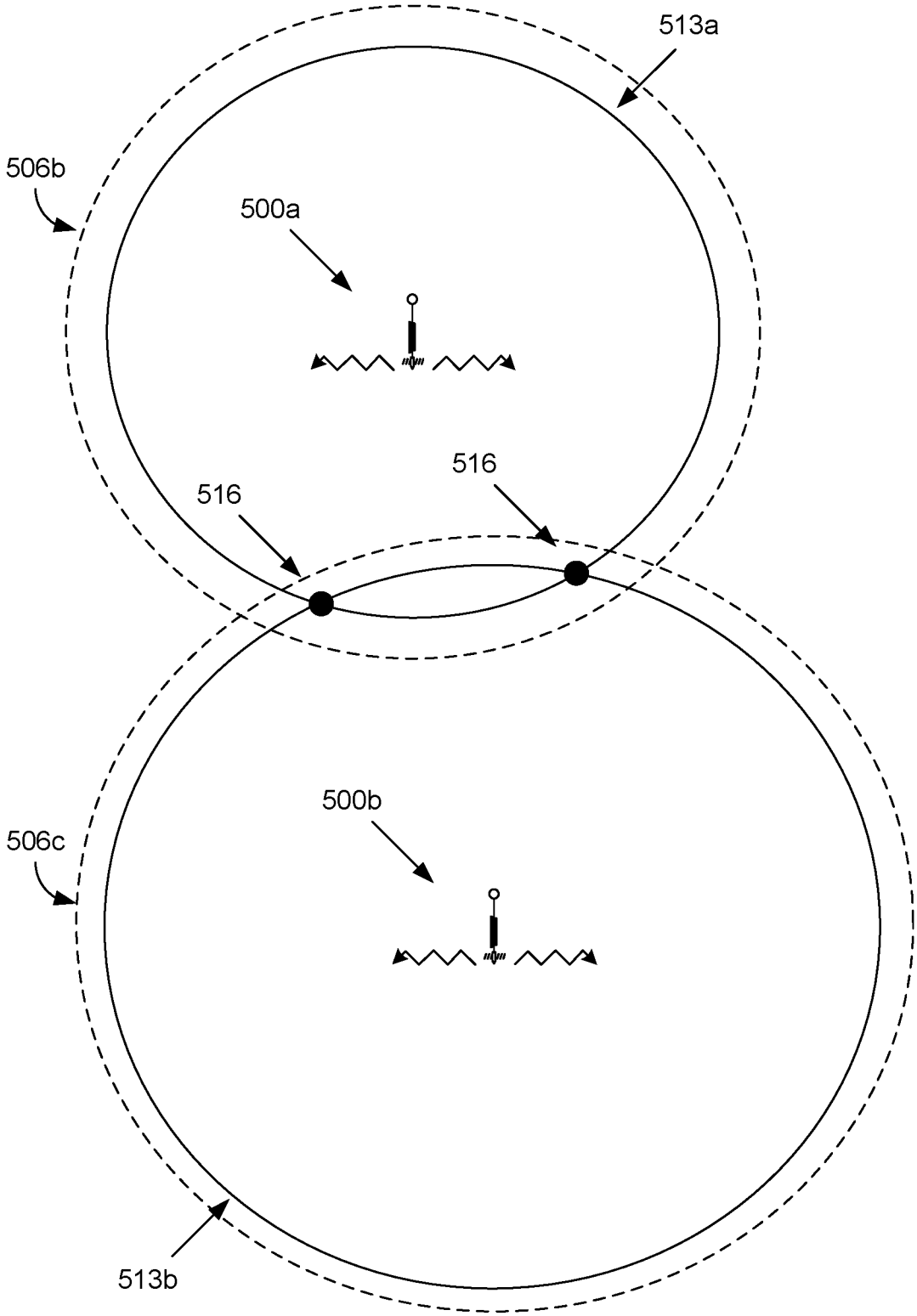


FIG. 24

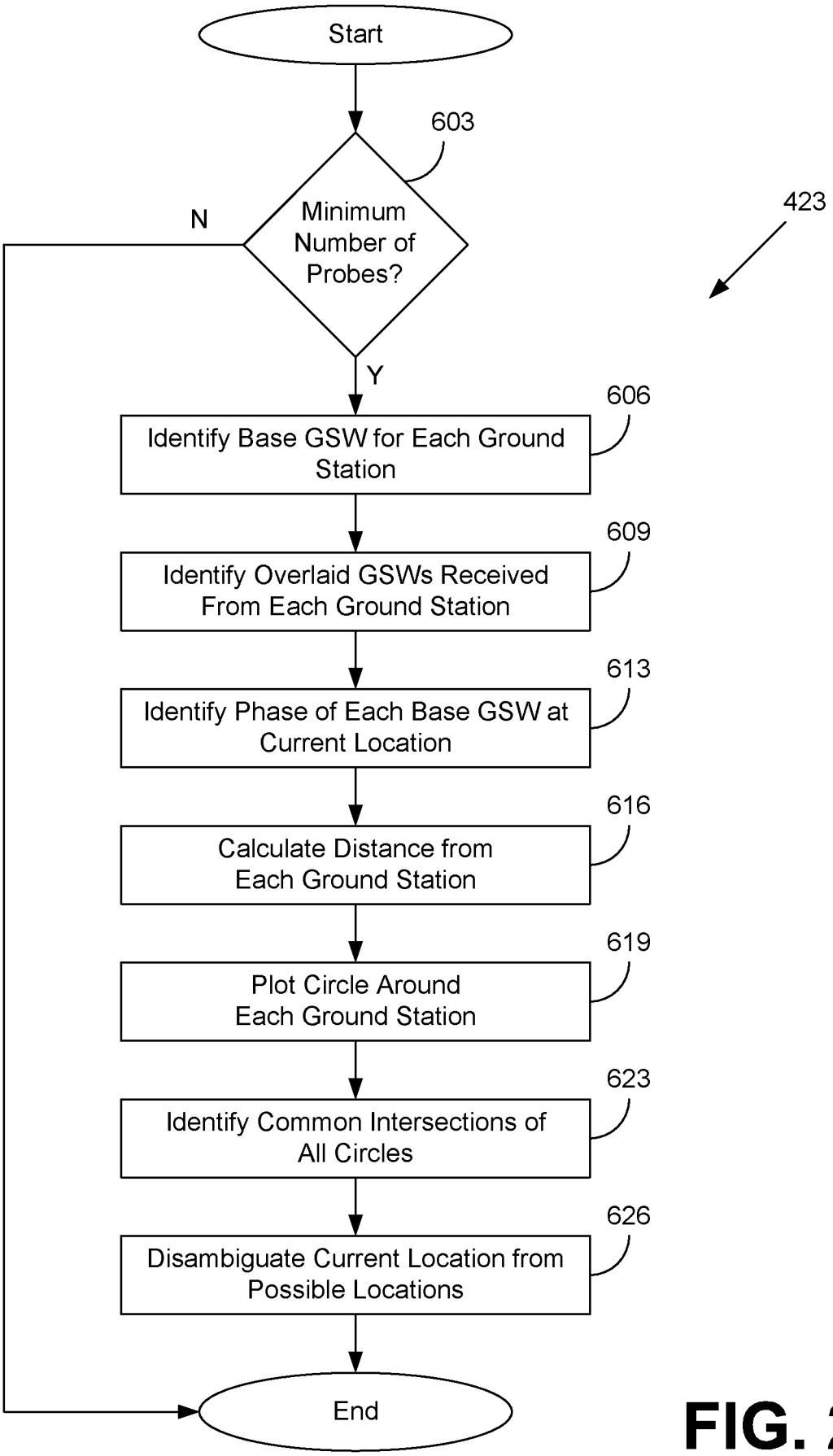

Start
603
Minimum Number of Probes?
N
Y
423
606
Identify Base GSW for Each Ground Station
609
Identify Overlaid GSWs Received From Each Ground Station
613
Identify Phase of Each Base GSW at Current Location
616
Calculate Distance from Each Ground Station
619
Plot Circle Around Each Ground Station
623
Identify Common Intersections of All Circles
626
Disambiguate Current Location from Possible Locations
End

FIG. 25

INTERNATIONAL SEARCH REPORT

International application No
PCT/US2016/047448

A. CLASSIFICATION OF SUBJECT MATTER
INV. G01S11/02 G01S5/14
ADD.

According to International Patent Classification (IPC) or to both national classification and IPC

B. FIELDS SEARCHED

Minimum documentation searched (classification system followed by classification symbols)
G01S H01P H04B

Documentation searched other than minimum documentation to the extent that such documents are included in the fields searched

Electronic data base consulted during the international search (name of data base and, where practicable, search terms used)
EPO-Internal, WPI Data, COMPENDEX, INSPEC

C. DOCUMENTS CONSIDERED TO BE RELEVANT

Category*	Citation of document, with indication, where appropriate, of the relevant passages	Relevant to claim No.
A	US 2014/252865 A1 (CORUM JAMES F [US] ET AL) 11 September 2014 (2014-09-11) figure 12B paragraphs [0027] - [0089] paragraphs [0141] - [0183] -----	1-15
A	US 2008/246647 A1 (HELLSTEN HANS [SE]) 9 October 2008 (2008-10-09) paragraphs [0022] - [0034] paragraphs [0050] - [0123] -----	1-15

-/--

[X] Further documents are listed in the continuation of Box C.

[X] See patent family annex.

* Special categories of cited documents :

"A" document defining the general state of the art which is not considered to be of particular relevance

"E" earlier application or patent but published on or after the international filing date

"L" document which may throw doubts on priority claim(s) or which is cited to establish the publication date of another citation or other special reason (as specified)

"O" document referring to an oral disclosure, use, exhibition or other means

"P" document published prior to the international filing date but later than the priority date claimed

"T" later document published after the international filing date or priority date and not in conflict with the application but cited to understand the principle or theory underlying the invention

"X" document of particular relevance; the claimed invention cannot be considered novel or cannot be considered to involve an inventive step when the document is taken alone

"Y" document of particular relevance; the claimed invention cannot be considered to involve an inventive step when the document is combined with one or more other such documents, such combination being obvious to a person skilled in the art

"&" document member of the same patent family

Date of the actual completion of the international search	Date of mailing of the international search report
7 November 2016	15/11/2016

Name and mailing address of the ISA/	Authorized officer
European Patent Office, P.B. 5818 Patentlaan 2 NL - 2280 HV Rijswijk Tel. (+31-70) 340-2040, Fax: (+31-70) 340-3016	Tancredi, Urbano

1

Form PCT/ISA/210 (second sheet) (April 2005)

C(Continuation). DOCUMENTS CONSIDERED TO BE RELEVANT

Category*	Citation of document, with indication, where appropriate, of the relevant passages	Relevant to claim No.
A	G.J. RICH ET AL: "The launching of a plane surface wave", PROCEEDINGS OF THE IEE - PART B: RADIO AND ELECTRONIC ENGINEERING, vol. 102, no. 2, 1 March 1955 (1955-03-01) , pages 237-246, XP055314964, DOI: 10.1049/pi-b-1.1955.0047 figures 3-6 sections (1) and (4)-(7) -----	1-15

1

INTERNATIONAL SEARCH REPORT

Information on patent family members

International application No
PCT/US2016/047448

Patent document cited in search report	Publication date	Patent family member(s)	Publication date
US 2014252865 A1	11-09-2014	NONE	
US 2008246647 A1	09-10-2008	CA 2613800 A1	02-09-2008
		CN 101256235 A	03-09-2008
		EP 1965223 A1	03-09-2008
		US 2008246647 A1	09-10-2008

摘要

公开的是使用引导表面波来确定定位的各种方法。识别从地面站发射并由引导表面波接收结构接收的基础引导表面波的波长和相位。识别从地面站发射并由引导表面波接收结构接收的重叠引导表面波的范围，其中，重叠引导表面波的范围被测量为基础引导表面波的波长数量。至少部分基于基础引导表面波的相位和重叠引导面波的范围计算引导表面波接收结构与地面站的距离。最后，至少部分基于引导表面波接收结构到地面站的距离来确定引导表面波接收结构的定位。

